Internal Sulphate Attack in Slag Blended systems

A Susceptibility Study

P. Arul Kumar

Faculty of Civil Engineering & Geo-sciences
Structural Engineering Track
Materials & Environment Department

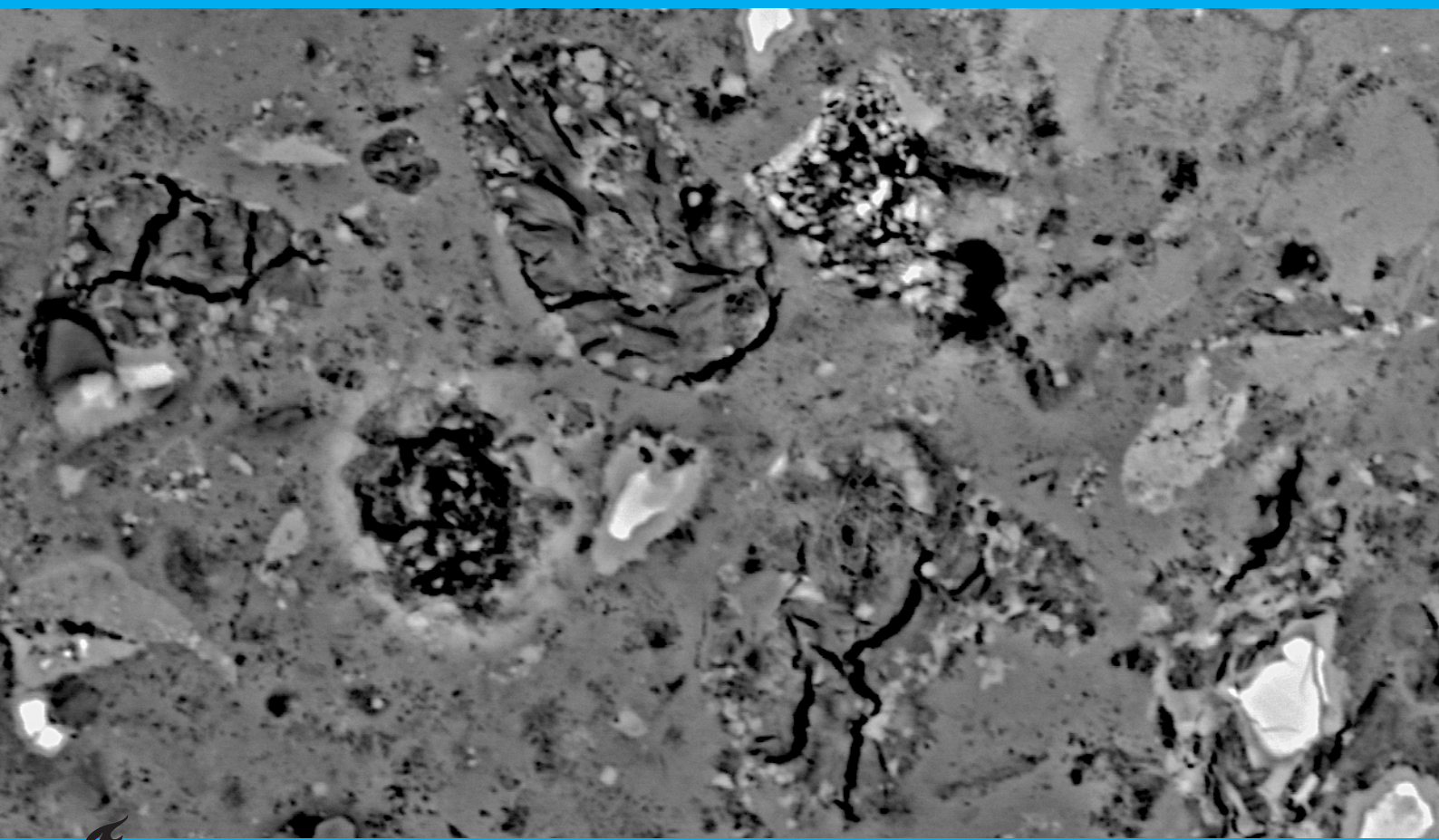

TU Delft

Internal Sulphate Attack in Slag Blended systems

A Susceptibility Study

by

P. Arul Kumar

to obtain the degree of Master of Science
at the Delft University of Technology,
to be defended publicly on 31^{st} August, 2020 at 15:00 pm.

Student number:	4782313	
Project duration:	Oct, 2019 – Aug, 2020	
Thesis committee:	Dr. O. Copuroglu ,	TU Delft, (Supervisor)
	Dr. B. Savija,	TU Delft,(Committee)
	Dr. K. Anupam,	TU Delft,(Committee)
	Ir. F. Filho,	TU Delft,(Committee)
	Dr. M. Pluis,	Spanbeton, (External Advisor)

TU Delft

Preface

செய்யாமல் செய்த உதவிக்கு வையகமும்,
வானகமும் ஆற்றல் அரிது.

(A favor done, not as return for another,
is more valuable than heaven and earth put together)

It feels great looking back at the challenging yet wonderful journey at *Delft University of technology*. I am humbled and grateful for the opportunities in the last two years; that helped me improve myself both professionally and personally. I would like to take this moment to thank the people who have been a part of this journey while adding meaning and joy to it.

Firstly, I would like to thank my chairperson *Dr.Oguzhan Copuroglu* for giving me an opportunity to work under his unique guidance. His constant support throughout the research with an eye for detail helped me solve the different challenges that came up during the research. His introduction to *Math Pluis* gave me the chance to collaborate with Consolis Spanbeton; whose knowledge and inputs gave this research an industrial application. Also, I would like to thank *Ir.Fernando* for his constant review on my work and patience in answering my questions whenever approached. *Dr.Branko Savija* and *Dr.Anupam Kumar*, although they joined the committee a little later their timely guidance and suggestions helped me validate my findings from this study.

My heartfelt gratitude for *Ir.Luis Miranda* for his constant support with GEMS software, without whom performing simulations would still be a far-fetched goal of mine. Being experimental research especially in the times of COVID-19; *Arjan, John* and *Maiko* were greatly supportive and encouraging. They made sure the facilities were scheduled and organized in such a way it was also safe for the students without any compromise.

In this moment, I would love to thank my father *Mr.Arul Kumar*, mother *Mrs.Vasanthi* and brother *Siva* without whom pursuing a Master's Degree away from home; would have still been a dream for me. Their sacrifice and support was the core source of motivation for me to keep facing challenging situations in life. A special mention to my closest friends in Netherlands *Ragav, Rahul, Ilma, Avin* along with my fellow mates from the Structural Engineering family, the times spent with them took away all the stressful periods and turned them into a cherishable memory. Lastly yet importantly many thanks to my best friends from India, *Preetha, Shruthi, Siddique and Praba*, for making feel less away from home every moment with constant support and love.

Enjoy reading the report!

P. Arul Kumar
Delft, August 2020

Abstract

With rapid industrialisation, the infrastructure sector has seen exponential growth in prefabricated concrete elements due to their speedy construction and efficient usage of material. Precast concrete elements have thus observed some deterioration due to increased internal temperature as a result of rapid curing, and also through deliberate heat curing techniques. This has led to researchers in the past to study the effect of such curing conditions on the durability aspect of the binders, especially their impact on Delayed Ettringite Formation. Precast elements such as railway sleepers, exposed to in the humid environment were thus prone to internal sulphate attack and needs to be investigated.

Use of Ground Granulated Blast Furnace Slag (GGBFS) as a substitution for binder content in conventional portland cement in the Netherlands has been prevalent since the early 1900s primarily because of its abundant resource from iron industry. The benefits of slag have been then exploited as it was one of the supplementary cementitious systems which along with being a sustainable solution, provides good resistance to environmental degradation such as chloride penetration resistance. However, their advantages surrounding extreme curing conditions have to be studied, unless used at optimised quantities.

The research focused on the potential of blast furnace slag systems to undergo internal sulphate attack due to high internal temperatures. The simulation of high internal temperature was done through heat curing inside an oven following which continuous storage under lime solution was carried out in order to saturate the system. Slag systems at low and high substitution levels (20% & 50%) were used along with a combination of coarser and finer surface areas, to investigate their subsequent influence was chosen for the study. Also, since infrastructure industry adopts CEM II & CEM III-A cement type, where the former was low slag concentration with moderate fineness and the latter with higher substitution level of slag in combination with high overall fineness, their potentials for DEF have also been studied.

For all the mixes, the influence of high curing temperature and exposure to moisture was studied through microstructural changes, pore size variations and mineralogical composition effect along with fineness on paste specimens. All studies were compared to reference systems of CEM I, which was observed to be the most detrimental due to DEF.

Test results indicate that at lower substitution levels of slag secondary ettringite forms in significant quantities in neat systems along with traces of carbo-aluminate phases in the case of slag systems. Also, higher substitution levels does not appear to completely suppress the formation of ettringite after exposure. Its formation in both the cases showed more or less no influence of fineness of slag added, except in the case of pore size distribution. The significant presence of carbo-aluminates was observed in the case of all slag systems that could prove to be beneficial as they do not translate to deteriorative expansion.

P. Arul Kumar

Contents

List of Figures

List of Tables

Nomenclature

AFc	Monocarbonate
AFm	Monosulphate
AFt	Ettringite
C2S	Dicalcium Aluminate
C3A	Tricalcium Aluminate
CH	Porltandite
CSH	Calcium Silicate Hydrate
DEF	Delayed Ettringite Formation
GGBFS	Ground Granulted Blast furnace Slag
IPA	Iso propyl Alcohol
PC	Portland Cement
SCM	Supplementary Cementitious Systems
SEM	Scanning Electron Microscopy
TGA	Thermogravimetric Analysis
XRD	X ray Diffraction

1

Introduction

Infrastructure is the main indication of a fast-growing economy and thereby integrating the country's development with the world. The global demand for such infrastructure is increasing rapidly, with the need for longer service life, fulfilled performance and increased durability playing an important role. Also, with population explosion and rapid industrialization, the need for faster and efficient construction techniques have driven the infrastructure segment from cast in-situ based to precast manufacturing; at the same time, not compromising on the properties and their performance. This new technological advancement also comes with the need to understand and adapt the concreting process to material research to meet the industry requirements.

Improvisations in concreting techniques are often implemented along with usage of innovative materials such as low carbon footprint cement comprising of slag, fly ash etc. and thus increasing the need to fully understand the science behind it. It has become paramount to consider the performance of such new materials both in terms of durability and integrity of the structure. Use of cementitious system alternatives can induce microstructure changes as well as physio-chemical changes such as pore structure density and hydration heat respectively that have to be investigated for service in real-time applications.

Innovations in raw-material usage integrated with concreting practices that provide enhanced properties and quick installations are delivered by prefabrication of concrete elements. To achieve these along with increased load-bearing capacity, such techniques involve rapid curing methods which may induce conditions that would prove to be detrimental for the structure itself.

Therein newly constructed and structures in-service experience degradation due to both man-made and natural factors. Concrete durability thus is one of the widely studied and discussed issues that engineers face to safeguard the structural integrity of different elements. The Netherlands spends around 30% of its annual infrastructure-related expenditure on inspection, to repair and maintain the existing infrastructure that faces degradation due to environmental factors[2]. Some of the commonly faced durability issues of concrete are corrosion that occurs in the steel in reinforcements, and sulphate attacks [3] .

Each application deals with corresponding durability conditions that have to be satisfied and thus creating the importance of predicting their susceptibility to degradation. In the case of the precast industry, high curing temperatures are experienced either through internal heat of hydration or through curing practices. Therefore indicating the possibility of durability issue related to **Delayed ettringite Formation (DEF)**.

Degradation of the concrete structure due to DEF despite being a rarely occurring phenomenon, the impact is quite evident and can prove to be dangerous if the needed precautions are not taken in predicting its formation [4]. Its occurrence in the past decade had been predominantly noted in the precast industry where the structural elements were subjected to heat curing conditions at elevated temperatures [1]. Mitigation of DEF, being associated with internal sulphate attack phenomenon, has previously involved the usage of fly-ash, slag and other pozzolans. This method is observed to restrict the availability of alumina and sulphates present and ultimately reduce the impact of sulphate attacks [5]. Thus, the alumina rich slag admixture is expected to have more resistance to internal sulphate attack and hence have the potential to be investigated in terms of composition and mechanisms.

Precast industries, thereby exploiting of the benefits of slag systems in the Netherlands, need to understand how this combination in concreting affect the hydration mechanism, in turn investigating the potential for DEF.

1.1. Research Significance

Over the past decade, a number of researches have been conducted in order to investigate the extent of damage that could occur as a result of Delayed ettringite formation in terms of expansion studies. Almost most of the studies primarily focus on several years of experimental monitoring to identify cementitious systems that may or may not be vulnerable to sulphate attack. Through this, scientists have aimed to understand the mechanisms involved and have subsequently reviewed alternatives in order to mitigate the degradation of structures due to DEF.

One such promising alternative is by the usage of blended systems which therein reduce the risk of ettringite formation due to several reasons on being a limited supply of aluminates in the matrix. Of the several blended compositions studied, ground granulated blast furnace slag has proven to be a good substitute for portland cement when combined in higher percentage replacement levels.

Although slag systems have been identified to show several positive benefits such as increased compressive strength, they are of particular interest when it comes to pre-cast applications due to adaptable curing strategies along with early high strength gain. Also, The Netherlands has seen substantial growth in usage of slag as supplementary cementitious systems as a result of abundant resource and sustainable construction practices. Considering these factors, along with the fact that Prefabricated structures undergo increased temperature conditions while curing, there comes the need to investigate the influence of such conditions on slag systems that may cause durability challenges, specifically DEF.

Slag pozzolans, despite being well established as a potential substitute for portland cement to deal with DEF, the underlying mechanisms that may be beneficially influencing the suppression of ettringite formation is not fully understood. Like any cementitious systems, physical parameters in conjunction with chemical parameters influence the durability properties of the structures. Cor-

relating the influences and mechanisms of those parameters such as fineness and composition, durability response of the system can be predicted for the potential to degradation.

Contrary to prevalent length and expansion measurement studies, investigation to predict the susceptibility of the specimen to DEF is sought as a preliminary step which would give a better understanding of the mechanisms involved by influencing component parameters and therein provide potential information for future prevention and/or expansion studies.

Since thermodynamic modelling enables fast-forwarded analysis in order to understand the phase changes as a result of high temperature during initial hydration, the simulations are therefore done subsequently for industrial blended systems. Here, the effect of high temperatures i.e. above 70 °C was studied with understanding the decomposition of sulpho-aluminate phases along with pore solution concentration changes.

This research thus aims to investigate the potential for slag blended systems to the susceptibility of internal sulphate attack through studies involving the phase prior to possible expansion often known as induction period.

1.2. Problem statement

"To investigate the susceptibility of Delayed ettringite formation in blended cement systems with slag with varying composition and fineness"

Sub Investigations:

1. Examination for susceptibility of secondary AFt formation after exposure period.
2. Observation on pore structure evolution as an effect of high temperature curing.
3. Correlation of phase change during exposure for understanding the mechanism during induction period.
4. Determine the effect of fineness on delayed ettringite formation and phase assemblage at high temp.

"Thermodynamic modelling investigation of cementitious systems with slag at elevated temperatures "

Sub Investigations:

1. Understanding the impact of temperature composition of slag on phase assemblage during hydration.
2. Observing the changes in pore solution concentration as a result of high curing temperatures.

1.3. Scope

Experimental Study:

Since the deterioration due to formation of secondary ettringite is instigated at the cement matrix level, the research is focused on understanding the mechanism of DEF at the paste directly. Also, the primary objective to study the possibility for crystal formation after exposure, the scope of the research is limited to susceptibility investigation.

Modelling Study:

The hydration products formed during early stages of curing at elevated temperatures play a major role in subsequent phase formation as a result of exposure. Thus, the phase assemblage before exposure period is modelled by maintaining constant elevated temperature , representing the high internal temperature experienced in real-time setting.

1.4. Limitations of the Study

- The carried investigation is conducted on small scale specimens and hence the effect of transport properties is not considered.
- The temperature cycle chosen is proportionate to the specimen dimensions whereas in the industry, often longer cycles are used.
- The exposure condition adopted though reported to have trivial effect on hydration , an ongoing research is done to standardise the testing conditions.
- The hydration degree adopted for modelling is empirical and thus is only partially representative of the experimental study.

1.5. Methodology

A flowchart describing the methodology adopted is given below.

2

Literature Study

Introduction

Sulphate attack is one of the commonly dealt durability issues in hardened concrete that can cause expansion and thereby leading to loss of structural integrity causing failure [6]. This kind of attack occurs either internally or externally depending upon the source of sulphate which may exist in a hardened state of concrete.

Delayed ettringite formation (DEF) is one such type of internal sulphate attack where the presence of sulphate source inside the concrete leads to degradation due to a combination of factors primarily in concrete that was cured at elevated temperatures although investigations have suggested their formation at normal curing conditions given the presence of significant sulphate content[7]. The basic mechanism of DEF is the decomposition of initially formed ettringite as a result of high concrete temperature and the subsequent re-formation of ettringite in the hardened concrete due to the precipitation of sulphate ions in the presence of sufficient moisture. Ettringite having needle-like crystal structure which when formed at the hardened state proves to be detrimental by causing distress inside the concrete leading to cracks.

Precast Industry Scenario

In construction practice, heat curing is often adopted in order to enable rapid hydration of binder and in turn enable fast removal of formwork. Thus, it is most commonly used in the precast industry. Apart from this, the structures experience high internal temperatures as a result of mass concreting as shown in figure 2.1, obtained from Spanbeton Pvt.Ltd. Such temperature regimens are not standardised and at times go beyond 70 °C , leading to possible ettringite decomposition. Therefore, they were predicted to be more susceptible to DEF [8]. The study on DEF was conducted with portland cement and found to be detrimental when cured at elevated temperatures. Also, real-life precast concrete sleepers have revealed damage due to delayed ettringite formation within 10 years of service the period, which had undergone elevated temperatures during casting [9].

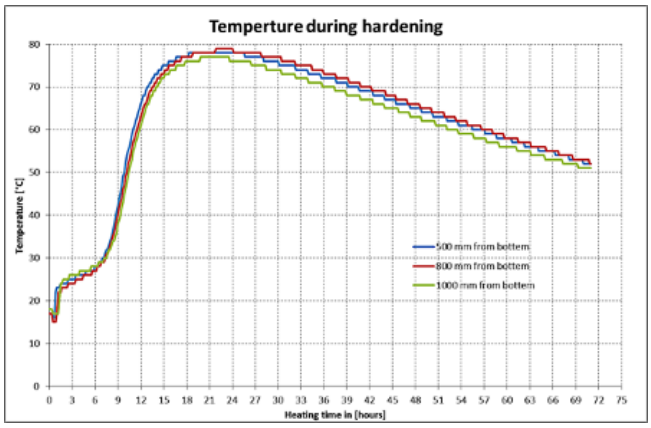

Figure 2.1: Temperature Signature as obtained from Spanbeton for concrete element.

The susceptibility of concrete to experience ettringite formation after hardening depends upon several important parameters and their configurations which influences the extent of its successive expansion in the system. Such parameters are studied extensively in the literature for different types of cement systems and in turn influence the reaction mechanisms. The factors thus causing DEF are discussed below:

Thermal Stability

During earlier stages of discovery of DEF in existing structures, it was hypothesised that initial elevated curing temperatures need not be the criteria for its occurrence. However, upon a microstructural investigation of the affected samples, it was concluded that the cases were specific to specimens containing a high level of SO_3^{2-} ions. The temperature at which concrete is cured has a direct impact on the reaction kinetics thereby influencing the products formed as a result. Experimental investigations were conducted to understand the adsorptive and desorptive capacities of sulphate ions prevailing in the hydrated cement phases at different temperature. It was concluded that the 100 % of the gypsum was consumed in 24 hours of hydration at an elevated temperature range of 65°C to 85°C along with the accelerated formation of ettringite within 1 hour of hydration contrary to slow formations cured at ambient temperatures. The quickly formed AFt also dropped in quantity as the temperature raised from 25°C to 65°C indicating its thermal instability[4].

Chemical Stability

It was understood that the decomposition of AFt into monosulphate was followed by the release of sulphate ions that were consequently adsorbed by hydrated cement phases such as C-S-H gel[10]. This phenomenon also occurs primarily due to the chemical demand of C-S-H and pore solution for sulphate ionic balance. The sulphate ions adsorbed onto the C-S-H are susceptible to dissolution given the suitable increase in temperature, higher pH environment and its charge capacity. It was exclusively investigated and concluded that despite immediate adsorption of sulphate ions by the C-S-H gel at elevated temperatures, its dissolution in the presence of sufficient moisture present in the matrix, as resulting in supersaturation of pore solution was considerably slower in the presence of aluminate sites for re-crystallization of AFt [11] leading to the formation in the concrete hardened state.

2.1. Mechanism of DEF

During cement hydration at normal concreting temperatures, C_3A being highly reactive forms primary ettringite in the presence of gypsum incorporated in the binder. Following which, due to the limitation of the amount of gypsum present, the ettringite thus formed further reacts with excess C_3A present and forms Monosulphate all while being present in the plastic stage.

There can occur a case when Monosulphate can exist even before depletion of gypsum due to reasons such as thermal and chemical instability of the ettringite formed under certain conditions primarily as an effect of elevated temperature during hydration either due to excessive heat of hydration or steam curing method commonly used in precast industries[12]. The mechanisms that develop due to such elevated temperatures hinder the existence of ettringite phases to be present during the plastic stage and later enable their re-appearance tending to be detrimental. Different stages of the DEF attack in terms of dimensional and chemical change, represented by a typical S-curve expansion as shown in figure 2.2 is discussed below.

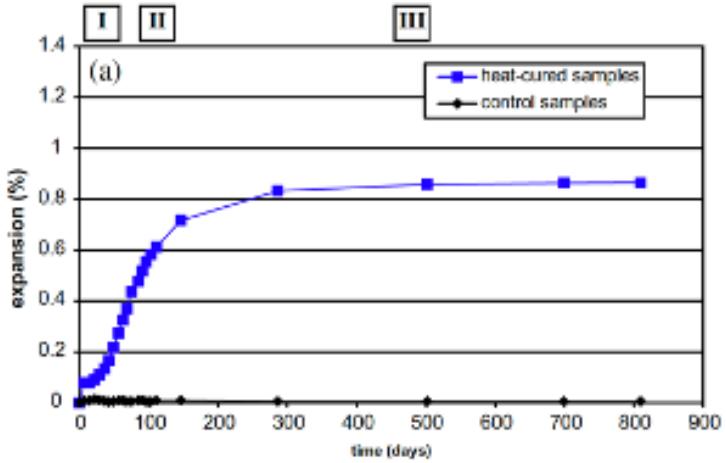

Figure 2.2: Typical Internal Sulphate attack expansion curve. [1]

Stage 1: Formation and decomposition of primary AFt

At elevated temperatures (>70°C), the stability of hydrated sulphate phases is disturbed causing thermal decomposition such as ettringite into a much stable phase of monosulphate. Almost all of the ettringite has been observed to be decomposed at prolonged high temperatures and the formed AFm phases rarely have appeared in the XRD analysis. The reason for the rare detection of AFm phases was primarily due to increases level of heterogeneous distribution of the formed phases. The disintegration of ettringite thereby has observed to release sulphate ions along with a substantial amount of alumina[4].

The desorbed sulphate ions are then subsequently adsorbed by hydration products present in the system that is also influenced by temperature. It has been reported that C-S-H gel experiences critical adsorption capacity at temperatures above 65 °C for sulphate ions and thus forming a porous layer after the initial set of the cement matrix. This new phase was termed as “Phase X” and

suggested that the extent of sulphate ions adsorbed had linear relation with temperature prevalent during curing. As a direct impact of thermal stability, competitive chemical kinetics occurs within C-S-H gel and hydrating alumina phases during the plastic stage. The presence of alumina has been detected to be present within the crystal structure of silica whereas the sulphate ions were present to be loosely bound[13].

Apart from the formation of sulpho-aluminate phases, a considerable quantity of sulphate reacts with alumina bearing compounds such as hydrogarnets. The kinetics behind, the possible phases are complex and often depends upon the composition of the cement[14].

Stage 2: Re-crystallisation of secondary AFt

After the final set of the hydrating cement matrix, it was reported that monosulphate was present along with sulphate ions adsorbed onto C-S-H gel. Upon the interaction with sufficient moisture, these ions subsequently undergo dissolution into the pore solution and in turn attracting mono-sulphate to take it up and recrystallize into AFt. It was thus confirmed that even though C-S-H gel does not directly contribute to the formation of secondary ettringite, it has a direct impact on the stability of the thus formed AFt through its adsorption capacity of both sulphate and aluminate. The primary trigger for the re-formation of ettringite is the source of sulphate ions which can be brought about through pore solution concentration. The saturation of pore solution enables desorption of sulphate ions from C-S-H and alumina by other minor clinker hydrates. Alumina required for the formation of ettringite in the presence of sulphate ions is provided by predominantly monosulphate[15]. Other alumina bearing phases such as hydrogarnets are highly stabilised and hence studies have shown recrystallised ettringite near alumina source, i.e. AFm phases. The phases are present at a submicrometric scale and thus follow reaction kinetics of dissolution and precipitation[4].

The regions and locations of the formation were studied in close relations to the mechanisms supporting expansion outcomes. Thus, an earlier indication of the presence for ettringite in the system was characteristic of the physio-chemical reactions involved.

Chemical equilibrium reactions involving in the monosulphate formation is given in 2.1

$$3CaOAl_2O_332H_2O(AFt) \leftrightarrow_T^{\overline{}+} 3CaO.Al_2O_3.CaSO_4(AFm) + 3Ca^{2+} + SO_4^{2-} + 12H_2O \tag{2.1}$$

Stage 3: AFt induced Expansion Mechanisms

The recrystallisation of ettringite is commonly denoted as delayed ettringite or in some cases secondary ettringite. Though the formation of ettringite after the hardening of the cement system is inevitable, their impact on the system response such as microcracking and subsequent expansion depends upon several underlying factors. Thus, several theories have been proposed in the past to highlight key mechanisms that may cause the expansion to the system.

Crystal pressure theory

In the early decade of investigations carried out in assessment of system expansions due to DEF, it was observed that there was no immediate impact on the extent of expansion with regard to the amount of ettringite that might be present[16]. This was also supported by researches conducted on the nature and morphological features of thus formed ettringite, which highlighted the importance of small and disoriented crystals that may be responsible for expansion. However, on observing expansion data, it was concluded that larger the amount of AFt greater the expansion recorded.

While several parameters influence the expansion rate and magnitudes such as reactivity and the presence of high sulphate to aluminate ratios, crystallisation pressure was studied explicitly to conclude that significant amount of crystals do not induce appreciable expansion. Rather, it was noted that the pressure prompted due to considerable dissolution and nucleation activity in an aqueous environment was responsible for expansions. The pressure (Pc) induced expansion theory was therein investigated in lime-rich Portland cement which depicted substantial expansion, supported by high reactivity (A) in the pore solution due to leaching of calcium ions from lime[17].The equation is described as shown in 2.2

$$Pc = \frac{RT}{V_s} ln(A) \tag{2.2}$$

R-gas constant, T- temperature, Vs- molar volume of crystal formed

The theory was also investigated, which concluded on the reason for the isotropic expansion of the system as a result of pressure-induced by ettringite situated in the micropores of C-S-H formed as a result of re-crystallisation during ambient humid environmental conditions[18]. This theory also suggested that this pressure counteracted by aggregate pressure does not allow expansion explicitly but creating micro-cracks due to tensile stresses which would then lead to further crystallisation when exposed to moisture conditions. Thereby leading to more damage in the second part of the formation caused by weakened paste microstructure and ultimately expanding the structure.

Swelling theory

During the same period, another arguable theory was explored and investigated that proposed an expansion mechanism as a result of water molecule uptake by amorphous ettringite system during re-crystallization. The crystallisation activity was further described as a result of solid to liquid solution interaction of the ettringite colloids that subsequently intake water and increase in volume. This mechanism thus suggested that it was necessary that there is high relative humidity present inside the system that could be achieved by supersaturation conditions[19]. Such conditions were further identified to initiate nucleation of delayed ettringite in micro-cracks through solution depositions. Highlights of the theory were also indicative that the ettringite did not form inside micropores of hydrated phases, and rather in the locations of sulphate rich regions, primarily close to monosulphate phases. Following which, the crystals accumulate and further grow in size thereby causing expansion through conformed crystal growth theory.

Several studied have been conducted to support either of the theories stated above and have also provided additional evidence that the formation of ettringite occurs at sites far from alumina rich hydrates, indicating that diffusion of ions through pore solution plays a major role for initiation[20]. Investigations on damaged structures were investigated for thus formed ettringite which was then reported to be found near the interfacial transition zone which predominantly contains porous C-S-H gel that could have been potential sites for SO_4^{2-} ion adsorption[12]. Since the primary source for the formation of ettringite occurs from the dissolved sulphate ions present in the pore solution the mechanism is stated as internal sulphate attack.

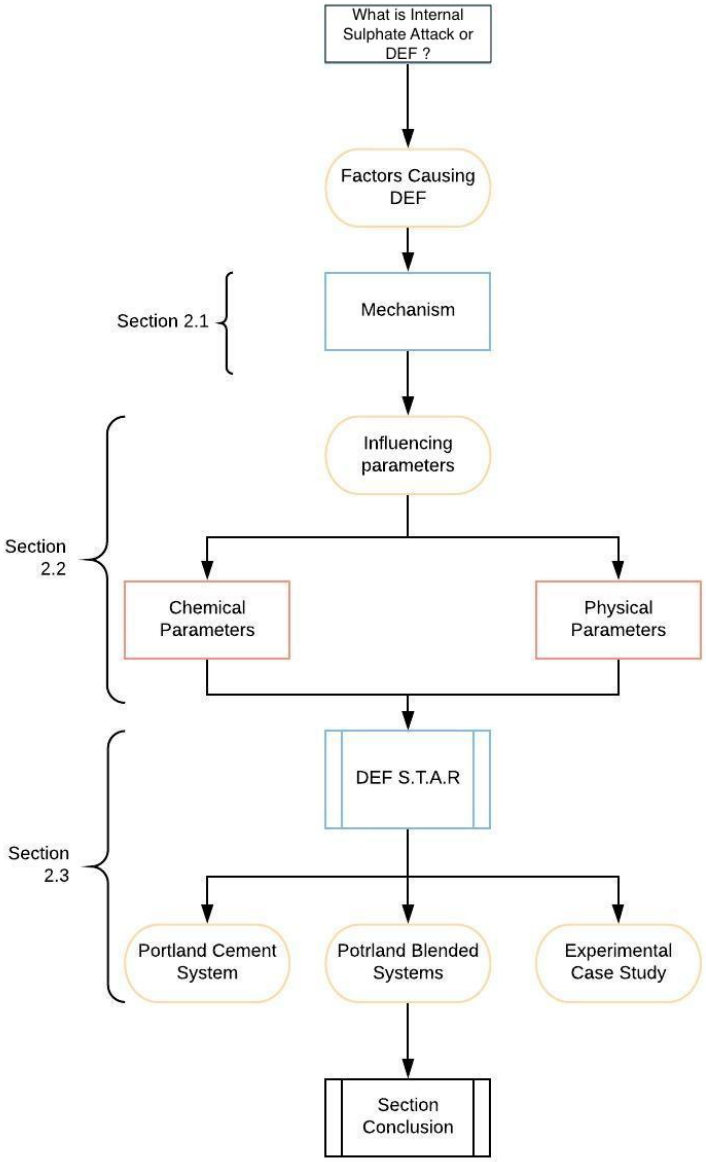

Figure 2.3: Part 1:Experimental Literature Study.

An extensive literature study was conducted to understand the different parameters involved and to define the scope of the research as shown in the flowchart 2.3 given above and was presented in the following sections.

2.2. Influencing Parameters

2.2.1. Chemical Parameters

Bogue Composition

The starting point of any chemical reaction occurs based on the presence of relevant reactive composition in the system. Thus, for ettringite to form irrespective of the temperature function, primary constituents are sulphate (SO_4) and alumina (C_3A)[4]. Where the former is provided by gypsum or Sulphated components and the latter is obtained from rapid hydration of one of the four main clinker components, Alumina along with other aluminate bearing phases in the later stages of hydration. As discussed in the mechanism for the re-formation of AFt, the different phases formed as a result of hydration at high temperature is directly influenced by the initial reactants, i.e. the bogue composition.

The influence of composition was also evident from studying individual phases formation studies such as the effect of high temperature on C-S-H formation and its subsequent ability to adsorb sulphate ions[13]. The dissociation of sulphate and its thermodynamic nature to reach equilibrium is affected considerably by the presence of oxide species present as a part of the clinker components. Importance of investigations to mitigate DEF induced expansion studies were also conducted by altering the system composition[7]. This enabled a conclusion based on an experimental study that, presence of anhydrites and silicates lowered the release rate of sulphate ions at elevated temperatures despite having higher amounts. Thus, re-iterating the impact of binder composition on the end phases present.

Most of the researches that have been conducted were focused on identifying the extent of concrete degradation with respect to expansion length. Thereby associating the extent of volume change to hydrated phases influenced by the initial composition of the cement systems. This further led to a considerable amount of experimental studies which provided guidelines and pessimum values of binder constituents that could indicate expansion later due to DEF[4]. The major finding was concluded that controlling the amount of alumina present in the initial system would limit the formation of ettringite even before thermal decomposition at a higher temperature, thus positively reducing further reformation of ettringite that could cause expansion. An investigation conducted by Kelham has revealed that cement types containing low C_3A content exhibited lower expansion rates. Subsequently the amount of C_2S present during hydration at elevated temperatures affects the stability of ettringite by attracting the aluminates towards the rapidly formed C-S-H phases along with sulphate adsorption[21]. Thereby experimental results of analysing different levels of clinker compositions showed the presence of only monosulphate and no ettringite.

Sulphate and Alumina Content

It was made evident that the presence of Al_2O_3 and SO_4 are paramount for calcium sulpho-aluminate phase formation.However, researches showed that the presence of high contents of the same does not always translate to deteriorating levels of ettringite formation in the hardened matrix. It was concluded that moderate levels of SO_3 content along with the negligible amount of Al_2O_3 would result in almost no ettringite, subsequently, an excess quantity of alumina would enable the formation of monosulphate in the later stages[22]. Also, studies showed that for an adequate amount of alumina for which not sufficient amount of sulfate is absent would eliminate the formation of AFt, while the latter's excessive quantity would create the chances of excessive presence of ettringite even at elevated temperatures[23].

Analysis of different substitution levels of alumina and sulphate present in the clinker brought about a parameter to assess the susceptibility of systems to ettringite formation that could cause a plausible expansion in hydrated systems. Broadly denoting the parameter defined by the molar volume ratio of SO_3/Al_2O_3 where the aluminate was contributed by amount of C_3A present. Early researches conducted on the same indicated that if the ratio was present above 0.5 or higher it would cause deterioration induced by DEF[24].

However, later expansion studies were conducted by varying the constituent ratio which concluded contradicting outputs stating that the initially set ratio criteria did not match for different systems[25]. Thereby highlighting the underlying mechanism influences despite probable values of sulfate and alumina contents. Ever since numerous experiments have been conducted to identify different pessimum ranges for specific cement substitutes with varying clinker ratios as well as systems that included SCM's such as fly ash and slag blended systems.

Alkali Content

Through early stages of research that showed a clear indication of the difference in the pessimum values of DEF index, it was evident that there could exist significant influence of other components of the cement binders such as minor components of oxides and alkalis. Thus, this speculation was followed by a series of tests by keeping the SO_3/Al_2O_3 ratio constant and subsequently varying the oxide compositions. One such test conducted by Lawrence et al indicated significant influence of MgO, explained by the presence of hydrogarnets C_3AH_6 that take part in high-temperature decomposition mechanism of ettringite[17]. Also, researchers conducted several trials to modify the earlier reported DEF indices to incorporate the influence of alkalis on delayed ettringite formation. So, developed a new equation that not only included the ratio of sulphate to aluminate but also combined alkali content expressed as sodium oxide equivalence as given below in equation 2.3.

$$DEF_{Index} = \frac{SO_3}{C_3A} \times 0.1 \times (SO_3 + C_3A) \times \sqrt{Na_2O_{eq}} \tag{2.3}$$

Also, a series of tests were conducted in similar preconditioning parameters conducted by Khelam, displayed higher expansions in specimens with higher alkali contents. The experimental study involved 12 hours of high temperature curing at 90°C and therein he proposed an equation to predict probable expansion as seen in 2.4[21].

$$\%Expansion = (0.00474 \times surface\ \ area) + 0.076 \times (MgO + 0.217) \times (C_3A + 0.0942) \times (C_3S + 1.27) \times Na2O_{eq} - 0.737abs|SO_3 - 3.7 - 1.02 \times Na_2O_{eq}| - 10.1 \quad (2.4)$$

It was however indicated through adoption and validation of the equation for different compositions that it proves correct only in the case of predetermined boundaries of the Khelam's data sets and cannot be applicable for generic scenarios. To add to these limitations the equation did not account for shrinkage observations in mortar specimens which were prevalent in specimens' tested.

The impact of alkali content is attributed to the rise in pH of the system that favours rapid adsorption of sulphate ions onto the surface of C-S-H and increased stability of the AFm phase proving unfavourable for ettringite formation. Also, alkali content appears to affect the extent to which ettringite can dissolve in close attribution with temperature effects. Higher the basicity of the pore solution, more is the absorptive capacity of C-S-H gel to take up the decomposed SO_3 ions in synergy with increased internal temperatures owing to thermodynamic balance. Thus, the two parameters together amplify the DEF process under relevant conditions.

2.2.2. Influence of Physical Properties

Elevated temperatures experienced as a result of high temperature curing and/or due to heat of hydration has been established as the main prerequisite for the decomposition of early-stage ettringite in wet cement paste. However, the reformation of the secondary ettringite is highly unlikely if supporting parameters are downplayed. Such supporting physical properties that go hand in hand with reformation are discussed below:

Environmental conditions:

Discovery of damaged structures due to DEF has been identified to have undergone humid and wet climatic conditions during the service period. Such environmental conditions meant constant or sufficient exposure of concrete elements to moisture which resulted in permeation of water from the surrounding into the cross-sections. Thereby, promoting an increase in the ionic concentration of pore solution attributed by dissolution or leaching and providing the starting point for recrystallisation of AFt. Thus, concrete elements present in dry and semi-arid environments have not shown any deterioration due to DEF, due to lack of moisture in pore solution to support transport properties.

The reformation of monosulphate to ettringite formation as supported by mechanisms involves movement of desorbed sulphate and aluminate ions followed by nucleation of crystals. Thereby indicating the presence of water present inside the systems that contribute to the saturation of the

pore solution by ions[26]. This simply requires the transport of moisture through the pores of the matrix that would, in turn, enable leaching of ionic species into the pore solution. Investigations were carried out to understand the effect of saturation of pore solution by the leaching ions and in correlation with different phases such as Ca/Si ratio of C-S-H, formed as a result of high-temperature decomposition. The study concluded that the supersaturation of the pore solution by leached calcium ions affect the newly precipitating phases especially ettringite[26]. This mechanism highlights the impact of pH levels that provide thermodynamic stability for recrystallisation.

Fineness:

The fineness of binder intrinsically exhibits reaction changes during hydration such as higher levels developing high heat of hydration due to greater reactivity and thereby contributing to temperature rise during curing. The fineness of SCM's also affects the chemical kinetics by influencing the pozzolanic activity. It has been reported that greater fineness of slag, leading to increased contact area in Portland cement blends promotes faster consumption of portlandite and faster realization of alumina due to heterogeneous nucleation, thereby inhibiting ettringite formation[27] . Fineness levels of blended cement systems were investigated and concluded that higher fineness levels indicated higher expansions. The fineness ranges were varied in close relation to the clinker and exhibited changes in pozzolanic activities that exhibit ted homogeneous nucleation eliminating the competition for alumina, that in turn affected the DEF. The impact of fineness is often coupled with other parameters such as alkali content and SO_3 content in the cement have been investigated and comply with the impact of individual influences along with finer blends of SCM's[28].

Micro-structure:

Although the hydration of cement phases during high temperature curing along with subsequent exposure to environmental conditions may lead to DEF, the internal physical structure of the cement matrix plays a major role. The microstructure of the systems determines the rate of diffusion of moisture and subsequent re-crystallization of phases influenced by pore structure distribution. Poorly connected pores, along with smaller pore sizes which may be a result of fineness effect would significantly prevent the entry of moisture and afterwards reflect on slower rates of dissolution of ionic species required for reformation.

Therein, the presence of micro-cracks would affect the connectivity of pores that have a direct impact on the transport properties leading to DEF[29]. High temperature curing or increasing in internal temperatures as a result of hydration heat evolution is often associated with the formation of micro-cracks in the paste structure. Thus, these act as potential sites for the entry of moisture along with subsequent re-crystallisation regions. Pre-existing micro-cracks that may have formed as a result of freeze-thaw actions have also resulted in negative effects of DEF, due to loss of integrity of system matrix. Thus, the quality of the microstructure characterized by pore size distribution greatly influences the probability of DEF.

2.3. DEF Studies Overview

2.3.1. Portland Cement Systems

DEF has been reported to have caused considerable deterioration in concrete elements subjected to high temperature curing over the past decade [30]. Examinations of deteriorated concrete samples showed significant bands of ettringite formations present in the Interfacial Transition Zones (ITZs), i.e. between the paste and aggregate that also showed considerable expansions. Also, DEF investigations were conducted on heat-cured railway sleeper elements that showed significant expansions and resulted in tie distresses[31].

Ever since the discovery of this durability issue associated with internal sulphate attack, early-stage researches were conducted to study the affected cement systems to understand the reason and mechanisms involved. Investigative studies were thus begun with the then most commonly used type of binder, Portland cement (PC) systems. During the initial days of understanding the factors affecting DEF, portland cement systems containing a higher amount of sulphates were proposed to be vulnerable[10]. However, this was later corrected through several experimental investigations conducted to understand better the mechanisms involved as stated in the earlier chapters. First steps were to understand the influence of cement compositions and physical parameters such as microstructure and fineness. This involved laboratory-scale concrete elements that were subjected to high-temperature curing and prolonged exposure to humid environments. Subsequently, length changes were measured to observe volume expansions. Expansion studies were also conducted on cement mortars that have undergone high internal temperatures as a result of the heat of hydration in mass concreting structures[32].

As conclusive statements based on the underlying reasons and mechanisms were drawn, the investigations were modified by testing portland cements varying in compositions and other parameters to develop binder systems that were least susceptible to DEF. The studies along with length change measurement included developing empirical models based on vast data collected from experiments conducted on portland cement systems to predict the susceptibility of new or yet to test cementitious materials to DEF. Models developed initially were based on empirical equations by considering conditions that are beneficial for deteriorative expansions. Later, researchers have also attempted to model the predictions based on scientific theories supported by the underlying mechanisms involved in portland cement degradation[17]. The models thereby developed were validated with existent expansion data provided in earlier studies. However, they hold limitations such as advocation of one theory of mechanisms and validity across cementitious systems other than portland cement, which would considerably change the mechanism[17].

2.3.2. Portland Blended Systems

One of the central results concluded from several experimental investigations conducted on portland cement was the effect of bogue composition on the susceptibility of systems to DEF. For which the reasons were well justified as explained in the earlier chapters. The key parameter for the formation of ettringite in the later stages was thus reported to be influenced by sulphate and aluminates in the system. Alternatively, limiting the re-formation of ettringite from monosulphate was identified to be a method for arresting DEF induced expansion. Thus, researchers began investigations on blended systems by partial replacement of portland cement with SCM's which would considerably reduce the portlandite presence which would otherwise be available for sulphate bearing gypsum phases that would subsequently be consumed by alumina present that is paramount for ettringite formation.

Also, experimental studies addressing durability issues surrounding sulphate attack have shown the positive effect of incorporation of pozzolanic materials into the portland cement blends primarily because of the consumption of portlandite, which would otherwise react with sulphate ions forming gypsum, followed by subsequent formation of ettringite from sulpho aluminates present in the system[25]. Recent studies on the use of nano-silica substitutes, at lower replacement levels (4 – 6%) have resulted in a significant reduction of expansions in the systems due to increased degree of hydration attributed by the small surface area of the reactants. Slightly higher substitution levels of fly ash at about 15 to 25% were reported to have expansion reductions. Since the substitution levels are mainly affected by the parent system composition, in the case of slag blends, higher percentage levels (> 25 %) were identified to mitigate expansion in the longer duration. A systematic study was also conducted to investigate the effect fineness of pozzolanic additions and concluded despite showing advantages in terms of substitution levels, coarser replacements proved to be ineffective in mitigation of damage due to DEF[25]. Also, reduced levels of $Ca(OH)_3$ available for gypsum formation, due to consumption by slag decreases the potential for ettringite re-formation considerably.

Ground granulated blast furnace slag (GGBFS) additions have therefore been demonstrated to have a considerable reduction in expansion lengths in comparison with sufficient replacement levels [33]. This was attributed to the considerable reduction of SO_3/Al_2O_3 ratio along with improvement in microstructure to porosity that would limit infusion of moisture considerably. Thus, expansion experiments have been conducted on slag blended systems with varying levels of replacement and other concreting parameters such as water to cement ratio. It was reported that slag substitution level as high at 50% was sufficient to completely eradicate the probability of ettringite formation during service period [33].

2.3.3. DEF Experimental case study

Researchers in the past decade has conducted several studies through experimental procedures to observe the effects of delayed ettringite formation. To develop a systematic analysis different tests and investigations conducted were identified and the widely reported procedures were studied. The aim of the study was to mainly identify plausible testing methods and characterization to obtain results in an orderly fashion. The list of literature studied, and the corresponding parameters involved are listed in Appendix A. The outcome of the case study is discussed below:

In terms of **objectives studied**, majority of the work conducted focused on testing specimens for the susceptibility to destructive volumetric changes induced due to DEF through length change data collected for long periods of measurements. The tests involved cases that included mortar and concrete specimens that further reduced the rate of dimensional change[20]. Widely, tests were done in comparison to a reference specimen that was most likely to undergo considerable damage during the exposure period. Subsequent microstructural analysis was also conducted primarily on damaged samples.

In the **experimental investigations,** conducted by the researchers in lab-scale tests, different sets of pre-conditioning methods and specimen selection have been reported. To begin with, concrete specimens were rarely explored for their length changes unless the samples were collected from existing structures such as rail sleepers and precast bridges. Most of the investigations thereby included investigations pertaining to mortar samples prepared using standard mixes, maintaining the w/c ratio for comparative analysis.

The **geometry and dimensions** of the specimens cast were adopted to suit convenient measurement of length change characteristics. Thus, prismatic specimens were cast with square cross-sections with the commonly reported dimension of 4x4x16 cm. Specimens with circular cross-sections were reported to facilitate mechanism studies including characterization research. In several literatures, the specimens were contaminated with sulphate solutions at about 2% – 3% by weight of binder to accelerate the formation of secondary ettringite. Scientists have also studied the comparative effects of different types of contaminants used and their relative effect on length changes measured. Despite a considerable amount of research conducted using sulphate contaminants for the acceleration of the tests, their representativeness of actual mechanisms that can occur in their absence has not been justified effectively.

Different **curing procedure** adopted for the prepared specimens have been reported, where the choice of temperature range was kept between 70°C to 80°C. While the temperature of study chosen happens to occur at more or less at the same aforementioned range, the duration of the temperature cycle reported were of considerable differences. Some of the early stage works described adopted directly real-time temperature signatures, which meant prolonged high temperature curing duration, even as long as 3 weeks. Later, the duration period was modified on the grounds of proportioned specimen sizes, reduced temperature signatures as short as 24 hours were adopted.

Exposure Environment to which the specimens cured at elevated temperatures are subjected to show significant differences as reported in the literature. In early-stage researches conducted the specimens were submerged either partially or fully into solution predominantly deionized water to accelerate expansion mechanism[34]. However, later it was studied that exposure to distilled water could instigate super leaching of ions and negatively influence expansion in the specimens. Thus, exposure solutions were modified, and lime saturated solutions were adopted to promote harmonic supersaturation of the pore solution[20].

From the conducted literature study it can be learnt that the effect of the composition of the clinkers has a significant influence on the formation of ettringite at corresponding conditions. The primary take away of the case study conducted was conclusive that no standard procedure is adopted to measure length change measurements or microstructural investigations that can be universally adopted to predict the susceptibility of systems to DEF. However, the most commonly reported procedure that is closely representative of real case scenarios was adopted to reduce and control errors thereby producing comparable results. Also, several types of research indicate the adoption of sulphate additives in the process of either casting of specimens or during exposure conditions to accelerate the expansion behaviour.Thus, their parameters along with the effect of slag fineness are studied through experimental program discussed in Chapter 3.

2.4. Thermodynamical Modelling

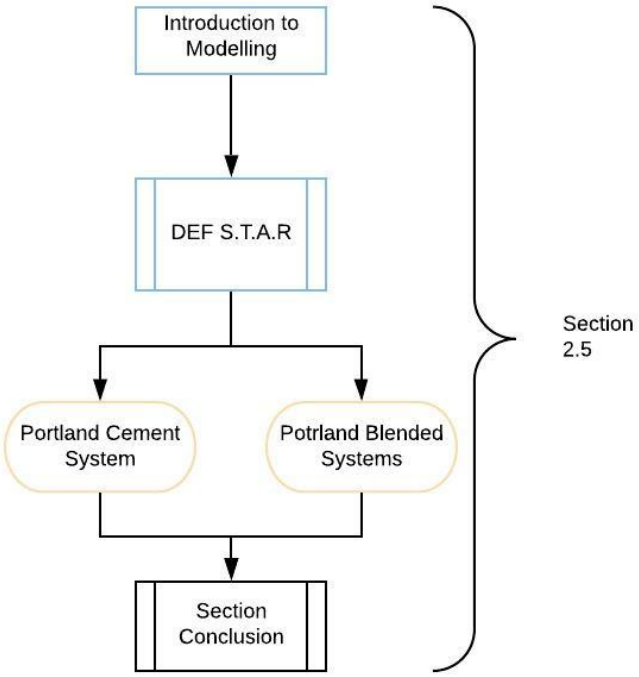

Figure 2.4: Part 2: Modelling Literature Study.

Literature study conducted to understand the fundamentals of thermodynamic aspects of cement hydration and its subsequent modelling is shown in the flowchart 2.4 given above.

2.4.1. Introduction

With fast approaching advances in material innovations providing the primary aim to improve performance along with sustainable solutions, the need to assess them has also become vital for research. Novel cementitious systems have come into prevalence in large scale industry adhering to improved performance and comparable benefits with conventional Portland cement. Despite being used in several sectors of the infrastructure field, extensive investigation is required and sort after to provide confidence in their application and also enable calculated modifications to suit, case-specific needs such as enhanced durability. Thus, extensive studies need to be conducted to modify the composition and surrounding parameters to control their structural performances.

Cementitious systems that are currently in the spotlight are the ones that enable significant replacement of traditional Portland cement following the need for sustainable systems along with improved durability properties. Such systems, namely supplementary cementitious systems (SCMs) have to be studied and investigated for their chemical responses in terms of hydration behaviour and pozzolanic activities upon changes in critical parameters such as chemical compositions, the temperature of hydration and other environmental factors.

For many years researchers have sort to experimental investigations to identify key properties and impact of several parameters to conclude on the performance of novel systems. These done and tested experiments through well-established is however time-consuming and bound to have the effect of human error. Anomalies and difficulty in controlling the boundaries of such tests have always created room for improvement. Thus, scientists in the past decade have worked extensively on mathematical models to predict and understand changes in cementitious systems enabling faster and more reliable results. With the support of basic experimental data and stating the science behind chemical reactions through a set of mathematical expressions have thus evolved to several systematic tools, one such being Thermodynamic Modelling of cement hydration. Thereby, considerably reducing the time and effort spent on probable uncertainty of laboratory experiments and yielding comparable results helping in predicting reaction products and properties.

Thermodynamic modelling of cement systems enables the prediction of cement hydrate assemblage, their composition in the aqueous environment based on the provided information of the parent or the reactant components of the system under study. They rely on the basic assumption that a restricted thermodynamic equilibrium is established between the solid phases formed and the pore solution during hydration. In this case, the unreacted clinkers continue to be present in the system suppressed by equilibrium conditions therein creating the necessary real-time hydration degree for the stipulated reaction. Despite this assumption, it has been studied through modelling calculations that, although in the early stages of hydration pore solution could be saturated with the hydration products formed, they tend to attain a meta-stable condition close to achieving thermodynamic equilibrium. This has been, however, proved comparable primarily for portland cement system, and there still exists ongoing research for blended systems.

Tools and software interfaces have been developed extensively in the past decade to accommodate complex equations and chemical interference with quick run time and providing accurate results. These tools also have inbuilt functions that have the platform to add experimental data and information. The tools operate with a predefined set of solubility data for the reactants in interest and run background geochemical codes to achieve equilibrium. One such popular tool is Gibbs Energy Minimisation Software (GEMS) for geochemical modelling. The principle and aspects of the modelling will be later discussed in Chapter 4.

2.4.2. Studies using thermodynamic modelling

Ever since the development of user-friendly interfaces to predict hydration, researches have conducted several simulation studies to correlate and verify the reliability of the results with available vast experimental data. With each simulation study, the modelling database has seen constant growth and update to match real-time compositions and hydration conditions to subsequently predict the effect of involved parameters. This section provides a brief literature study on several works done using thermodynamic modelling pertaining to hydration simulation of cementitious systems.

Portland Cement systems

One of the primary interests was to predict different hydration products as a function of time for common systems such as Portland cement and observe the changes in the phase assemblage along with changing stoichiometry in terms of saturation indices for 28 days[35]. The first significant inputs to thermodynamic computations were provided by a series of simulations conducted by Lothenbach and colleagues to understand the chemical hydration characteristics of PC. Their work provided information regarding solid solution interactions with cement constituents, identifying pore solution composition, and also impact of hydration parameters such as temperature and pressure.

The first set of studies were conducted to model the hydration of Portland cement at ambient temperatures to predict the phase assemblage as a function of time. The input parameters included providing kinetically modelled data for the reaction rate of clinker compositions adopted from empirical equations. The study included also the effect of different w/c ratios and subsequent analysis of pore solution composition[36].

Portland Blended Systems

With the development of standard database sets for ordinary portland cement, the application of thermodynamic modelling saw significant contributions to study the effect of supplementary cementitious systems' effect in combination with PC, to predict hydration phase assemblage and pore solution concentration.

One major revelation was the effect of reactive calcite present in the composition of the binder that revealed the possibility of Monocarbonate stabilisation as opposed to the formation of monosulphate during early hydration stages. With this finding, subsequent studies were also conducted

on the effect of the addition of reactive limestone to PC system [37]. With regard to SCM's, the effect of fly ash addition in combination with limestone was also studied that depicted the positive effect of calcite reactivity in an aluminium rich environment. Also, ternary blended systems in a combination of fly-ash, metakaolin and portland cement have been extensively studied to compute the optimized composition beneficial to set parameters and conditions[38].

Thermodynamic modelling of hydration phase assemblage for systems containing blast furnace slag has been studied to understand the consumption of portlandite along with hydrogarnet formations [39]. The subsequent effects of their activation reactivity with regard to alkali-activated systems were explored and substantiated the uptake of ions during hydration [40]. The substitution mechanisms with portland cement activation were also explored to observe the changes in Ca/Si ratio along with Al content's effect on the phase assemblage at ambient temperatures[41]. With regard to the effect of temperature, slag blended system in combination with CEM I, subjected to nuclear waste disposal temperatures were simulated across regimes spanning from 20°C to 80°C to observe the phase change evolution with increasing values of heat[42].

From the understanding of the benefits of thermodynamic modelling of cementitious systems, and the possibility to model slag blended systems to observe the hydration phase assemblage in relation to elevated curing temperatures is studied

3

Experimental Research Program

To observe the phase changes and understand the influence of the different parameters involved along with investigational case study, an experimental program was devised that could provide information necessary within the scope of the work.

The influence of slag replacement and its fineness in the case of custom blends along with industrial binders with comparable slag percentages as of custom blends was also investigated. For a comparative analysis CEM I, a neat binder was chosen as a reference mix.

The description of materials used and preparation of the specimens to stimulate high temperature at the core of the structural elements was discussed in sections 4.1 and 4.2 respectively. To instigate suitable environmental conditions for initiation of Internal Sulphate Attack, exposure conditions as described in section 4.3.

Before mixing, the commercial binders and pure slag admixture a quantitative chemical compositional analysis was conducted through XRF test to identify major oxides present along with minor impurities. Following the exposure period, subsequent testing was conducted on specimens to identify the mineralogical changes using TGA and XRD analysis. Pore structure evolution was studied through MIP tests and subsequent phases are visualised through SEM image analysis. The tests descriptions are discussion was section 4.4.

3.1. Materials

The study comprised of standard binder which was manufactured by ENCI cement factory, that were CEM I 52.5, chosen as the reference system, CEM II/B 52.5 and CEM III/A. Along with this, 4 different types of mixes were prepared by mixing CEM I 52.5 Portland cement with pure slag pozzolanas varying in their fineness by mill grinding provided by ECOCEM Pvt Ltd. Slag with varying percentage replacement with respect to PC was dry mixed using Hobart mixer following the standard protocol of 3 min for all mixes. Overview of the binders used, and their primary oxide compositions provided below in Table 3.1.

Table 3.1: Physical Properties of Commercial Binders.

Type	**Density** (kg/m^3)	**Fineness** (m^2/kg)
CEM I 52.5	3150	530
CEM II/B-S 52.5	3090	489
CEM III/A 52.5	3030	600
GGBFS	2890	410 and 610

3.2. Specimen Preparation

Micro-structural changes occur ideally in the system matrix and hence samples were prepared using neat binders with a constant w/c ratio of 0.45. The table below displays the different mixes prepared with varying percentage replacement levels slag in the case of laboratory prepared blended mixes along with industry provided ready mix samples. Slag present in the blended systems was prepared with 2 varying fineness, namely low fineness and fineness in comparison with alkali activator used, i.e. portland cement as given in Table 3.2 .

Table 3.2: Properties of Custom Blended Binders.

Specimen ID	**Slag %b.w.o.b**	**CEM I %**	**Fineness** (m^2/kg)
20C	20%	80%	410
20F	20%	80%	610
50C	50%	50%	410
50F	50%	50%	610

b.w.o.b – by weight of binder, C-coarse, F-fine

Stimulating environmental conditions and inducing supersaturation of cement matrix under laboratory conditions requires larger exposure times. Also, since the primary goal of the work was to observe hydration products' formation at the end of the exposure period, and not observing expansion data, small specimen sizes were adopted also keeping in mind the possibility of ion leaching. Paste studies were also chosen to eliminate any anomalies that might occur as a result of paste to aggregate interaction.

Thus, smaller circular disc specimens with 35 mm diameter and 5 $\pm$ 2 mm thickness were prepared by casting larger cylindrical specimens with the same diameter and subsequent cutting. The following steps were carried out for the preparation of the specimens.

Casting: Dry mixes of the binders were proportioned carefully in high accuracy weighing balance and mixed in the mixer for about 1 min. Following which, careful addition of water in proportion to the binder content was added and then mixed for 2 min before their transfer to the cylindrical mould (see figure 3.1. The prepared mixes were hand compacted using a small needle and sealed with polyethylene sheet to prevent moisture loss while curing. The moulds were also sealed externally and kept horizontally on a mechanical roller that was made in-house for a period of half an hour to prevent bleeding.

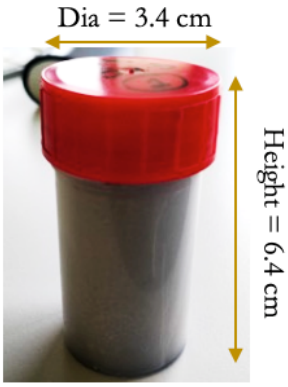

(a) Cast cylindrical moulds

(b) Sheet protection for 100% humidity

Figure 3.1: Cast specimens in cylindrical moulds.

Curing: As the study involves the effect of high-temperature curing, artificial increment in temperature was adopted to mimic the curing signature that normally occurs in precast industries and thereby scaled down to suit the specimen dimensions. Cast specimens were placed inside the controlled heating oven and humidity was maintained to 100 percent by sealing the moulds with polyethylene sheets and lids to create air-tightness. The temperature regime [21] thus used was also commonly reported in studies involving expansion experiments and the details are described below in Table 3.3:

Table 3.3: Temperature Signature.

Period	Temperature°C	Duration (hrs)
Immediately after Casting	20-25	3
Increase	90-100	10
Decrease	20-25	12

The specimens were kept in ambient laboratory temperature of 20 °C - 25 °C for 3 hours and then transferred to the oven where the temperature was observed to rise to 90 °C at the rate of 15°C per hour and maintained at 80°C for about 10 hours before taking out the moulds to cool down to 25 °C gradually. The specimens are kept at again room temperature for about 12 hours before demoulding and prior to exposure.

During the period of curing, the temperature was measured using a thermocouple embedded inside of the specimens and continuously noted to observe the temperature changes as shown in figure 3.2.

(a) Thermocouple

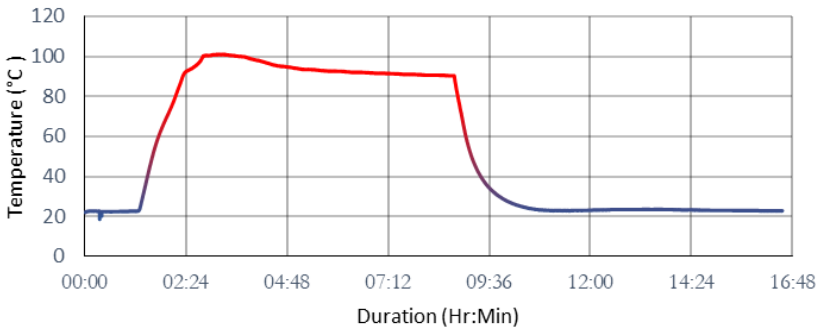

(b) Temperature Signature

Figure 3.2: Measured Temperature Profile.

Cutting: Following the curing period, the samples are demoulded. The larger cylinders were marked for thickness lengths and cut using high-speed equipment across the cross-section as seen in figure 3.3 . To ensure the influence of external moisture, non-water-based coolant was used, i.e. ethanol whole cutting. The cut discs were kept in individual containers and labelled according to their type of exposure.

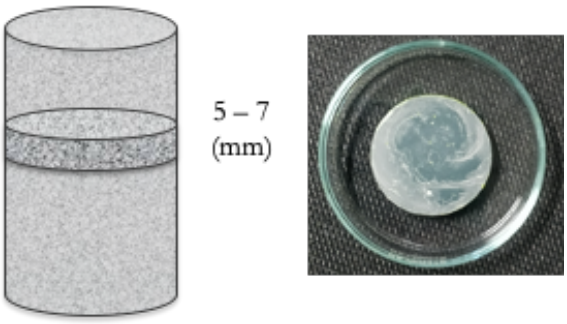

Figure 3.3: Cut dimension and shape of specimen after curing.

3.3. Stimulation of Environmental Conditions

Cast and cut specimens were organised and classified according to their type when they were transferred to airtight containers to prevent exposure to carbondioxide that could interfere with the hydration process. The specimens along with lime saturated solution were kept at an ambient temperature of 20°C throughout the exposure period as shown in figure 3.4 .

For stimulating supersaturation condition which was as studied from the literature review was one of the primary requirements for instigating DEF, the specimens were placed inside lime saturated solution in the containers. The volume of lime solution used was adopted to ensure sufficient saturation of the pore solution along with limiting leaching of ions that might cause negatively enhanced trigger by altering the pH of the pore solution. Thus, the volume of exposure fluid to Volume of solid of 2.5 was used[43]. Also, the solution was also renewed every 2 weeks to prevent over-saturation of the exposed solution.

Figure 3.4: Specimen stored in lime solution for exposure.

It was reported in earlier studies that the re-formation of ettringite in ordinary portland cement was detected at 45 days of exposure for concrete specimens and significant expansion was observed after 90 days for concrete specimens. In a recent study, slag blended systems also showed no considerable expansion i.e. it was less than 0.04 % at the end of 200 days[33]. This period of exposure where limited expansion occurs was indicated as the induction period and also where no swelling was prevalent. Hence, similar exposure duration was considered for the study. Also, given a reduction in specimen size the formation of ettringite was expected to be accelerated despite the shorter duration.

3.4. Tests Conducted

To monitor the microstructural changes and understand the phases assemblage due to high-temperature curing, testing intervals were adopted, where specimens were tested during the exposure period. The tests were conducted on specimens immediately after heat curing and after 90 days of exposure. Herein, the results corresponding to the period of immediately after curing will be indicated as **D-0** and the end of the exposure period as **D-90**. At each interval, the specimens were conditioned, and samples were prepared to suit different test methods during which meticulous care was taken to not damage the samples' microstructure. Procedure to prepare samples for various tests is described below:

Step 1:Hydration stoppage

The most important step prior to testing was to ensure that the specimens can be stored for an indefinite period adhering to unforeseen circumstances and also to prevent the influence of environmental conditions such as atmospheric moisture and CO_2 which might cause microstructural changes and affect the sample conditions. This was of utmost priority as the tests were conducted to be representative of the time of the specimens under study.

Several practices are present to stop hydration of specimens, the first step being the removal of physically bound moisture in the free pore solution. Different methods have been studied extensively for understanding the benefits and limitations of each method in terms of damage to microstructure. The commonly practised hydration stopping procedure was through drying techniques that ensure faster and efficient removal of free water present in capillary pores when done at

temperatures above 60°C. However, special crystals, specifically AFt was observed to decompose at temperatures even as low as 48°C, thereby losing valuable information of the system. Thus, after careful assessment of different alternative techniques to prevent decomposition of calcium sulpho-aluminate phases, which are highly sensitive to temperature changes, the most suitable method of Solvent Exchange procedure was carried out.

The specimens were air-dried after being taken out of exposure solution for few minutes and then again submerged in Isopropanol (IPA) solution for 2 weeks which enables almost all of the free water present was replaced by it. This was followed by a quick drying procedure, where the specimens were removed from the IPA solution and placed in 40°C oven for 10 hours, thereby removing the organic solvent to evaporate from the system. Specimens were taken out of the oven were placed in desiccators before test specific sample preparation to prevent exposure to environment over silica gel spheres, which were then frequently renewed.

Step 2: Sample Preparation

The specimens having undergone hydration stoppage was thus subjected to different exercises to obtain samples to suit different tests conducted for analysis. For TGA and XRD analysis, the sample for interpretation comprises of powdered particles obtained from the conditioned specimens. It was understood from the literature that specific crystals were sensitive to physical impact due to friction and abrasion practices, again ettringite crystals were identified to be damaged. Thus, the physical crushing of specimens was avoided, and a mechanical vibrator for 40 seconds was used to obtain the powders. For Image analysis, polished sections were prepared after epoxy impregnating the face of the specimen. To measure the pore size distribution of specimens, chunks samples were prepared with little pressure to break the specimen.

Since the study aims at understanding the influence of parameters in cement blends through comparison, the same procedure and techniques for all the specimens were ensured. For instance, the sample weight for the TGA test was controlled to have a difference of about ± 0.002 g for all specimens.

3.4.1. pH Test

The alkalinity of the pore solution was indicative of its ionic concentration experienced during exposure to a saturated environment. When the specimens were stored in a neutral environment such as distilled water for a stipulated period, there occurs an ionic concentration gradient between the pore solution inside and the exposed solution. This results in leaching of ions to obtain equilibrium condition. Based on the concentration, the alkalinity of the pore solution was representatively determined.

The cast, cured and cut disc of each specimen type was placed inside a tightly sealed container with de-ionised water. pH measurements were carried out using an electrode that comprises of an electrolyte usually made up of KCl solution, and connected to a microchip. When the electrode was placed inside the solution to be measured, and as the current was passed through the electrode

charging it with negative electron charge, it attracts the Hydrogen ions (H+) towards it. This was measured in terms of voltage which was then processed by the chip to compute the pH value using the Nernst Equation is given below:

$$E = E_0 + (0.591 * pH_{sample}) \tag{3.1}$$

E- Measured Voltage , E_0 *- Standard Voltage*

From the measured pH values , interpretation of the alkalinity was done and correlated with the phase changes occurring during exposure.

3.4.2. Thermal Gravimetric Analysis

Thermogravimetric Analysis (TGA) is a test procedure that involves continuous measurement of dynamic loss of mass when the sample is heated at a constant rate under inert environment usually nitrogen atmosphere. The information of different phases present in the sample under analysis was obtained based on the basic principle of phase decomposition at characteristic temperatures along with loss of bond water through dehydration. Although there might occur some overlap of decomposition temperature for different phases, the predominant phases observed are tabulated below in the Table 3.4.

Table 3.4: Phase Decomposition Temperatures.

Temperature range °C	Phase Decomposition
20-415	CSH-Loss of Bound water
80-300	Sulpho-aluminates
420-550	$Ca(OH)_2$

Powdered samples were measured and placed inside a special crucible that has been priory calibrated for the temperature range and rate of increase for all the specimens. The crucible with the sample was placed in a holder with a weight loss measuring sensor attached at the bottom. The sample was then enclosed by a hood that purges nitrogen atmosphere in order to provide an inert environment while temperature changes occur. Since the interest in the observation of carbonation and subsequent phase analysis is beyond the scope of this research, the temperature range used for TGA test was between 40°C to 700°C increasing at a rate of 10°C/min.

To analyse the TGA data, 2 different techniques were adopted. The primary requirement to identify characteristic temperatures where the transitioning of phases onsets was conducted. Following which, observation with respect to mass loss was investigated at intervals of temperature ranges corresponding to determined phase decomposition peaks from derivative of TGA curves.

Further, to identify the decomposing phases and their association with peak temperatures, Derivative Thermogravimetric (DTG) results were obtained that was measured as the derivative of mass change over thermal changes i.e. dm/dt. The DTG thermogram can show the peaks generated thereby providing information on transformations that have occurred, in this case, decomposition of phases.

3.4.3. Mercury intrusion Porosimetry

Mercury intrusion Porosimetry (MIP) is a technique adopted to visualise the distribution of pores present in the specimen tested through representative samples. It works on the principle by which the empty pores were filled with non-wetting liquid, preferably mercury under pressurised conditions, subsequently measuring the volume of pores filled corresponding to the diameter size of the pore measured in micron meters. The relation between pressure applied and corresponding fill of pore sizes is given by Washburn's relation as follows [44]:

$$P_c = \frac{-4\gamma \cos(\theta)}{d} \tag{3.2}$$

P - pressure,γ - surface tension of liquid,θ - contact angle of liquid, d – pore diameter

Samples prepared after hydration stoppage procedure were placed inside penetrometer, sealed with a lid and the mass of the entire assemble was measured. The procedure to measure the porosity comprised of two steps, the low-pressure run, where the mercury was filled up inside the penetrant up unit atmospheric pressure where larger pore sizes falling around capillary diameters were filled. This was followed by a high-pressure run, where the pressure inside was raised up to as high as 400 Mpa filling up smaller pore sizes of the sample covering gel pore diameters. The instrument used was designed to measure the pore size range of 4 nm to 400 μm.

All accessible pores were filled by the mercury through induced pressurising and pores seizes smaller than 4 nm was not accounted. The entry pore diameter was the information that was recorded and not the actual size of the inner pores. The data that was recorded at each pressure step increase was stored by inbuilt software in term of differential intrusion volume for each corresponding pore diameter. Thus, characterisation of the specimen in terms of the pore size distribution (PSD) and total porosity was measured. Breakthrough pore diameter (Øth)and characteristic diameters that provide insight on the durability of the specimen was also subsequently measured.

3.4.4. X-Ray Diffraction Technique

Cement systems contain hydrate phases which may be amorphous or crystalline in nature. One of the popular methods to identify the phase composition was through identification of the crystal structures which are characteristic of crystallographic planes. These planes depict the way in which the atoms are arranged in the crystal and demonstrate subsequent properties. Few such arrangements are indicated by cell names such as cubical, hexagonal etc.

The atoms present in such a specified arrangement may act as an obstacle for an incoming electromagnetic wave if and only if its wavelength matches that of the size of the obstacle. The phenomenon was known, and diffraction and the principle wave used in this method is X-Rays, and thus the term X-Ray Diffraction (XRD). Thus, the diffracted waves are thus captured by sensors representative of the specific crystal structure providing the information of the phases present. The intensity along with the interference of the diffracted peak is therein characteristic of lattice spacing of the crystal structure whose relation is given by Bragg's Equation below.

$$n\lambda = 2d\sin(\theta) \tag{3.3}$$

n – *whole number*, λ *-incoming wavelength*,θ *-diffraction angle*, d – *lattice distance*

Powdered samples were compressed onto a surface of the holder and flatness was ensured in order to enable maximum diffraction intensity without dispersion. The wave source was directed in such a way that it scans over an angle of 180 °C with the x-rays covering the plane of the sample at each incident angle. The diffracting ray was then captured by a detector that was also set in motion so as to capture the waves at different angles. The detector measures the intensity of the wave along with the angle at which it was diffracted. This information was then correlated by Brag's equation providing different phase patterns with intensity and angle of diffraction in y-axis and x-axis respectively.

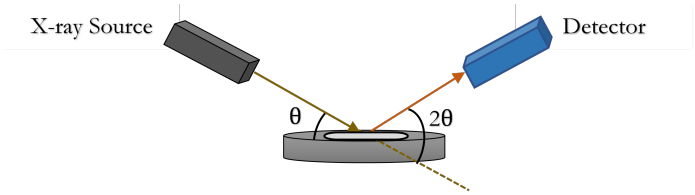

Figure 3.5: XRD Schematic.

The phase patterns were qualitatively analysed to identify their existences in the samples using Xpert High score plus software. A background noise cancellation followed by a refinement scheme was applied to identify the dominant peaks present. Following which, peak search was performed by adopting External standards technique to identify the crystal and amorphous phases present. The idea behind it is matching the lattice distance of crystal structures given in the database to the computed d value from the test's diffraction angle.

3.4.5. Scanning Electron Microscopy

The composition of the hydrated cement paste system is characteristic of different elements which have atoms that interact with electrons coming from a beam source. When an electron from the source comes in contact with electrons present in the different energy shells of the atoms, the repulsion pushes the incoming electron away from the nucleus. This deflected electron is known as Back Scattered Electron. It is then captured by a moving detector, that measures the intensity coming from specific locations and processed to produce a grayscale image.

When the same electron sources when shot at a specific interaction area or spot with a voltage high enough to knock out an electron from the atom's shell, another electron from the outer shell falls to replace the lost electron for stabilisation. This stabilisation occurs with loss of energy, that is released in the form of characteristic X-rays for different elements. The signals were also captured by the detector measuring its intensity and processes it to provide information on the elements present (see figure 3.6):

Polished sections were prepared for the specimen to be observed and placed inside the chamber of the machine. Vacuum environment is made by the use of pumping system in order to prevent interaction of incoming electron beam with moisture and other particles in the chamber.

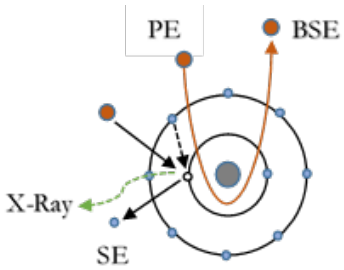

Figure 3.6: SEM Schematic.

Optimum working distance and spot size, along with voltage of incoming beam is set and at adjusted magnification backs scattered images were obtained. For elemental analysis , electron beams were focused at selected point of interaction were of interest and outgoing x-rays were detected.

The intensity of the micro-graphs obtained were representative of atomic densities corresponding to different phases present in the specimen under observation. Heavier elements, i.e. with high atomic number tend to scatter more electrons upon interaction and reflects a brighter gray scale of image, while the lighter elements appear to have darker intensity. Combining the observations through micro-graphs and micro-analysis for elemental composition conclusions were made.

The described tests were conducted systematically and the results were presented in chapter 5.

4

Thermodynamic Modelling Research Program

4.1. Fundamentals

Thermodynamic equilibrium computation enables the prediction of stable solid phases in an aqueous environment that may exist under given environmental conditions such as temperature, and pressure. The reactions are characterized by the component's standard parameters namely solubility, entropy and enthalpy that enable formation in a given system. Such information is compiled through chemical experiments are said to be constitute thermodynamic data base.

In order to attain the thermodynamic equilibrium state two primary methods can be adopted and incorporated in geo-chemical modelling programs as below[45]:

1. **Mass Balancing Law**: that states the apparent conservation of mass of the component that may enter and react in the given system. The information for mass balance is obtained through reactivity of the solids in the solution along with equilibrium co-efficient often denoted as K. The balancing of the equations is computed through iterative procedures following Newton-Raphson steps.

2. **Gibbs Free Energy minimization** : that provides information on the minimum amount of energy required in order for the components to react at the given temperature and pressure. It's given by the expression as below:

$$\Delta G^{O} = \Sigma \gamma_i \Delta G^{0} = -RT(lnK) \tag{4.1}$$

Δ G$^{\circ}$ *refers to Gibbs minimisation energy* , γ *– stoichiometric co-efficient, R gas constant, K –mass action constant, T –temperature*

In the current modelling tool (GEMS), the Gibbs free minimisation energy principle is used primarily because no prior information and subsequent assumptions have to be declared during calculation of equilibrium for the phases present. The method therefore adopted by GEMS is that it computes all possible combinations of phases that can be formed based on stoichiometric mass balancing along with charge equilibrium state every step primarily driven by the Gibbs free energy expression of the compounds in reaction and formation.

Since thermodynamic properties of solids and aqueous species vary with temperature considerably, these parameters are also taken into account in the tool for the reactions. The temperature dependence is given by the equation for solubility constants (KT) as 3-term approximation[46].

$$logK_t = (0.4343/R) * ((\Delta S_T{}^0_0) - (1 - lnT_0) * \Delta_r C_P^o - \frac{\Delta_r H_T^0 - T_0 C_P^0}{T}) + lnT_0 \Delta_r C_p^0) \quad (4.2)$$

Δ Cp,To : Heat capacity at standard temperature, Δ S – Entropy , Δ H- Enthalpy and To is standard temperature =25 C

4.2. Modelling Strategy

4.2.1. Characterisation of Binders Used

The composition of the different industrial binders as obtained and studied in chapter 6.1 is used as the primary input for the modelling tool to observe the subsequent phase changes predicted through simulation.

In the case of CEM I 52.5, bogue composition was calculated to obtain the four main clinker phases along with minor oxides were included in the modelling. Since the effect of oxide composition and clinker phases are comparable, the later was used for neat portland system, while the former was used for slag blended systems such as CEM II/B-S and CEM III/A. The oxide composition for slag present in them is computed relative to the percentage of slag present in the overall constituents.

4.2.2. Hydration Model

In order to observe the phase change of the predefined composition of binder systems, a degree of hydration for the clinkers was assumed to occur as a dissolution and precipitation mechanism. This approach was studied and recorded by Parrot and Kiloh, and was used in the model.

The model describes the hydration process with a set of empirical equations that considers the lowest value for hydration rate among the different clinkers as the dependent rate step. For oxide hydration degree the lowest rate corresponding to CEM I 52.5 clinkers is used in the case of portland cement part in slag blended system. The set of equations are described below[47]:

$$(Nucleation)R_T = \frac{K1}{N1} * (1 - \alpha_t) * (-ln(1 - \alpha_t))^{(1-N1)} \quad (4.3)$$

$$(Difusion)R_T = \frac{K1 * ((1 - \alpha_t)^{\cdot 6})}{1 - (1 - \alpha_t)^{\cdot 3}} \quad (4.4)$$

$$(HydrationShell)R_T = K3 * (1 - \alpha_t)^{N3} \quad (4.5)$$

Where Rt is the rate of hydration, α is degree of hydration, K,N are constants obtained by Parrot.

For hydration degree of slag oxides[αt], an empirical expression obtained by previous researchers that accounts for the surface area as well as temperature is given below[41]:

$$\alpha_t = ([A * lnT] + B) * S_{sg} * \exp\frac{-E_{sg}}{R} * (\frac{1}{T} - \frac{1}{T_o}) \quad (4.6)$$

where,

$$A = -0.16 * \%Slag + 12.81 \quad (4.7)$$

$$B = 0.33 * \%Slag + 4.30; S_{sg} - Surfacearea, E_{sg} - ActivationEnergy \quad (4.8)$$

4.2.3. Database

Thermodynamic modelling requires solubility data that comprises of standard entropy, enthalpy and activity constants in order to compute geochemical equilibrium reactions. These data have been obtained through experimental work over the past few decades and are available in open source data base sets for specific materials. Specific data sets for cementitious systems comprising of phases such as hydrogarnets, ettringite, portlandite and CSH gel have been compiled and given in software friendly formats for computations. The data base thus used for the simulations is present under the title cemdata07 containing data for several cement phases which have been critically reviewed and corrected in earlier studies [37].

Data for Higher Temperatures:

The thermodynamic data for solubility at higher temperatures can either be experimentally measured or can be computed empirically using interpolation with existing temperature measurements. The second method is adopted in the GEMS tool, which uses the apparent Gibbs free energy measured at standard temperature (25°C) , to compute for higher temperatures[46]. The computation is discussed in detailed in Damidot et al and is out of the scope of this current research.

Following the principle and strategy described in this section, and with the tool (GEMS), thermodynamic modelling simulations are obtained and discussed in chapter 5

5

Results and Discussion

5.1. Characterisation

Preliminary characterisation of the binders involved in the industrial mix as well as the custom mix was done to understand the influences of oxide compositions. XRF technique was adopted to identify the primary oxides present in the dry mixes and normalised by weight to 100% and given below in 5.1 and 5.2. A detailed composition and properties are given in Appendix B.

Table 5.1: Oxide Composition of Industrial Binders.

Oxides	CEM I 52.5	CEM II/A-S 52.5	CEM III/A 52.5	GGBFS
CaO	65.96	59.50	48.64	37.63
SiO_2	19.65	22.64	27.78	34.51
Al_2O_3	4.25	6.38	9.70	14.04
SO_3	2.84	2.85	3.64	1.60
Fe_2O_3	2.78	2.25	1.40	0.04
MgO	2.22	3.85	2.63	9.80

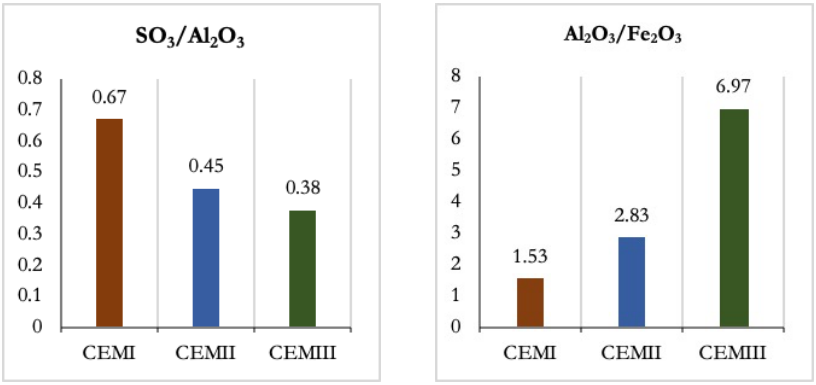

Figure 5.1: Molar Oxide Ratio for Industrial Blends.

Through the extensive literature study, it is clear that the bogue composition of the paste matrix plays an important role in predicting possible expansion characteristics. Reflecting on the individual oxide influences, the following inferences were derived.

Industrial Blended Systems

The amount of alumina and sulphite present in the reference system, (i.e.) in CEM I cement, reflects ratio higher than 0.5. This is depicted to have an impact decomposition of AFt formed during early hydrations along with excess AFt present as a residue after heat curing. In the case of slag blended industrial mixes (i.e.) CEM II/B-S and CEM III/A, the amount of alumina present is considerably higher with respect to sulphate. Although one should consider that, the amount of alumina available for sulpho-aluminate products could be much lower due to the presence of slag, in turn, increases the ratio of SO_3/Al_2O_3. Therefore, the influence of lower availability of alumina actually indicates the lack of ettringite present during early stages of heat curing. Also, it is important to note that the amount of magnesia present in CEM III/A cement indicates the possibility of hydrotalcite formation from the available carbonates from polymers, both during temperature curing as well as during subsequent storage in a lime solution. This would reflect on further reduction of available alumina present during heated hydration as well as during curing under room temperature to directly contribute to alumina bearing phase formation[4]. Hence, comparing Alumina to Ferrite ratio, CEM III/A depicting higher value would thus result in lower formations of sulpho-aluminate phases relative to a lower ratio in the case of portland cement.

Table 5.2: Oxide Composition of Custom binders.

Oxides	20C & 20F	50C & 50F
CaO	43.30	51.80
SiO_2	31.54	27.08
Al_2O_3	12.09	9.15
SO_3	1.83	2.21
Fe_2O_3	0.82	1.5
MgO	7.94	5.8

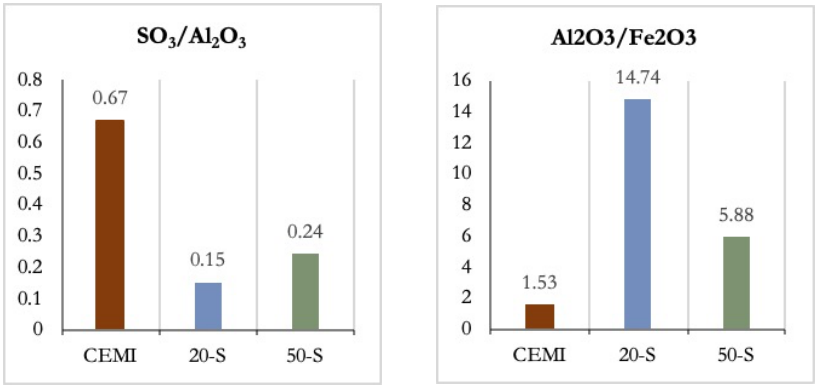

Figure 5.2: Molar Oxide Ratio for Custom Blends.

Custom Blended Systems

In the case of custom mixes, the sulphate to aluminate ratio is considerably lower in comparison with CEM I, which is justified by the replacement of neat clinker by slag, which would increase the amount of alumina present, with a majority of coming from the former. However, with higher percentage levels of replacement (i.e.) for 50C and 50F mixes, the ratio is much noticeably higher, indicating enough pessimum value of about 0.25, as previously reported by Khelam, [21]for ettringite to be present and subsequently decompose at elevated curing temperatures. In both mixes, the amount of magnesia is considerably higher in comparison with the reference system, that increases the possibility of hydrotalcite formations resulting in lower alumina present for sulpho-aluminate phases.

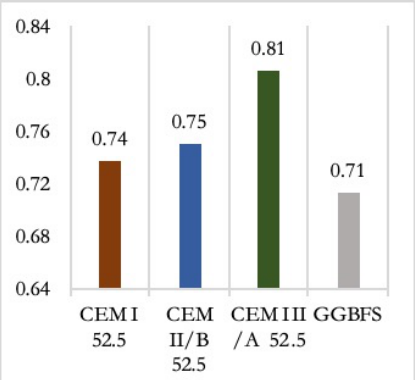

Figure 5.3: Alkalinity of the binders.

The **alkalinity** of the binders is calculated using the equation given below in terms of sodium oxide equivalence per 100 g by weight [19].

$$Na_2O_{eq} = Na_2O + (0.658 * K_2O) \tag{5.1}$$

From the values, it can be understood that even at a higher percentage of slag composition in the case of CEM III/A system, higher alkalinity was seen as computed. However, in the following section where specimens undergoing leaching and subsequent pH measurements, the alkalinity computed did not appear to translate in the former in the case of high fineness systems. This influence is further discussed in Section 5.2

It is thus important to carefully assess the formations of sulpho-aluminate phases during exposure, as alkalinity reflects the favourable pH conditions for their formations. Also, due to comparable values of alkalinity for CEM I systems and pure slag, the alkalinity for custom-blended systems were in similar ranges.

Carbonate Influence

Since the oxide composition of slag systems infer lower sulphate ratios, it indicated the possibility of carbo-aluminate formations upon exposure to a saturated environment that bypasses the ettringite phases. Thus, the presence of carbonate in unhydrated binders was measured using TGA –Mass spectrometry technique that measures the intensity of evolved molecular elements such as sulphates and carbon dioxide with corresponding mass loss. The results are shown in figure 5.5 and 5.7.

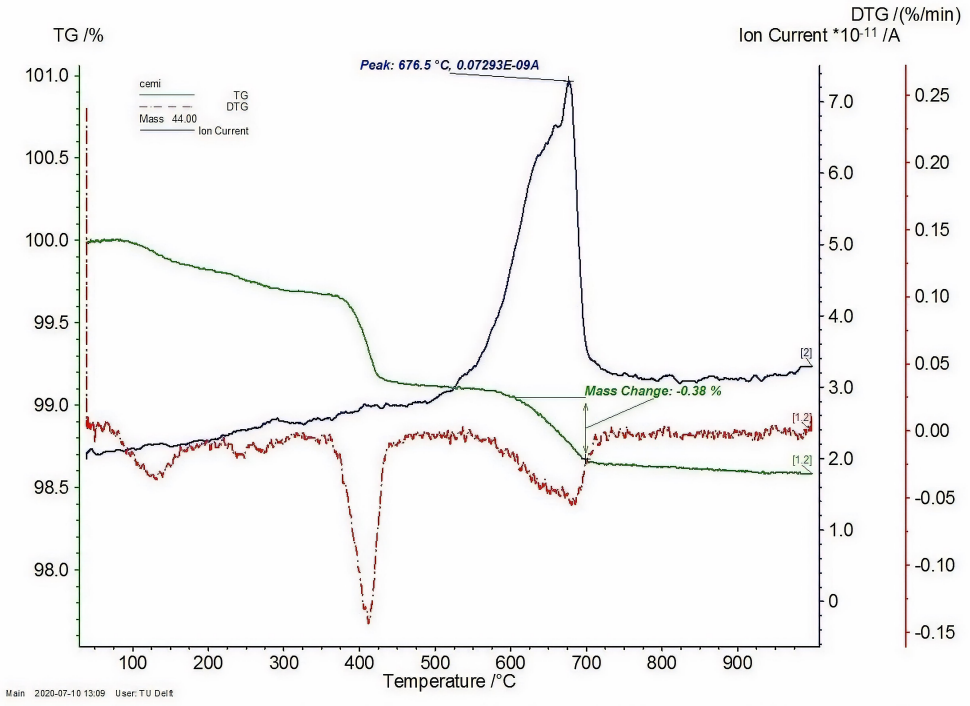

Figure 5.4: CEM I gas spectrometery.

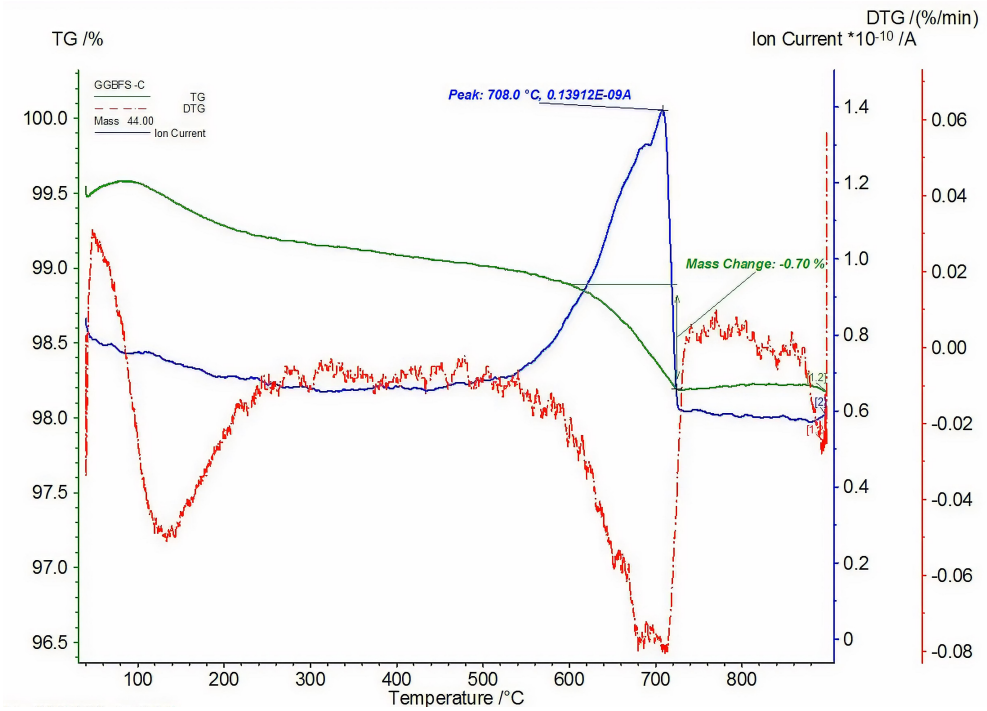

Figure 5.5: Pure Slag gas spectrometry.

The mass spectrometry graphs appear to considerably overlap with the thermal mass loss data indicating that characteristic temperature close to 700 °C indeed correspond to carbonate species such as calcite and vaterite being present in the binders. Thus, TG analysis was performed for the slag binder mixes.

Figure 5.6: CEM II/B-S Thermal Analysis.

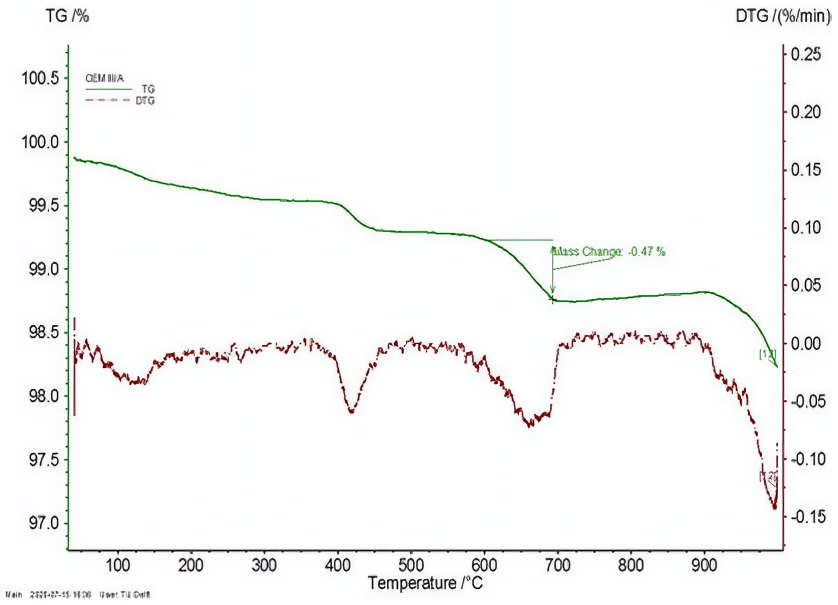

Figure 5.7: CEM III/A Thermal Analysis.

As observed from the thermographs (fig 5.7), CEM I, the neat system showed a lower percentage of mass loss at about 0.4 % and for pure slag system, the mass loss was almost double at about 0.8 %. It is therefore evident that the presence of carbon, possibly from calcite and limestone present in the clinker, at a percentage higher than 0.4 could promote significant elimination of sulpho-aluminate formations, primarily in combination with sulphate to aluminate ratio less than 0.5, depicted in the case of all slag blended systems[48]. However, in the case of CEM II/B-S system, despite lower percentage of carbonate mass loss, due to the presence of increased Al_2O_3/Fe_2O_3 ratio, its subsequent effect on carbo-aluminate formation is predicted.

5.2. pH Measurement

Specimens exposed to saturated environments undergo phases changes which were considerably influenced by nature and characteristics of pore solution which acts as either a buffer or catalyst to enable crystal formations. The key ingredient contributed by pore solution is the ions present as a result of dissolution from existing hydrates present in the cement matrix. The dissolution is triggered to achieve thermodynamic equilibrium, the ions thereby present in the pore solution either increase or decrease the alkalinity of the systems. This alkalinity therein influences the nature of ionic interactions which later enable the formation of new hydrates in the cement base. Change in the pH environment was monitored at different intervals and are shown in figure 5.8.

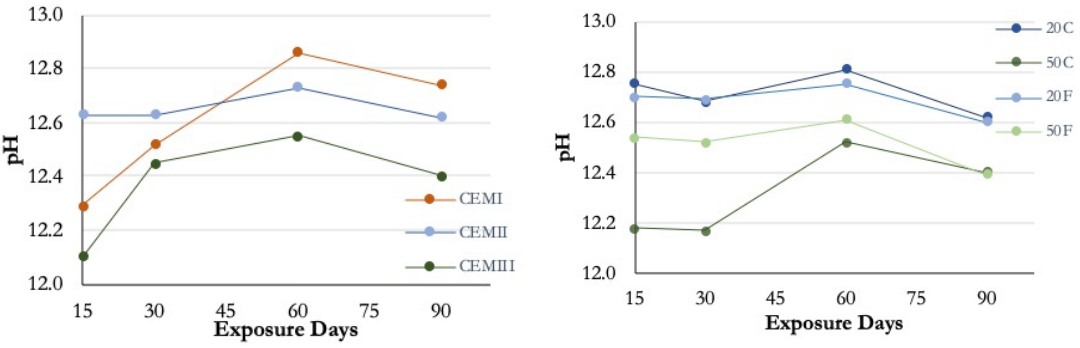

(a) Industrial Binders

(b) Custom Blended binders

Figure 5.8: pH Measured during Exposure.

At the start of the measurement, 15 days after curing, the alkalinity of CEM I neat system was at the lower ranges. The difference could be indicative of higher quantities of sulphate ions that could have gone into the pore solution decreasing the alkalinity momentarily. Since the amount of sulphate is relatively lower in composition as observed for the slag systems, the above effect is negligible for the same however was observed only in the case of CEM II/B-S system. For CEM III/A, despite having high alkali content, the effect of temperature is suspected to have instigated the formation of hydrogarnet species formation, which increases the alkali uptake intensity [49]. Thus, this justifies lower pH reading during the early stage of measurement.

Alkalinity measured at the beginning of exposure for slag systems showed higher values i.e. above 12.6 for CEM II/B-S system as well as low percentage slag custom blends (20C and 20F). With a higher composition of slag in the case of 50% slag substitution and CEM III/A system, alkalinity was relatively lower for the reason mentioned above.

The effect of slag fineness on the alkalinity is more prominent only in the case of high substitution i.e. for 50C and 50F custom blends, a reflection of which could have increased the consumption of portlandite and subsequent uptake of Na and/or K ions to form C-Na/K-S-H and in turn reducing the hydroxyl content in pore solution[50]. This effect is minimized for lower substitution levels as a result of an excess of clinker composition present.

Measurements taken in the following intervals revealed an increase in alkalinity, that could be associated with the consumption of sulphate ions for subsequent formation of sulpho-aluminates

during exposure. Result of which is apparently was recorded to be higher than that of slag systems.

Measurements taken thereafter showed minor differences in the case of systems with 20% slag composition, for both industrial blend (CEM II/B-S) as well as custom mixes. Blended systems with high fineness i.e. about 600 m2/kg, along with 50% slag composition showed a clear increase in alkalinity. This could be associated with increased alkalinity as measured for CEM III/A system, also in closer ranges for 50% custom blended system that during exposure lead to leaching of adsorbed alkali ions. The increase is noticeable in the case finer slag system with 50% composition (50F and CEM III/A) due to increased consumption during elevated temperature curing as a result of increased reactivity.

It has been reported that the pH values corresponding to the alkalinity present at the range of 11-13 in the pore solution, favours the suitable thermodynamic environment for the formation of sulpho-aluminate phases, more specifically delayed ettringite formations. As the observed pH values were well within the range, calcium-aluminate crystal formations were expected during the exposure period. In the upcoming chapters, this has been therefore verified.

5.3. Mineralogical Changes

5.3.1. Thermogravimetric Analysis

Thermal analysis conducted on samples immediately after high temperature curing to observe the phases present in the specimens. Since high temperature curing predominantly affects calcium sulpho aluminate phases, the range of decomposition temperatures of 90 °C to 300 °C was studied, along with portlandite presence due to possible consumption by slag in the replacement with Portland cement content.

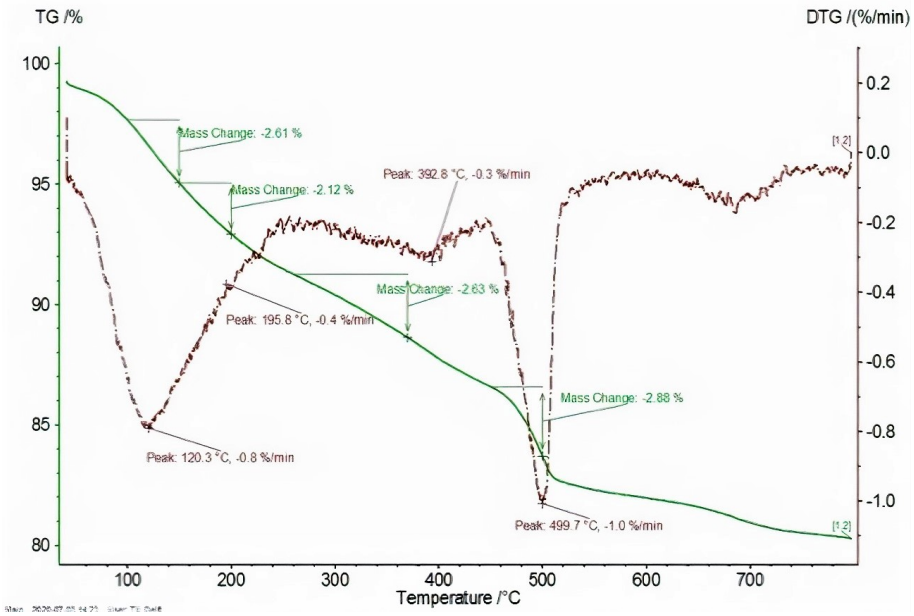

Figure 5.9: Characteristic Peak and Mass loss%.

The first peak observed at 120 °C (see figure 5.9), corresponds to the predominant decomposition of ettringite and some minor quantities of CSH gel phases along with other sulpho-aluminates. This peak is followed by a significant endothermic heat loss as a result of bound water in the portlandite phase at a range between 450°C and 500°C. In the case of systems with a considerable amount of magnesium oxide present, another distinct peak at between 300°C and 400°C corresponding to hydrotalcite phases was also observed.

Prior To Lime Solution Exposure

The DTG curves for the samples tested immediately after curing to identify the characteristic peaks as seen in figure 5.10. The endothermic peak appeared to be closely overlapping for all the systems studied, thereby indicating no differentiation in the measurements with regard to peak shift at characteristic temperatures. The peak corresponding to the temperature of 120 °C, was observed to be lying in close limits, with negligible difference between the industrial mixes as well as in the case of custom mixes. No difference in the peaks is an indication of the total decomposition of almost all available ettringite phases that could have formed initially and thus it can be understood that the peak primarily corresponds to the C-S-H and C-A-S-H gel formation for neat system and slag systems respectively.

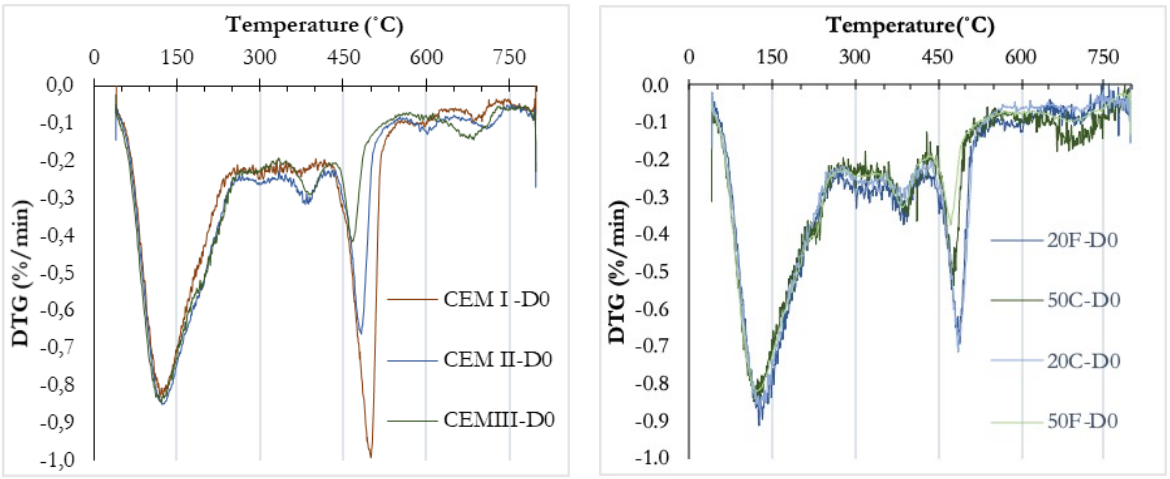

Figure 5.10: Thermograms Measured Before Exposure to Lime solution.

A clear decrease in peak intensity at a temperature around 500 °C was observed, which is justified by the consumption of portlandite with a corresponding increase in slag composition. This difference was observed to be consistent in both industrial blends as well as custom mixes. Also, an interesting observation is noted with regard to portlandite peaks between slag concentration of different fineness levels. The difference though insignificant at lower replacement (20%), it shows an evidently smaller peak for finer slag concentration at higher replacement level i.e. at 50%. This supports the theory that, with an increase in replacement level, the effect of fineness is dominant on the degree of hydration that is responsible for the consumption of portlandite by slag particles amplified by the increased availability of slag grain's reactive surface.

In the case of slag systems, owing to high quantities of magnesia present in comparison with CEM I, neat system, significant peak at the temperature range between 350˚C and 400 ˚C is observed,

that corresponds to hydrotalcite phase. Also, a small but visible peak was observed in the range of 650 °C to 700° C, indicating the presence of carbonates in the case of slag systems, especially for higher replacement level (50%).

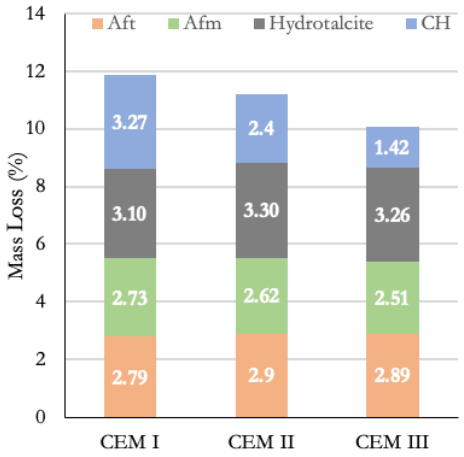

Figure 5.11: Mass loss percentage for Industry Blends.

In order to quantitatively compare the extent of decomposing phases while performing thermal analysis, mass loss percentages by weight of the measured sample were calculated and shown in figure 5.11 and 5.16. From the widely and repetitively reported decomposing temperature ranges corresponding to each hydration products[51], the mass loss percentage is computed from thereby obtained TG curve. Thereby percentages were obtained for all the samples and are graphically represented in figure 5.11.

From observing the mass loss at the interval of 450°C to 500°C, which is reported to be temperature range corresponding to a total loss of Portlandite, it is evident that there is a considerable decrease in the amount of Portlandite present with an increase in slag content, owing to the replacement levels in comparison with neat CEM I mix. This supports the primary reason being the consumption of CH during hydration by slag minerals through secondary hydration.

Drawing a comparison within the slag blended systems in both, industry mix as well as custom mixes, despite a higher percentage of slag in CEM III/A, 50C and 50F, no significant difference in the mass loss at temperature range corresponding to ettringite phase was observed. It must be noted that since the silicate hydrate phases such as C-A-S-H and C-S-H also decompose in the same temperature range, the values computed could be representative of the same. Therefore, the mass loss in the calculated temperature range may not be directly indicative AFt.Hence, an increased amount of mass loss for the slag blended systems is justified as consumption of portlandite which in turn directs to the increased content of C-A-S-H phases, whereas in the case of CEM I system, the hydrogarnet phases were absent, reflecting on smaller mass loss is observed.

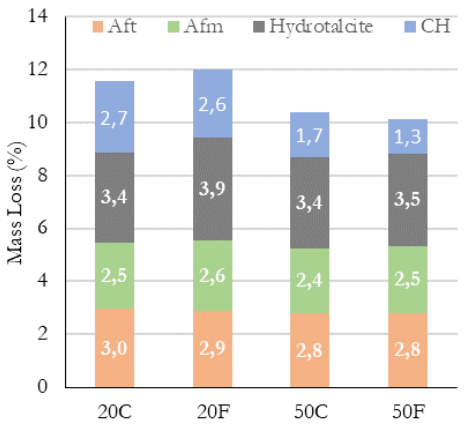

Figure 5.12: Mass loss% for Custom Blends.

Observing and comparing custom-blended slag mixes with neat CEM I cement type (figure 5.16), there is a significant reduction in the mass loss value of Portlandite, again supported by its consumption by slag during hydration. As a result of increased fineness of slag that would reflect on its increased reactivity, it was expected that a lower amount of portlandite content would be observed in the case of 20F and 50F mixes. However, on the contrary, the amount of portlandite depicted little difference in the case of high fineness slag blends, which could be associated with the agglomeration effect of slag

particles even at high temperatures, that restricts its reaction with portlandite[33].

Here again, the presence of hydrogarnet phases, through mass loss at 120 C is observed without much difference between different fineness levels of slag. This results partly contradicts earlier studies that have indicated the influence of slag fineness in comparison with binding clinker. According to it, the increased reactivity of high fineness slag is associated with heterogeneous nucleation characteristic, that enables accelerated phase formation of C-A-S-H gel, despite being kinetically slow reaction under conventional conditions[52].In the case of 20% slag system, its impact appears to be minimised due to the effect of high Al_2O_3/Fe_2O_3 ratio, due to which binding capacity of alumina towards the magnesia is increased. This is also confirmed by higher mass loss for hydrotalcite phase.

However, this effect was not seen in the case of 50% slag system, i.e despite increased slag composition, a similar amount of C-A-S-H was observed. This could be possibly due to dilution effect that causes lowering of degree of hydration in high fineness slag along with a smaller ratio of Al_2O_3/Fe_2O_3.

Presence of AFm content was computed showing minor differences within slag blended systems. The presence of AFm phase indicates two possible reasons. One, the ettringite formed during hydration would have decomposed during high-temperature curing forming the more stable AFm, and the other, the direct formation due to insufficient sulphates present in the systems during early hydration stage. With respect to CEM I, higher sulphate to aluminate ratio is indicative of the increased formation of ettringite during early hydration and subsequent decomposition to monosulphate. Thus, indicating the above stated first possibility. Also, the mass loss value was above that of slag systems, clearly indicating a larger amount of early ettringite that was formed and decomposed to form AFm, owing to higher SO_3 ratio.

In the case of CEM II/B-S and CEM III/A systems as well as for custom blends with slag, higher AFm mass loss with respect to reference system than expected, could be attributed to the initial availability of aluminates required for the formation of ettringite in the early stages of hydration was consumed by a significant amount of Magnesia present in the system leading to the formation of hydrotalcite and hydrogarnet phases. This is again supported by the increase in mass loss percentage corresponding to its characteristic temperature for hydrotalcite species. Thereby, supporting the second possibility for the presence of AFm.

After Exposure

The microstructural phase changes were subsequently monitored after 90 days after the commencement of exposure, with the requirement to observe sign of delayed ettringite formation, which would further be supported by XRD and image analysis.

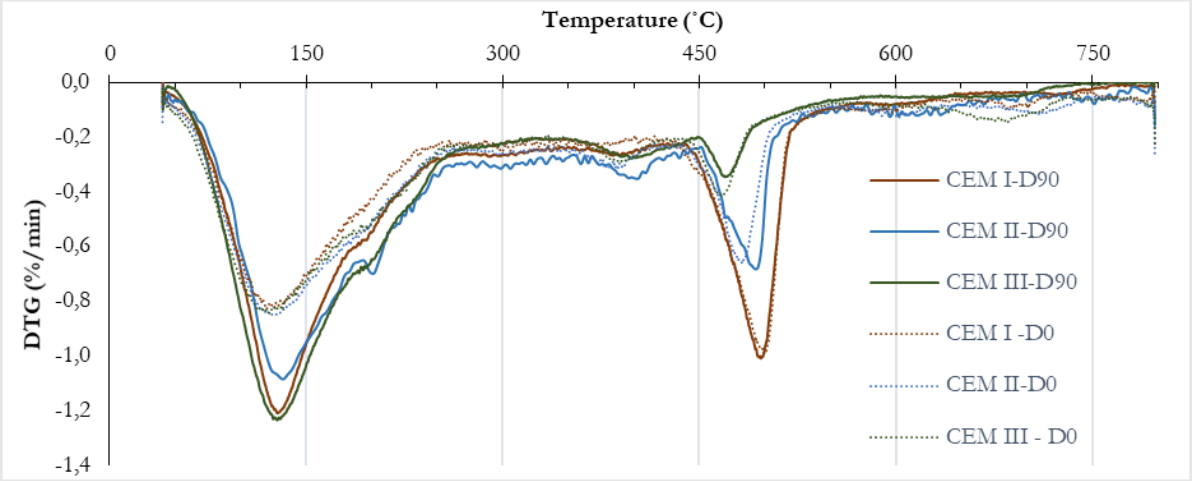

Figure 5.13: DTG curve Comparison for Industry Blends.

Observation from the DTG curve and the correspondingly computed mass loss shows an increase in peaks at 120°C (See figure 5.13 and 5.14. The increase could be associated with ettringite formation in the case of CEM I system as the possibility of C-A-S-H formation is negligible due to significantly lower Al_2O_3/Fe_2O_3 ratio, along with higher SO_3/Al_2O_3 ratio that promotes ettringite formation. This change is also demonstrated in high mass loss difference before and after exposure.

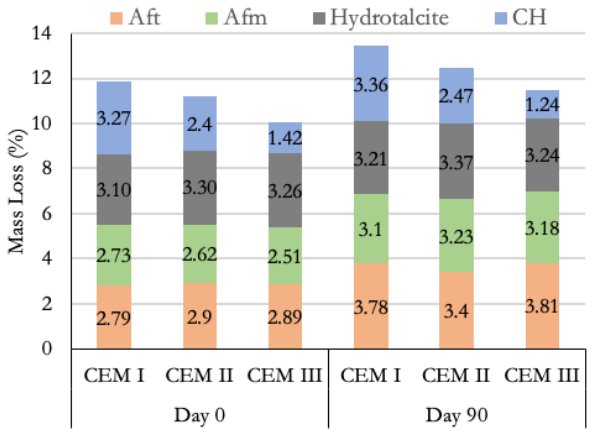

Figure 5.14: Mass loss% for Custom Blends.

On the other hand, slag systems' 120°C peak, mainly for 50% composition(CEM III/A ,50C and50F) (see fig 5.15) , have a higher potential to correspond to hydrogarnet formations due to reduced sulphate ratio along with an increased binding capacity of alumina to form hydrotalcite phases. The contribution of ettringite to the increase in peaks is therefore expected to be minuscule.

For CEM II/B-S system as well as in a custom-blended system with 20% slag, the effect of both ettringite formation, as well as the trivial formation of C-A-S-H, is observed with its increase in peak. The difference in mass loss percentage for the former is more evident when compared to the latter system, dominated by the formation of C-A-S-H phase in high percentage slag.

A reduction in portlandite peak is observed in the case of CEM III/A system, which indicates its reaction with slag particles to form C-A-S-H gel. This effect is not seen in the case of CEM

II/B-S system as well as 20% custom mixes, understood by the information that the percentage of slag present is low when compared to CEM III/A. However, a minor increase in the peak for portlandite is observed for 50% custom blended systems, contrary to CEM III/A binder. This could mean that due to the possible the effect of lower alumina to ferrite ratio, the tendency to form hydrogarnets is relatively suppressed in comparison with CEM I system. Therefore, indicating less portlandite consumption.

Along with this, an increase in peaks corresponding to hydrotalcite phase is observed for CEM II/B-S system, reflecting on the impact of high Al_2O_3/Fe_2O_3 ratio. No obvious difference for CEM I system with regard to portlandite and magnesium peaks is observed. The peak changes were also consistent with the mass loss variation between Day 0 and Day 90 results.

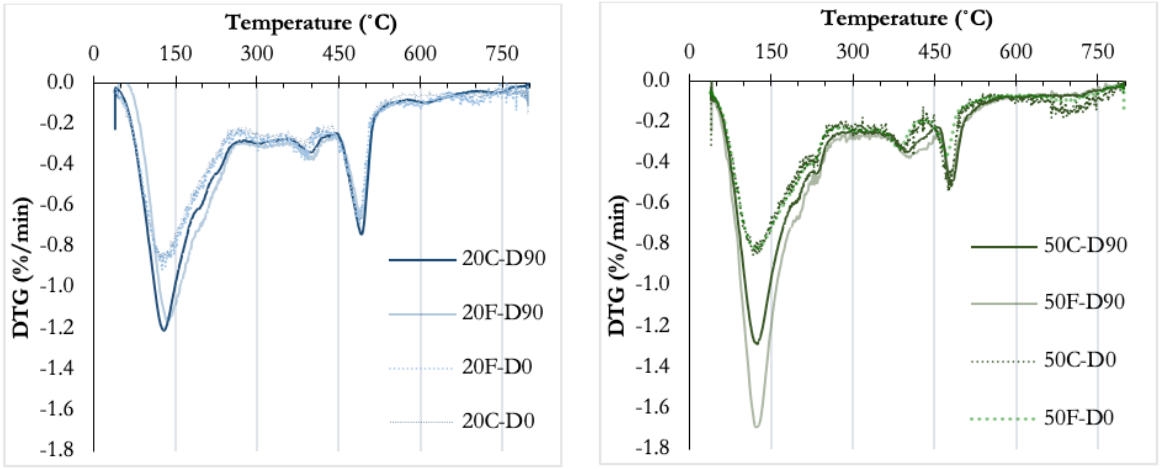

Figure 5.15: Thermograms Measured After Exposure for Custom blended systems.

An increase in the mass loss percentage corresponding to AFm phases was observed for all blends, however, the increase was more pronounced in the case of slag blended systems. This result could correspond to the effect of lower sulphate ratio necessary to instigate the formation of more monosulphate phases in contrast to ettringite.

Trivial reduction in the mass loss was observed with respect to hydrotalcite phase in the case of custom-blended systems with 20% slag and marginally with 50% slag. The moderate partaking of aluminates in the formation of monocarbonates and sulpho-aluminate phases during exposure as well as in the formation of hydrogarnet species could be a possible cause for the observed reduction.

A reduction in calcite peak was also observed in the case of slag systems after 90 days of exposure attributing to the possible formation of carbo-aluminate phases, supported by low sulphate ratios in the systems. This is later verified in XRD analysis.

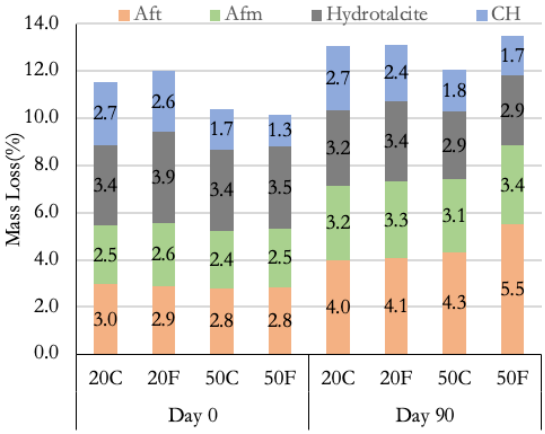

Figure 5.16: Mass loss% for Custom Blends.

Comparing within the custom slag blends, the effect of fineness is more distinct for the high percentage of slag i.e. between 50C and 50F systems. This is seen in a significant difference in the C-A-S-H temperature range, where the corresponding peaks of coarser and finer slag do not overlap. The effect of agglomeration as predicted at the beginning of exposure appears to not have surpassed the increased reactive surface under saturated pore solution environment during and after exposure.

5.3.2. X-Ray Diffraction Analysis

Characterisation of hydrated phases in the prepared mixes both industrial blends and custom blends is done by X-ray Diffraction methodology as discussed in section 4.4. The phases observed immediately after heat curing i.e. prior to lime solution exposure is analysed to identify the early stage hydration products and subsequent changes is observed by analysis of samples after 90 days of exposure at ambient temperature.

The analysis was done to identify primary peaks corresponding to crystalline phases that is predicted to be present in the samples analysed and to observe if it is analogous with thermograph information. A qualitative analysis is also carried out by observing the intensity of the peaks obtained. The characteristic peaks identified for all the types are shown in Appendix C and a sample pattern in figure 5.17. From the results obtained through peak identification, the phases observed in the different mixes are given in the table 5.18 and 5.19. The observations are discussed below:

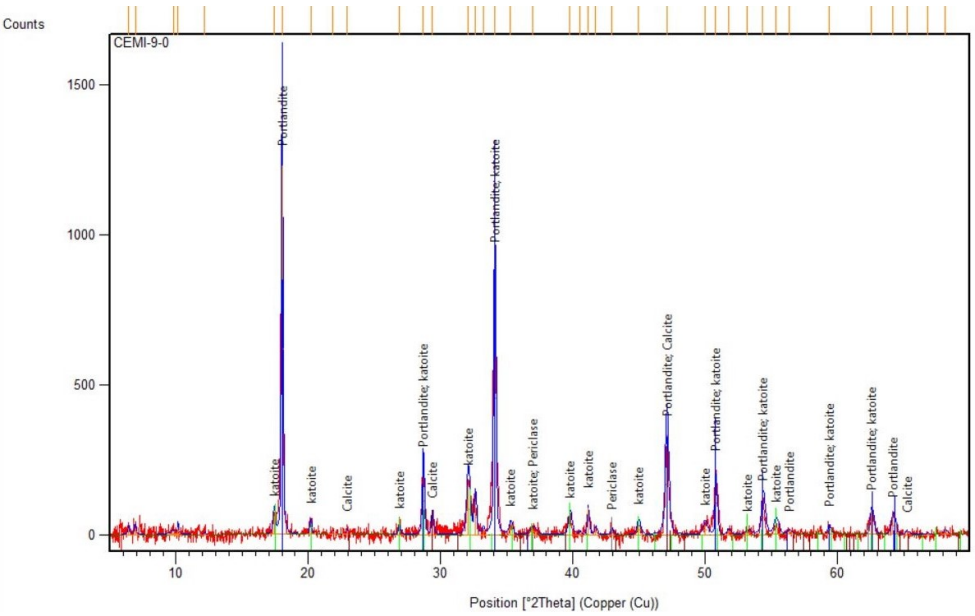

Figure 5.17: X-ray Diffraction Pattern for CEM I Before Exposure to Lime Solution.

Before Exposure

Figure 5.18: X-ray Diffraction peaks identified before exposure to lime solution.

Phases	CEM I	CEM II	CEM III	20C	20F	50C	50F
Portlandite	✓	✓	✓	✓	✓	✓	✓
Katoite	✓	✓	✓	×	✓	✓	✓
Dolomite	×	✓	✓	✓	✓	✓	✓
Ettringite	×	×	×	×	×	×	×
Periclase	✓	×	×	✓	✓	✓	✓
Monocarbonates	×	×	✓	×	×	✓	✓
Hydrogarnet	×	×	×	✓	✓	✓	✓

Immediately after high temperature curing, it was suspected that ettringite formed during early hydration would have decomposed to release sulphates into the pore solution or to be taken up by silicate hydrates. Congruent to this, no trace of ettringite was found in all the types both industrial blends as well as custom blends. Although this observation does not comply with the TGA results , were small traces of ettringite was shown , it must be understood that the reason for it may be limitation for XRD measurement limited to identify only major concentration of mineral peaks and that minor amounts of ettringite phases could be difficult to detect.

With high weight concentration of magnesia present in all slag blended systems, present of dolomite was found as a result of their subsequent hydration with calcite and hydrotalcite where portlandite can be partly consumed [36]. With hydration degree further increased, no traces of magnesia were detected, owing their participation into dolomite formation.

Traces of hydrogarnet phases were detected in industrial slag blends, which was as expected. While high temperature curing is said to affect sulpho-aluminates, it was also understood that siliceous hydrogarnet phases that normally do not persist at temperatures below 80°C, were instigated at higher temperatures[32]. Thereby justifying their presence. However, their absence in the case of industrial blends could be a result of effect of reactive silicate present in the system as a part of alite and belite clinkers, in combination with available alumina from clinker as well as slag composition.

After Exposure

It is evident that ettringite was present in industrial mixes at accountable intensities. This confirms the reformation of ettringite which was originally absent in the samples before exposure. Also, confirming to the considerable amount of magnesia present in the unhydrated blends, presence of Dolomite and Periclase is justified. Also, it is interesting to note that carbo-aluminate phases were identified in the industrial slag blends and their absence in neat Portland cement system i.e. CEM I. This can be explained in the line of available alumina and sulphate content present, wherein the case of slag systems, the reduction of SO_3/Al_2O_3 ratio accommodates the available carbonates to maintain thermodynamic equilibrium in calcium-aluminium bearing phases. Thereby resulting in

Figure 5.19: X-ray Diffraction peaks measured After exposure.

Phases	CEM I	CEM II A	CEM III	20C	20F	50C	50F
Portlandite	✓	✓	✓	✓	✓	✓	✓
Katoite	✓	✓	✓	✓	✓	✓	✓
Dolomite	✓	✓	✓	✓	✓	✓	✓
Ettringite	✓	✓	✓	✗	✗	✗	✗
Periclase	✓	✓	✓	✓	✓	✓	✓
Monocarbonate	✗	✓	✓	✓	✓	✓	✓

the formation of moncarbonates.

It can be understood that the moderate ratio of sulphate to aluminates lying closer to 1 for the case of plain Portland cement, implies sufficient amount for the formation of ettringite and in turn suppressing the formation of carbonate phase. On the contrary, with lower ratios i.e. below 0.5, shows the formation of both carbo-aluminates and sulpho-aluminate phases.

In the case of custom-made slag blended cements, primary phases identified were portlandite, Mg bearing phases and monocarbonates. No significant traces of ettringite was detected. This can be understood from the hydration mechanism, that there is a comparable reduction of sulphate to aluminate ratio, much less than 0.3, indicating no sufficient amount present to form ettringite or monosulphate. Thereby, correspondingly increase the presence of monocarbonates.

Significant peaks for magnesium bearing phases were also identified congruent with the high molar percentage of MgO present in the unhydrated mixes. This presence also reflects on the availability of alumina for sulpho-aluminate phases, wherein carbonate phases get formed during exposure

5.3.3. Pore Structure Evolution

Cement paste comprises of characteristic pores and voids which were responsible for durability performance of the system on the whole. This effect is studied by observing the microstructural changes in terms of pore-size distribution which may be a result of the reformation of primary phases such as ettringite and portlandite. As discussed in section 2.2, the porosity of the system is influenced by the fineness of the binders and thus their impact is studied by analysing MIP results.

Prior to Exposure

It can be observed that the characteristic pore diameter shows a significant drop as the slag content increases seen in figure 5.20. Slag blended systems indicate a much-refined pore size distribution primarily comprising of smaller peaks that lie in close ranges without much variance in comparison with CEM I system where significant peaks do not lie in closer proximity. This may be attributed to the higher content of slag in the former type that reacts with portlandite to cause similar pore diameter change.

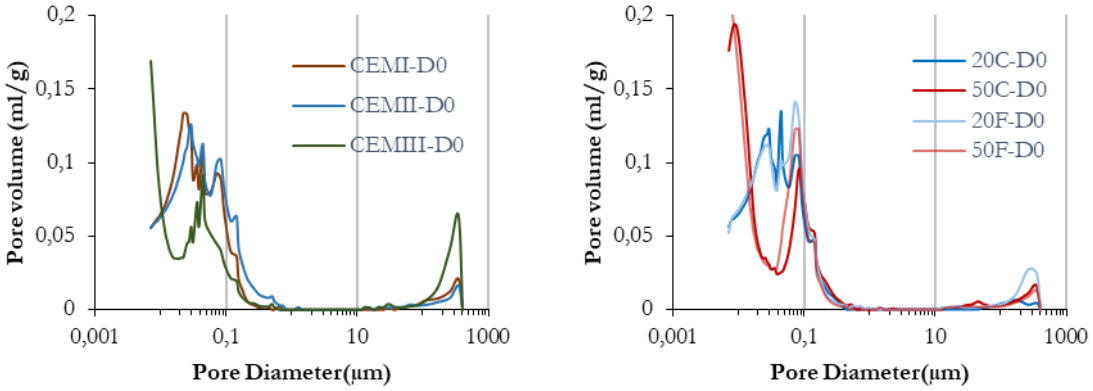

Figure 5.20: Pore Size Distribution for Day 0.

The range of pore dia between 0.01 µm and 0.1 µm is indicative of the formation of Portlandite which is verified in the case of slag systems as the corresponding peaks were smaller where slag reaction with CH occurs [53]. Also, the higher significant peak corresponding to pore dia range above 0.1 µm is indicative of the formation of C-S-H gel phases.

However, a significant peak at pore dia greater than 100 µm for CEM III/A system with was observed on the contrary to portland cement system. This could be related to the agglomeration of the binder mixes associated with higher fineness effect which may have not reacted during curing[54]. Similar differences were also observed custom mixes with varying fineness and slag content, however, the peak variance was more significant at lower percentage replacement of slag. Thus lower slag content along with higher fineness difference depicted more capillary pores contrary to higher slag replacement showed converging capillary pore presence for different fineness levels.

Analysing the pore volume variation in the different systems, CEM II/B-S and CEM III/A system with higher slag content, showed dominance in the lower pore dia range of 4 to 20 nm in comparison with CEM I, which alternatively showed coarser pore volume variation with the presence of pores lying in higher diameter range. Within the two slag systems, lower pore volume present in the range between 0.4 µm to 1µm for CEM III/A, indicates a higher degree of hydration as a result of increased fineness of the binders during early hydration[53].

For custom blended mixes, the total porosity for lower replacement level of slag is comparatively lower than that of CEM I system. However, at higher replacement level (50%), the porosity is much higher, indicative of slag reaction to portlandite for C-A-S-H and CSH gel formations that were porous[55].This difference is furthermore evident in the case of higher fineness of 50% substitution level, confirming the effect of the reactive surface area of slag. The increase in porosity is reflected by pores lying in the diameter range of 4 to 20 nm, again representative of silicate hydrate gel formations[55].

After Exposure

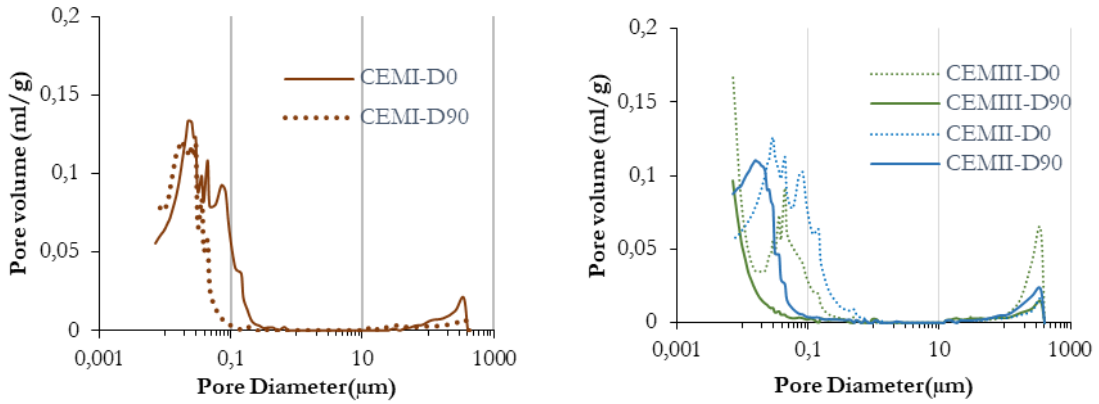

Figure 5.21: Pore Size Distribution for Day 90 - Industrial Blends.

After 90 days of exposure, the pore size distribution for CEM I and CEM II/B-S systems showed a minor evolution of characteristic pore diameter that still persists in the similar range. The difference is more apparent for higher slag substitution along with increased overall system fineness of CEM III/A, where a clear shift in the characteristic pore diameter is observed (see figure 5.21.

In the case of industrial mixes, reference mix of neat portland cement showed decreased in total porosity considerably lower than slag blended system. Since crystal growth theory suggests that secondary ettringite formations were more likely to occur in regions of porous media of the matrix, it is clearly reflected in the case of CEM I system. Here the reduction pore volume with diameter ranger higher than 20 nm is indicative of the same (see figure 5.22).

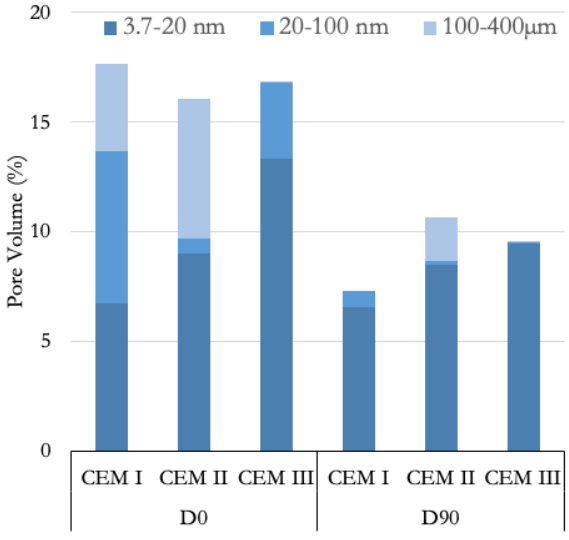

Figure 5.22: Pore Volume Variation for Industry Blends.

CEM III/A system showed an increased level of refined structure, indicative of higher fineness of the system, in comparison with the reference mix especially with pore diameter ranges closer to larger capillary pores i.e. above 100 µm. Significant reduction in pore volume percentage in the range of .02µm to 0.1µm reflects the presence of crystals of ettringite formed within the capillary and gel pores[56].

It should also be noted that despite crystal formations in the above range for CEM II/B-S, there is no significant reduction in the pore volume as a result of the same. This could be attributed to the formation of hydrotalcites phases that were also responsible for the consumption of alumina, a primary source for ettringite formation[57]. Since the presence of magnesium in the bogue composition is confirmed along with high aluminate to ferrite ratio that is

responsible for the rate of alumina consumption, the possible formation of the corresponding magnesium bearing phase is proposed..

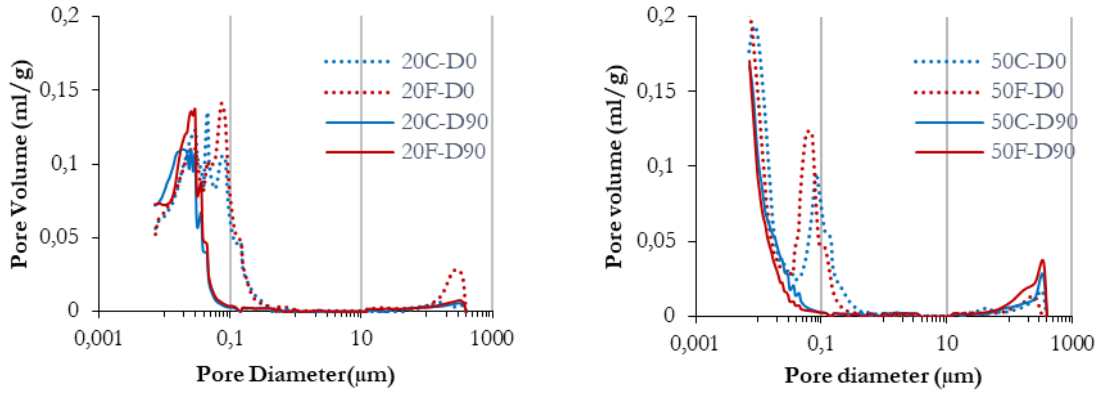

Figure 5.23: Pore Size Distribution for Day 90 - Custom Blends.

Observing the overall shifts in pore size distribution after 90 days of exposure, low replacement level of slag i.e. 20 %, there is a reduction of pore diameters at less than 0.1µm (see figure 5.23. This shift is evident for both lower as well as the higher fineness of slag. However, the change in the characteristic pore diameter is more prominent with a higher replacement level, with close diameters for different fineness-es. For lower replacement level i.e. at 20 %, critical pore dia overlaps for both the ages only at coarser grain size, along with a peak shift. This could attribute to the enhanced reaction of slag, leading to more CSH gel formations, dominating the overall pore refinement due to whole system hydration[53].

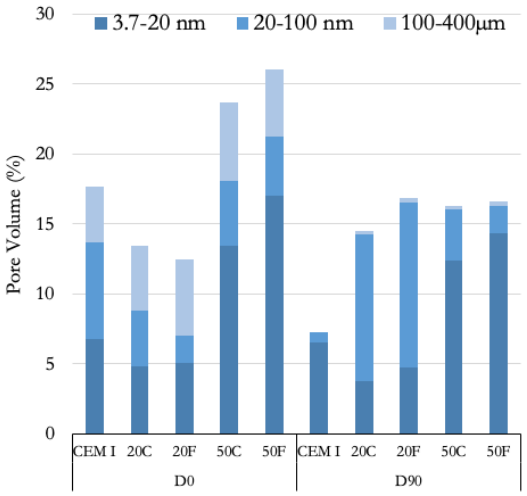

Figure 5.24: Pore Volume Variation for Custom Blends.

Along with the shift in size distribution, the pore volume present in the range of 0.02 µm to 0.1µm shows a considerable increase for 20% slag custom blends (See figure 5.24). This range indicates the presence of portlandite, supporting the fact that a lower degree of hydration attributed to lesser slag contents and their consumption of CH[53]. Also, possible formation of ettringite crystals in this range, as they mostly comprise of capillary pores and gel pores. Pore size reduction in the lower ranges i.e. < 0.02µm, though not very significant, reveals the possible formation of calcium aluminate crystals. The close levels of pore volume difference could be because, although crystals were present at the smaller pores, in turn, decreasing the volume, could be counteracted by decalcification of CSH leading to increase in porosity. The decalcification occurs as a result of dissolution under exposure conditions, for it to precipitate into ettringite crystals[57]. Correlating the pore volume changes to crystal growth theory, which states that ettringite forms at the inner hydra-

tion products of CSH were not congruent, as pore volume increase in these lower ranges is not significant[53].

In comparing before and after exposure pore volume variation for 50% slag replacement, there appears clear reduction in the ranges of 0.02µm and 0.01µm, which could possibly be due to formation of ettringite crystals precipitated from calcium bearing phase, C-S-H, that in turn reflects in increased pore volume at a diameter less than 0.02µm. The refinement of pore structure in the latter ranges could also indicate the formation of Magnesium bearing phases such as periclase and hydrotalcite, due to the considerable amount of Mg present in slag composition[57].

Along with changes in pore size distribution and volume variation before and after the exposure period, characteristic pore diameter changes were also observed. The characteristic pore diameter represents the largest entry pore diameter that influences the saturation of the matrix's aqueous environment responsible for transport properties and is characteristic of the specimen. This value gives qualitative information on the permeability of the system under observation and in turn its durability.

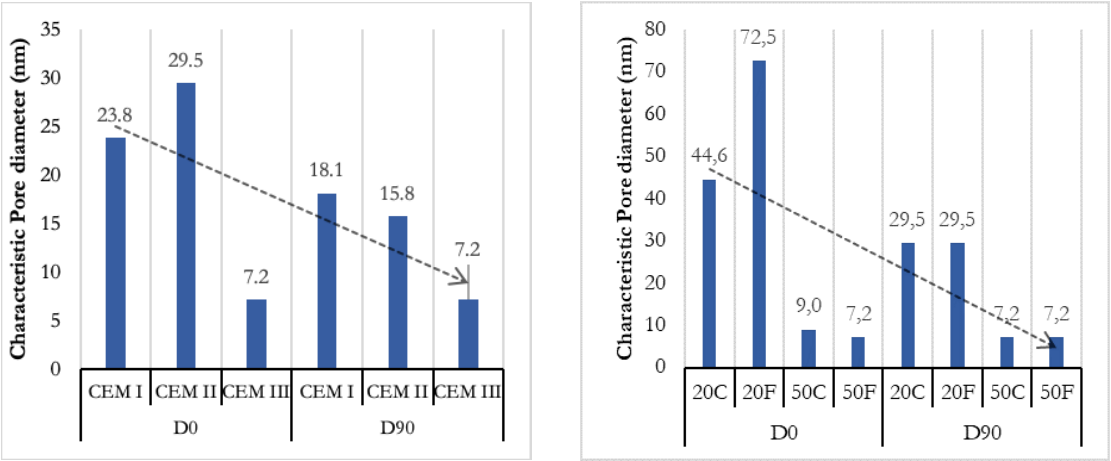

Figure 5.25: Characteristic Pore Diameter Variation.

From the graph presented above (5.25)it can be seen that the reduction in the characteristic pore diameter is more evident in the case of CEM I system, as well for low percentage slag composite systems, i.e. for CEM II/B-S as well as custom-blended 20C, 20F. Whereas for a high percentage of industrial slag blend (CEM III/A), almost no significant difference is observed. A similar observation is recorded for 50% custom blended slag system with an analogous fineness (600 m2/kg). In the case of low percentage custom slag blends, (20C and 20F), the effect of fineness is more prominent in the early stage hydration and at later stages during exposure appears to be indistinguishable. This reflects that the effect of fineness is diminished with increasing exposure period.

The overall reduction in the characteristic pore diameter as understood by analysing the volume change and pore size distribution is indicative of both crystallisation of secondary phases as well as partly by subsequent hydration of the binders.

5.4. Micro structural Phase Analysis

In order to obtain visual evidence of ettringite and ettringite like sulpho-aluminate phases present along with other microstructural changes such as hydration phases and porosity, semi-quantitative image analysis was conducted on polished sections of the specimens at ages primarily after heat curing and at the end of the exposure period. The first examination is conducted through micro-graphs obtained through back-scattered electron image analysis. Following this, point analysis was conducted at different positions in the samples to quantitatively confirm the different phases which were suspected to be present in the micro-graphs. The point analysis was used to verify through elemental identification of the hydration products plot through atomic weight ratios.

5.4.1. Micro structure Examination

Before Exposure

Immediately after curing SEM micro-graphs were obtained and observations are discussed below. The visual examination revealed similar characteristics for all the different types studied and thus the observations are compiled in this section. The obtained raw images are added to Appendix D for reference.

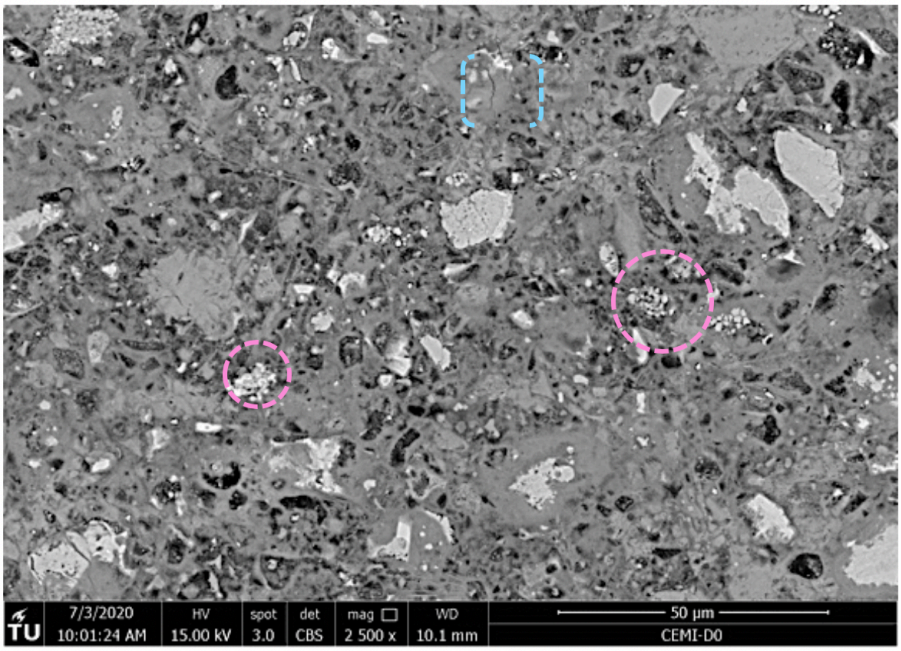

Figure 5.26: CEM I :Before Exposure to lime solution sample micro-graphs.

Key: Belite, Micro cracks, Unhydrated slag

In all the sample types, the pore structure revealed higher porosity, especially in the case of coarse substitution of slag i.e. 20C and 50C and also in CEM I system. This observation is therein in line with the pore size distribution measured in chapter 6.4.

A considerable amount of belite clusters were observed in the samples suggesting the possible mechanism where alite hydration is accelerated due to high-temperature curing and slower hydration of belite. A considerable amount of unhydrated slag grains were identified in all slag blended

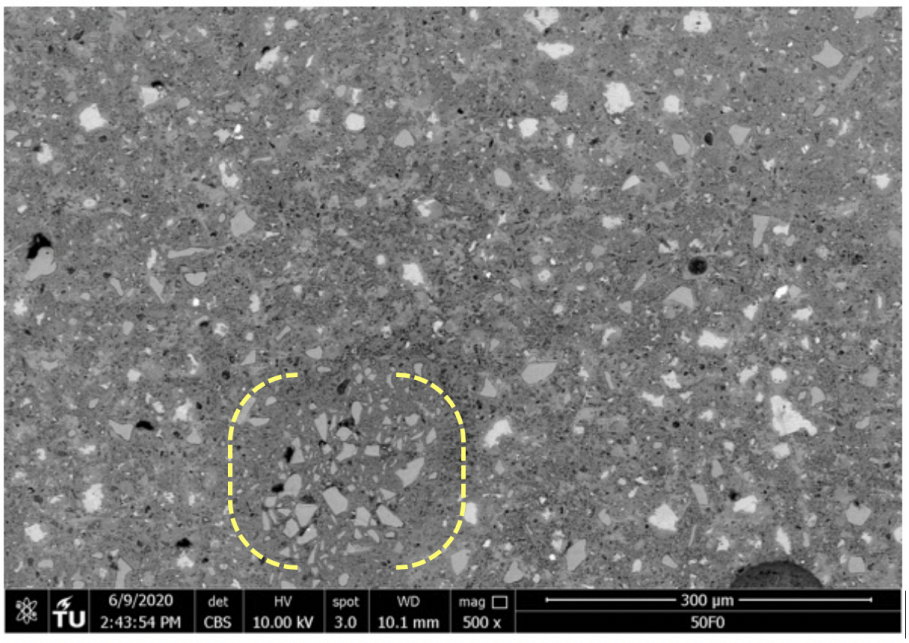

Figure 5.27: 50F :Before Exposure to lime solution sample micro-graphs.
Key: Belite, Micro cracks, Unhydrated slag

systems. A distinct feature in the case of high fineness slag blended system was observed, that indicated possible agglomeration of the slag particles as seen in fig. Micro-cracks were observed scarcely within slag grains and within hydrating C-S-H gel-like phases. This could be an indication of thermal stresses induced during high-temperature curing.

With regard to sulpho-aluminate phases, distinct streaks were rarely identified, especially in the case of slag blended systems. The observation is expected because, as a result of elevated curing temperatures, ettringite would have decomposed leaving behind monosulphate crystals.

However, the size of the crystals thus formed are said to be in sub-micron scale and often dispersed underneath other hydrating phases. Thus, causing difficulty in their identification.

After exposure

Observing the global paste system of CEM I at a lower magnification, revealed the pore structure was no refined and an overall porous matrix was identified. This finding shows to be in correlation with the porosity measurements, which also revealed a less refined distribution after 90 days of exposure.

Higher scale visual examination of the cementitious matrix revealed significant number of small streaks suspected to be of ettringite heterogeneously spread in the observed study area of the specimens (see figure 5.43). Also, concentration of ettringite clusters were also visible mixed amidst CH hydration products. It was also noted that these clusters were present in relatively porous matrix, supporting the fact that they are the potential sites for crystals to form with less counteracting pressure. In some regions, the clusters were located in close proximity to each other indicating possible rich source of aluminates as well as sulphur during early hydration. The streaks of ettrin-

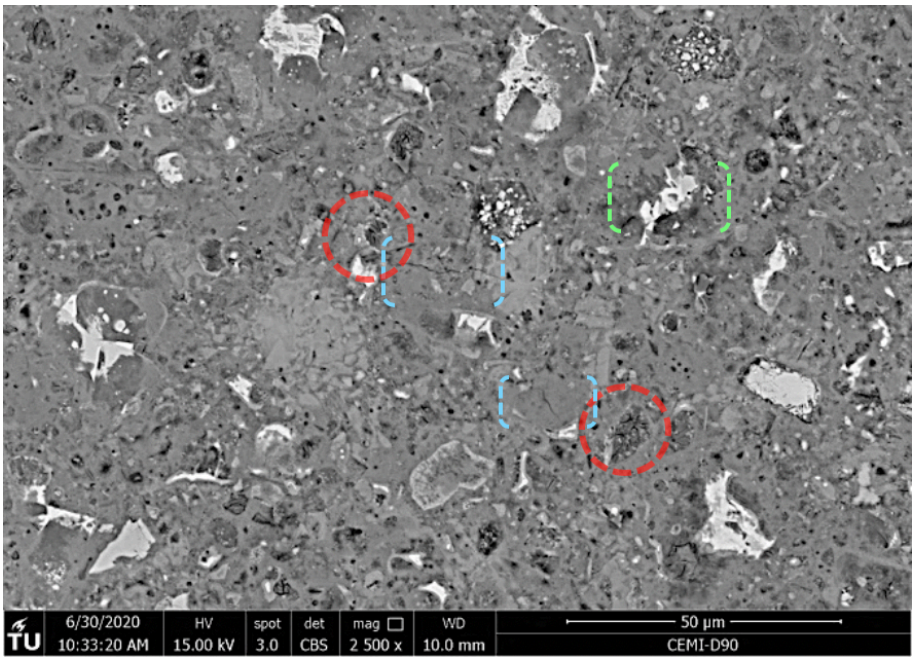

Figure 5.28: CEM I D90 micro-graph after exposure to lime solution.

Key: Aluminate phases, C-S-H gel, Micro-cracks, Hydrated Slag, Unhydrated Slag

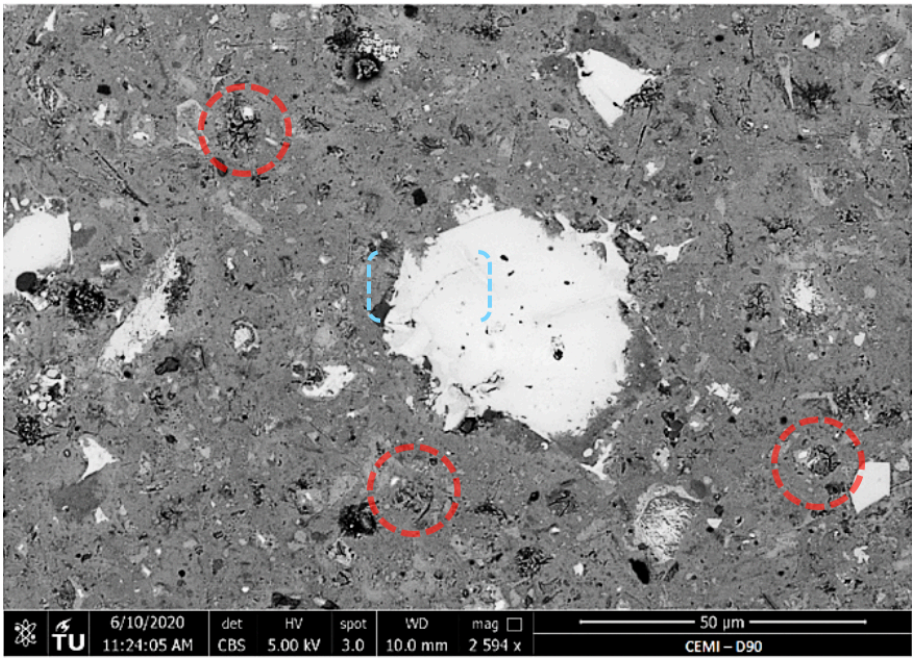

Figure 5.29: CEM I D90 micro-graph after exposure to lime solution.

Key: Aluminate phases, C-S-H gel, Micro-cracks, Hydrated Slag, Unhydrated Slag

gite were identified to be around the scale dimension of less than 5-6 µm, while the clusters of ettringite were in the higher range at about 10 µm.

Evidence of ettringite veins were also identified near the outer products of C-S-H indicating their formation from the adsorbed sources of sulphur. No significant streaks were located within the

C-S-H rims. Evidence of micro crack propagation from the ettringite clusters were also identified indicating crystallisation pressure induced during their subsequent formation.

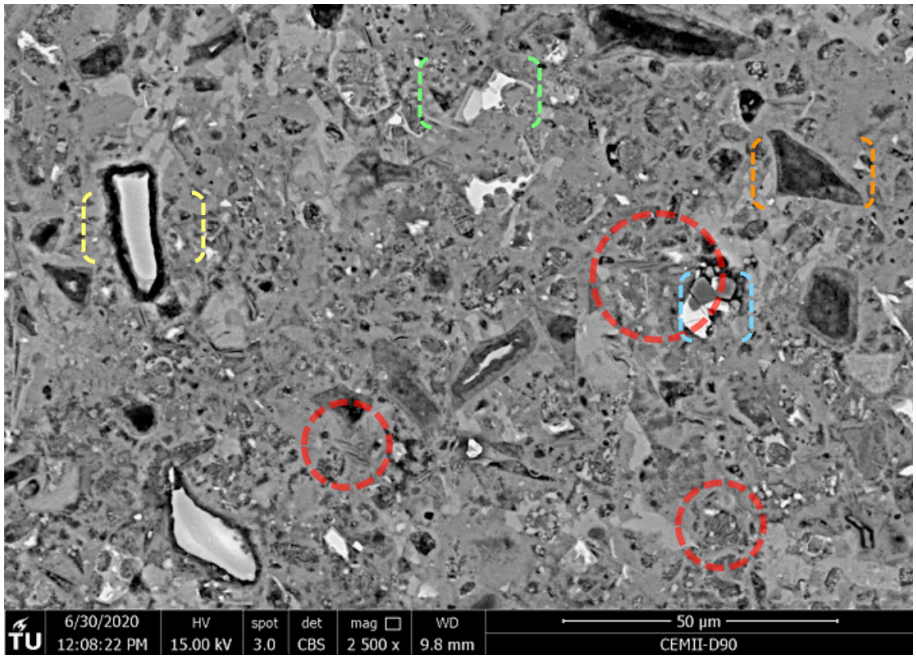

Figure 5.30: CEM II/B D90 micro-graph after exposure to lime solution.
Key: Aluminate phases, C-S-H gel, Micro-cracks, Hydrated Slag, Unhydrated Slag

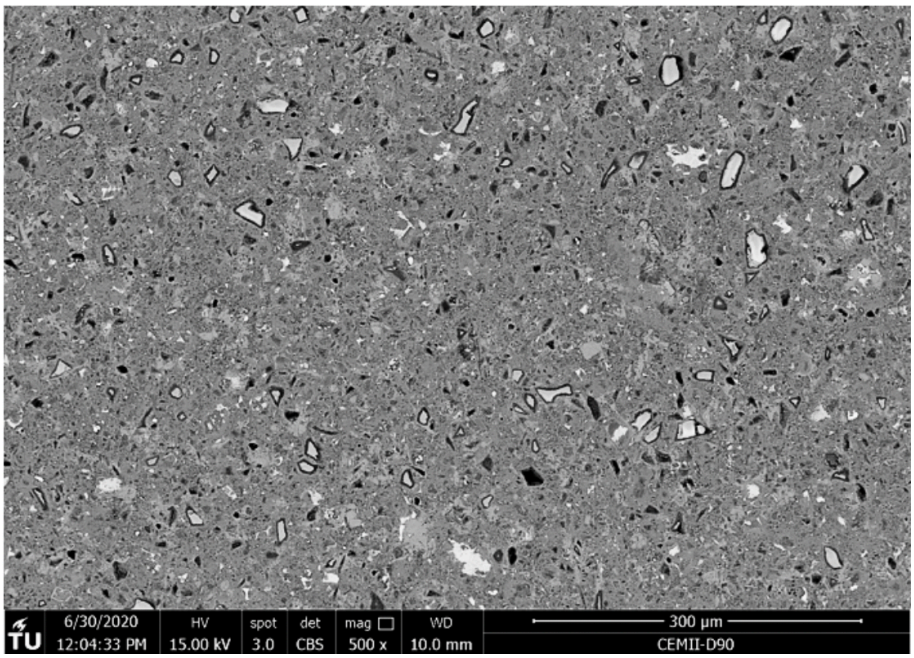

Figure 5.31: CEM II/B D90 micro-graph after exposure to lime solution.
Key: Aluminate phases, C-S-H gel, Micro-cracks, Hydrated Slag, Unhydrated Slag

For CEM II/B-S type, an observation at a lower magnification scale was made through which a partially refined pore structure was recognised, with patches of porous matrix regions. This observation was found to be in correlation with pore size distribution obtained as a result of the MIP

experiment. At this magnification, grains of unhydrated slag was observed and hydrated silicate hydrates were also identified.

Higher magnification was chosen in order to identify sulpho-aluminate phases and their subsequent locations(see figure 5.31). Individual veins of ettringite were observed to be heterogeneously distributed in the system matrix at regions of hydrated silicate hydrate gel formations. Smaller clusters of ettringite like streaks were also noticed in the hydrated cement matrix. These clusters were also located in regions surrounding hydrating CSH gel formation with few spots of alite mineral in the vicinity, indicating that crystal formations were characteristic of sulphur sources that could have been adsorbed during heat curing by the former.

Ettringite formations were located in relatively porous parts of the system matrix reiterating the possibility for easier crystal growth. Presence of neither discrete nor cluster formations of AFt was observed within CSH hydration product although micro-cracks were situated in inner CSH gel products in some cases. Discrete veins of ettringite were observed at dimensions less than 3 µm, and clusters were identified at the range of 3µm to 5 µm approximately.

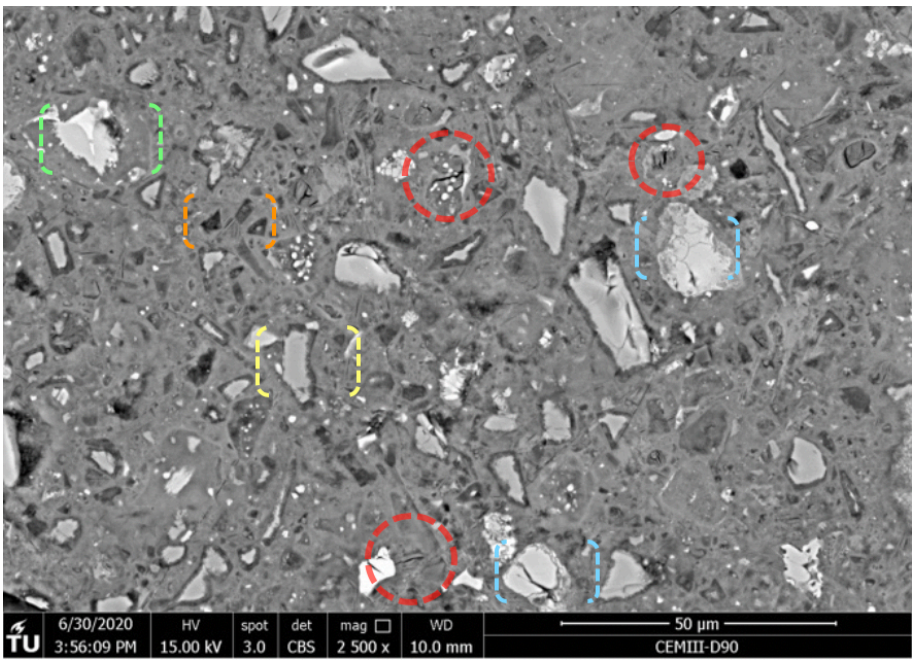

Figure 5.32: CEM III/A D90 Micro graph after exposure to lime solution.

Key: Aluminate phases, C-S-H gel, Micro-cracks, Hydrated Slag, Unhydrated Slag

For CEM III/A specimens, contrary to CEM I, the over-all pore structure appeared more refined and with smaller patches or porous regions. This observation again was in line with porosity measurements, that indicated increased refinement of pore size distribution with the characteristic pore diameter lying in the lower scale regions.

Inspection at higher magnification revealed the presence of ettringite streaks distributed heterogeneously in the matrix (See figure 5.33). However, a lesser number of individual streaks were

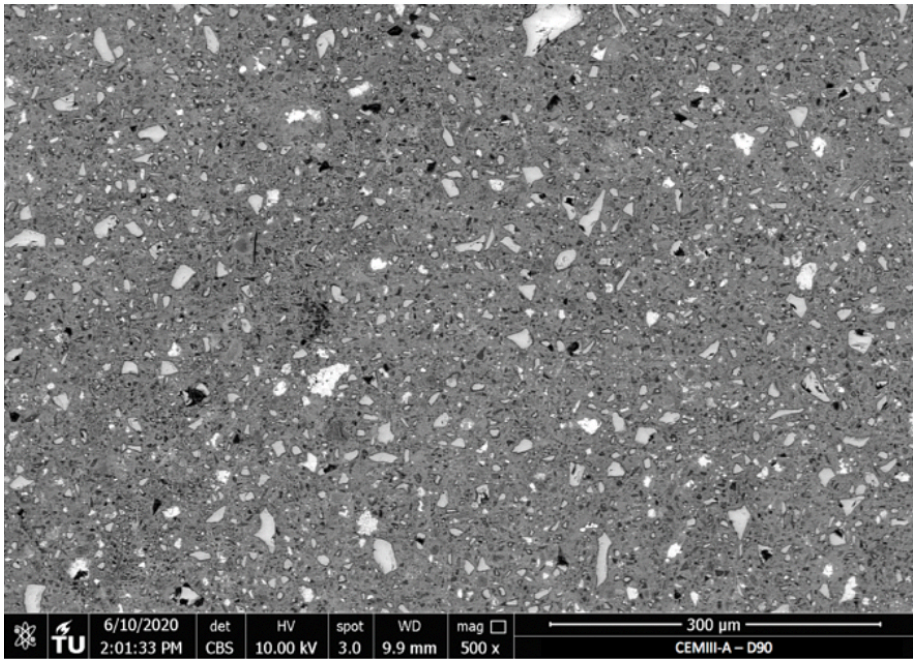

Figure 5.33: CEM III/A D90 Micro graph after exposure to lime solution.

Key: Aluminate phases, C-S-H gel, Micro-cracks, Hydrated Slag, Unhydrated Slag

identified unlike in the case of CEM I system. The cluster of ettringite veins was located in porous regions given by the darker gray-scale, and in some regions near hydrating clinker grains. Micro-cracks were identified within cement clinkers with incidents were traceable propagation to ettringite streaks was identified.

There appeared ettringite streaks also near unhydrated slag grains, along with micro-cracks within the grain. Discrete veins of ettringite were present in the dimension of less than 4 µm and rarely larger than 5 µm. The cluster of ettringite streaks was observed to have dimensions less than 5 µm in most cases, although evidence of larger clusters with a scale of about 15 µm was found. The clusters, in general, were not located in close proximity to each other unlike in the case of CEM I system.

Apart from individual observations for AFt like phases, a distinctive property of C-S-H hydration product was observed at 90 days of exposure for all the types of industrial blends. This property was that two different gray-scales of hydration products concentric to each other were identified. The difference is commonly referred to as inner product and outer product, which change with atomic densities and composition. The outer product, with differentiable lighter grayscale, indicates the formation of early-stage C-S-H as a result of high-temperature curing. Subsequently, the inner product with darker grayscale represents the C-S-H formation during exposure to a lime solution at ambient temperature. Although micro-cracks were located in the C-S-H products, no evidence for streaks of ettringite in the sub-micro metric scale was identified within them. This highlights the mechanism that the ettringite has formed away from the free ionic sources of sulphate despite the presence of microstructural spaces, such as micro-cracks.

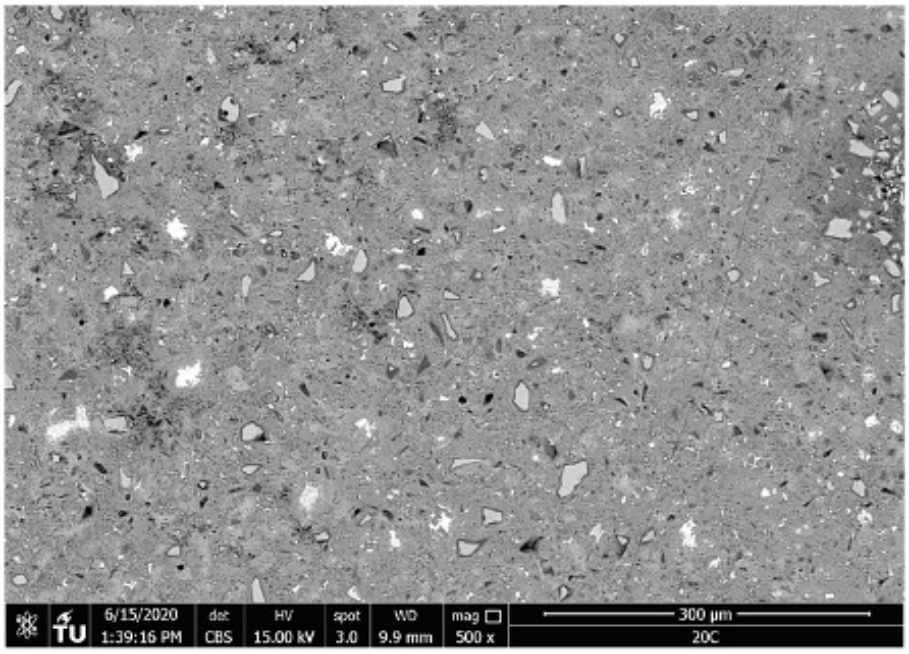

Figure 5.34: 20C-D90 :After Exposure micro graphs.

Key: Aluminate phases, C-S-H gel, Micro-cracks, Hydrated Slag, Unhydrated Slag

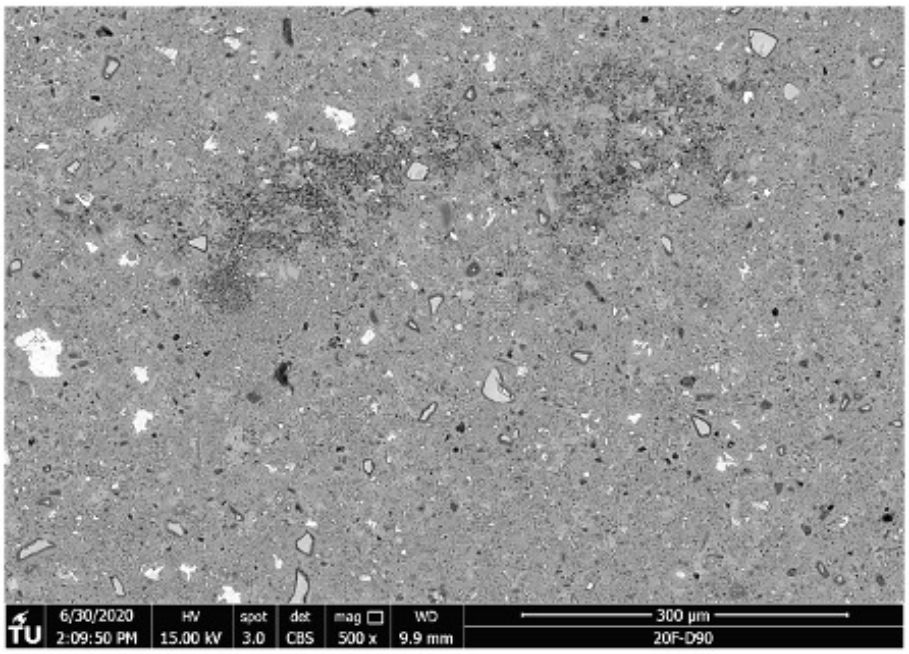

Figure 5.35: 20F-D90 :After Exposure micro graphs.

Key: Aluminate phases, C-S-H gel, Micro-cracks, Hydrated Slag, Unhydrated Slag

Observing the porosity of low slag percentage systems i.e. 20%, the blended matrix with coarser slag showed homogeneous distribution of porous media, while the system with finer slag

composition exhibited a much-refined matrix although patches of the porous environment were located (See figure 5.35). This appeared to be in line with porosity measurements, wherein coarser slag, a broader peak corresponding to characteristic pore diameter was obtained, whereas for the case of finer slag much-refined distribution supported by a narrow peak for characteristic pore diameter was observed.

At higher magnification as well as lower magnification, the presence of unhydrated slag grains were more prominent in the case of coarser slag contrary to finer slag composition. This difference could be indicative of an increased degree of hydration exhibited by slag as a result of increased surface area for a reaction while for coarser slag, even after 90 days of exposure reaction rate had less impact.

Microcracks were observed for both the systems, minorly spanning across slag grains and majorly in hydrating clinker grains, i.e. within the C-S-H gel formations. The associated micro-cracks were clearly detached from any ettringite like formations appearing in the vicinity. The two-tone characteristic of hydration C-S-H gel formations were also witnessed in the systems with a varying fineness of slag, as a result of which, lighter grey area indicating early hydration due to heat curing and darker concentric regions indicating subsequent hydration products during exposure.

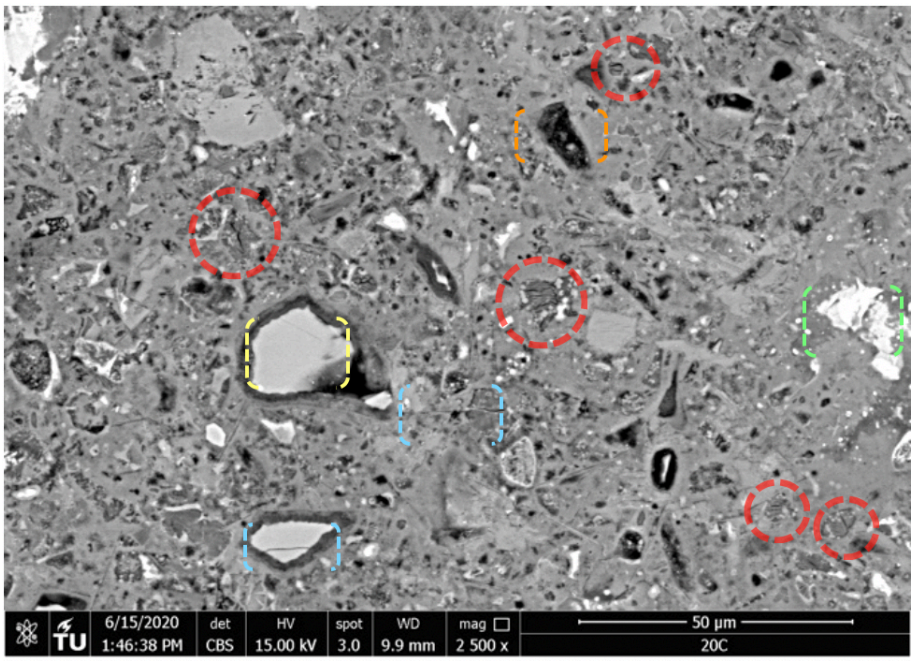

Figure 5.36: 20C-D90 :After Exposure to lime solution micro graphs.

Key: Aluminate phases, C-S-H gel, Micro-cracks, Hydrated Slag, Unhydrated Slag

Blended systems with coarser slag (20C) showed clear evidence of ettringite like streak formations predominantly as clusters rather than individual veins (see figure 5.37). The sizes of those clusters were observed to have scale dimensions less than 5 µm and in one particular case even as large as 50µm, although more of larger formations were difficult to locate. In some regions were ettringite like veins were prevalent micro-cracks appeared to have emerged indicating potential

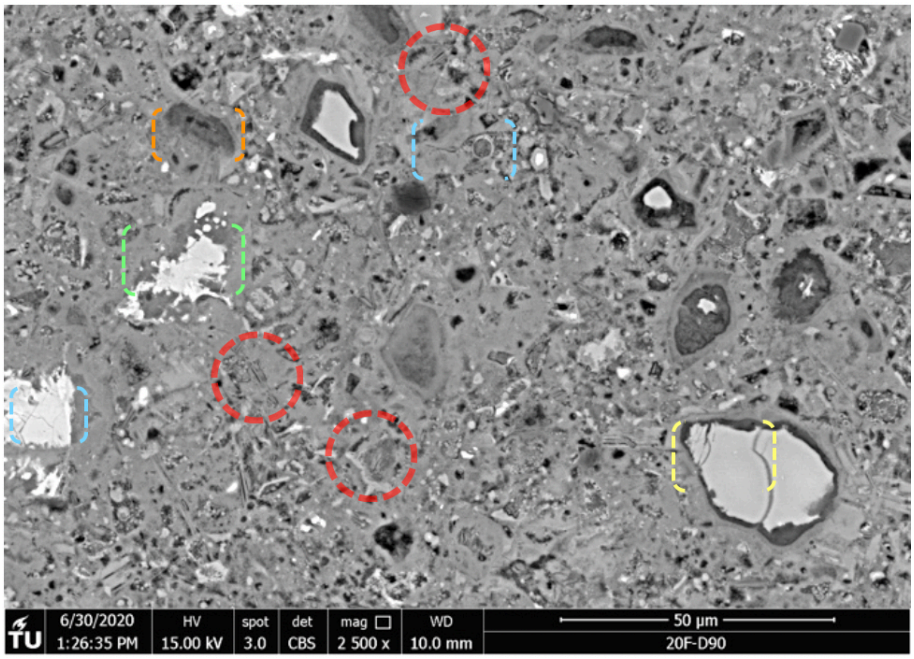

Figure 5.37: 20F-D90 :After Exposure to lime solution micro graphs.

Key: Aluminate phases, C-S-H gel, Micro-cracks, Hydrated Slag, Unhydrated Slag

crystallisation stresses around them. However, the dimensions of the crack were limited to less than 1µm.

With respect to finer slag systems (20F), ettringite like veins appeared more significantly as discrete lines and scarcely as clusters. This could be indicative of the refined pore structure, due to which transport properties required for ionic saturation of pore-solution could have been limited, causing it to be formed at isolated regions. Here again, the dimensional width of the streaks was identified to be less than 1µm in scale. At the observed area, no significant crack propagation was identified emerging from the ettringite like streaks.

For slag systems with higher replacement levels i.e.50%, the overall porosity appeared refined in comparison with lower slag composition (See figure 5.39). No apparent difference in the porosity distribution was observed at higher magnification for varying fineness of slag composition. The observation is again is congruent with porosity measurements were the dominant pore volume was present at pore diameter range of less than 0.02µm, representing finer pore size distribution.

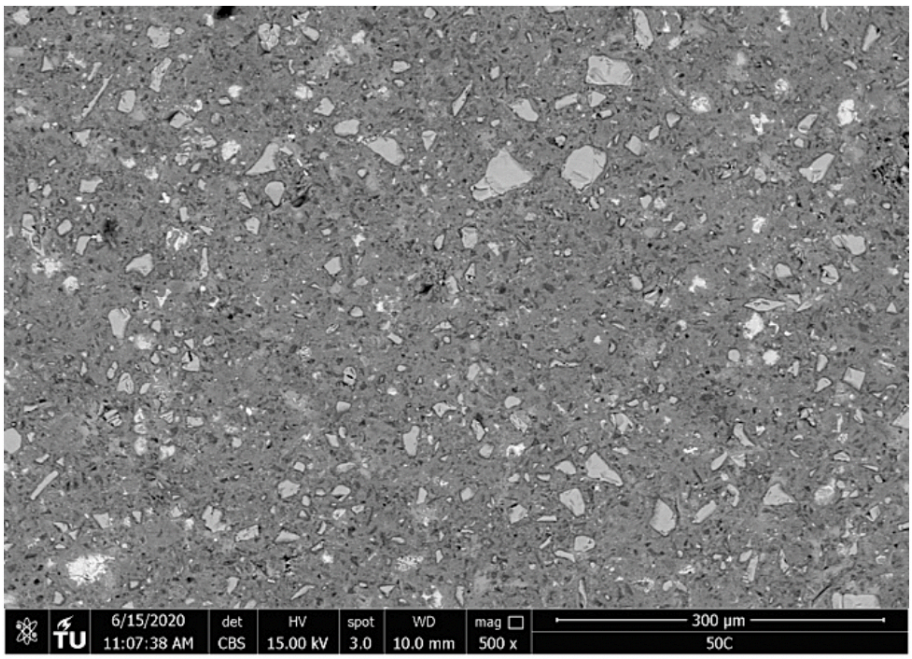

Figure 5.38: 50C-D90 :After Exposure to lime solution micro graphs.

Key: Aluminate phases, C-S-H gel, Micro-cracks, Hydrated Slag, Unhydrated Slag

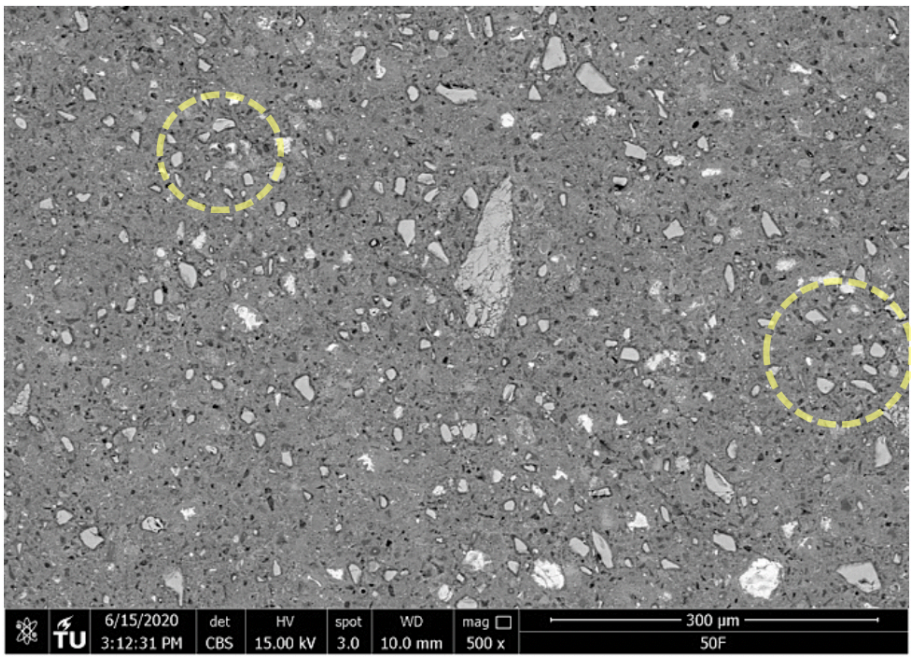

Figure 5.39: 50F-D90 :After Exposure to lime solution micro graphs.

Key: Aluminate phases, C-S-H gel, Micro-cracks, Hydrated Slag, Unhydrated Slag

Inspection on the slag phases in both the systems revealed an overall lesser presence in the case of the matrix with higher slag fineness as opposed to the matrix with coarser slag composition. The differences are symptomatic of increased reactivity of slag adhering to the larger surface during hydration. However, the available unhydrated slag grains present in 50F system, showed agglomeration of granular particles, unlike 50C system, where a more homogeneous distribution was observed. This aligns with earlier studies by researchers, which stated the possibility of accumulation due to a wide margin of fineness between the clinker and pozzolanic material [54].

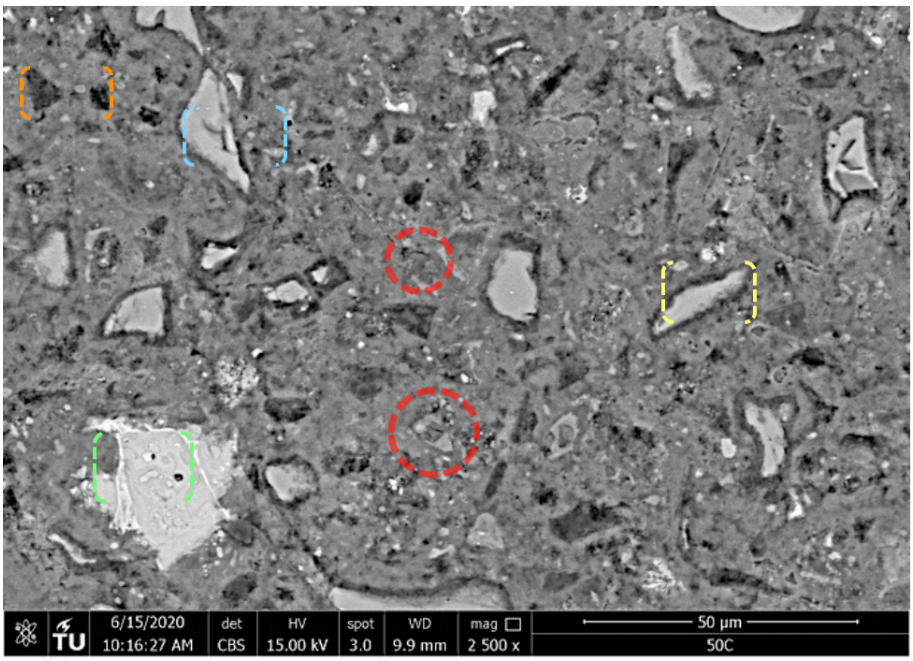

Figure 5.40: 50C-D90 :After Exposure to lime solution micro graphs.

Key: Aluminate phases, C-S-H gel, Micro-cracks, Hydrated Slag, Unhydrated Slag

Investigation for locating ettringite like streaks revealed their sparse presence in the observed areas for both systems with higher slag composition (50C and 50F) irrespective of varying fineness (see figure 5.41. Whichever was identified veins were primarily discrete and not connected to any apparent micro cracks present. The formations of the veins were observed to be present amidst outer C-S-H gel formations and seldom in the vicinity of hydrated slag grains with the discrete veins having the dimension of about 1µm scale. Clusters of ettringite like streaks were altogether absent contrary to lower slag replacement systems.

Since the appearance of sulpho aluminates such as ettringite and monosulphate, along with the appearance of carbo aluminate phases do not have distinct properties, it is almost uncertain to conclude the phases that have formed with similar form. Thus, in order to distinguish between them, a micro-analysis was conducted on the observed areas, with electron beam shot at the suspected incidences of ettringite like veins.

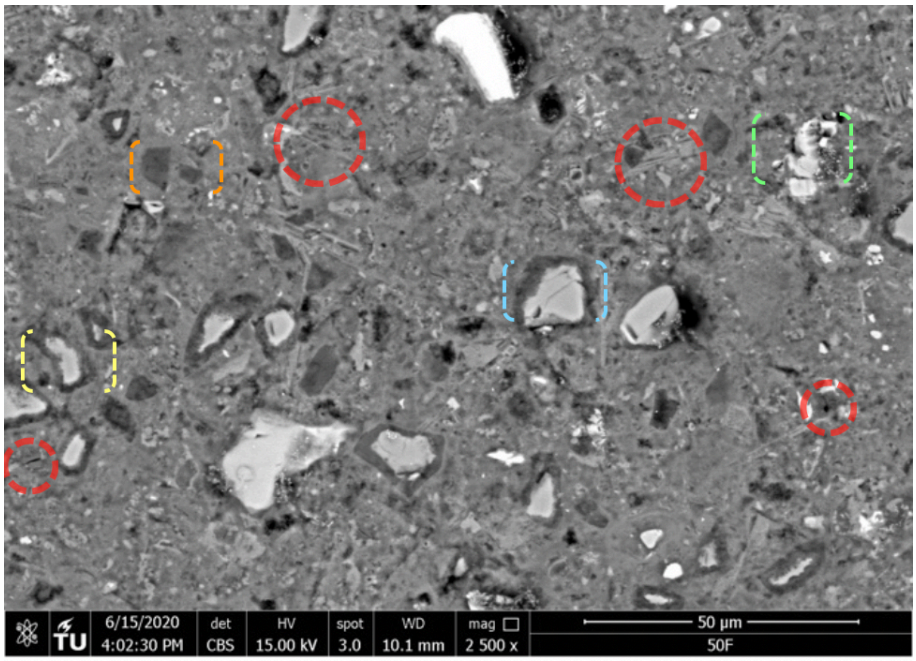

Figure 5.41: 50F-D90 :After Exposure to lime solution micro graphs.

Key: Aluminate phases, C-S-H gel, Micro-cracks, Hydrated Slag, Unhydrated Slag

5.4.2. X-Ray Micro-analysis

To confirm the presence of sulpho-aluminate phases and to differentiate accurately between, AFt, AFm and mono-carbonate phases if any, the micro-analysis was conducted. Here, point observed and suspected to be streaks or veins of ettringite were shot with an electron beam, that would, in turn, emit energy in the form of X-rays, that is characteristic of different elements present. Since the area of shooting is at the micrometre scale, the possibility of other elements to be present in the vicinity may cause misinterpretation of the phase's present underneath it. Thus, atomic concentrations of the elements were plot in ratios for improved accuracy.

A scatter plot containing these different points were obtained with the Al/Ca molar ratio in the x-axis and S/Ca ratio in the y-axis. In such a typical plot, the orange line along the line of increasing sulphur to calcium ratio represents the stretch in which the existence of AFt phases was identified. At a lower ratio of S/Ca, for a similar ratio of Al/Ca, is indicative of AFm phases. A much lower concentration of Sulphur even below 0.5 at higher concentrations of Al/Ca ratio is said to represent monocarbo-aluminate phases[36].

The area between the orange line and grey line indicates the possibility of ettringite and monosulphate phases predominantly, while the area between the grey line and yellow line indicates the presence of primarily monosulphate and Monocarbonate phases. The pure phases were indicated as the red triangle and green triangle for AFt and AFm respectively.

Point Analysis was conducted at 3 different positions within the specimen and the detailed plots are added in Appendix D. The summary of the results is discussed below with reference figures. It should be noted that the specimen matrix is heterogeneous and thus for conclusive results further detailed point analysis, through complete scan is advised.

Before Exposure to Lime solution

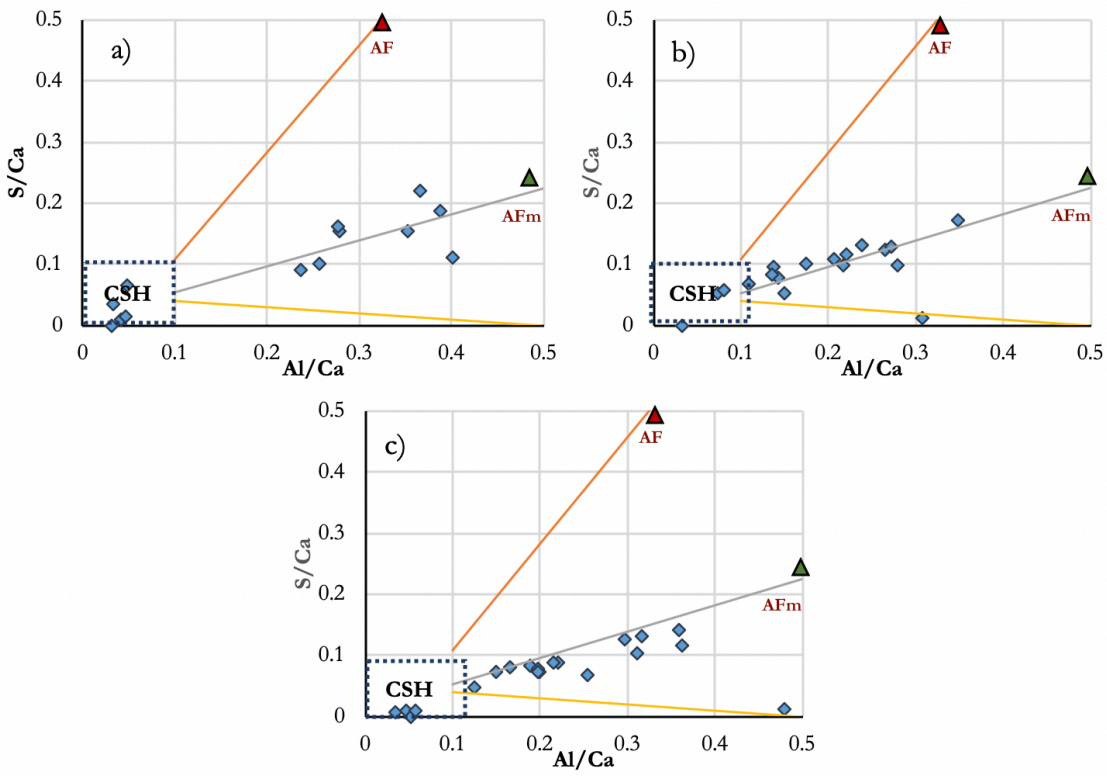

Figure 5.42: Before Exposure Micro-Analysis :a)CEM I , b)CEM II/B-S ,c)CEM III/A .

Point analysis of all three industrial binder system revealed the predominant sulpho-aluminate phase as to be monosulphate and no trace of ettringite as shown in fig 5.42.

The characteristic points corresponding to monosulphate showed relatively smaller sulphate ratio for slag blended systems in comparison with a neat system containing only portland cement. This is expected as a result of smaller sulphate to aluminate ratio in relation to CEM I system.

Micro-analysis was omitted as the identification of sulpho-aluminate phases through visual examination in order to perform point analysis was not viable, unless a full scan was performed. However, based on the results in XRD and TGA analysis, that were in agreement with each other and hence the subsequent phase changes were discussed for after exposure period observations.

After Exposure to Lime Solution
Industrial Blended Systems

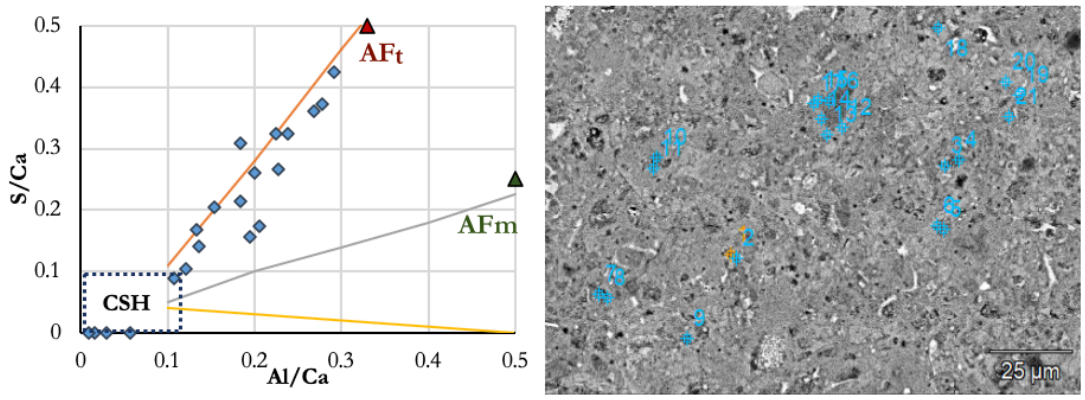

Figure 5.43: After Exposure Micro-Analysis for CEM I 52.5 .

In the above figure, points of atomic ratio along the stretch of ettringite ratio line indicate the presence of AFt. Fewer points with Sulphur ratio lying below 0.2 were identified, stating that there was a lesser monosulphate phase present, justified by the conversion of primary AFm to AFt upon storage under lime solution. The points present closer to the origin is indicative of outer CSH gel formations that could have overlapped during spot analysis. This result is in conjunction with XRD results, that indicated the presence of only AFt after 90 days and no AFm phases.

In addition to the identification of sulpho aluminate phases, a global random point analysis was done on the specimen in order to identify other dominating phases. Of which, it was noted that minor concentrations of magnesium were found, along with a significant concentration of carbon intermixed with the outer CSH gel hydration products. This result is indicative of the presence of magnesium bearing phases, such as dolomite and hydrotalcites, again consistent with XRD results.

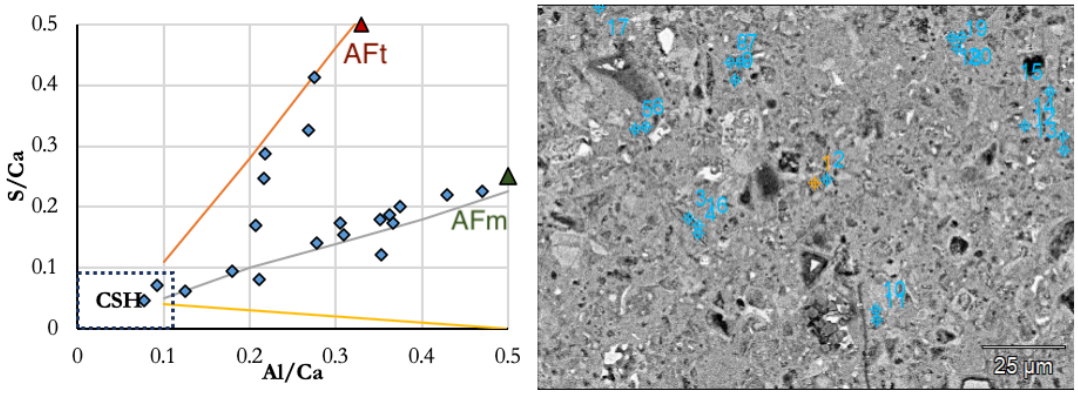

Figure 5.44: After Exposure Micro-Analysis CEM II/B-S .

In the case of CEM II/B-S specimens, the points analysed were observed to be spread along AFt stretch with increasing sulphur ratios. Along with this, fewer points also indicated by lower sulphur ratios i.e. below 0.2 with increasing Al/Ca ratio confirmed the presence of monosulphate and/or carbo-aluminate phases.

Since the limits for AFm and Monocarbonates lie within the range as observed, it can be understood by the elemental ratio of the different phases that, at a higher concentration ratio of Al/Ca corresponding to lower concentration of sulphur i.e. below 0.1, it could be indicative of carbo-aluminates and at higher concentration of sulphur i.e. between 0.1 and 0.2, is representative of AFm phases. From this understanding, it is concluded that the specimen analysed at the region could have minor quantities of both AFm and monocarbonates after 90-day exposure.

These results were again, align with XRD results, that suggested a high concentration of ettringite and minor presence of carbo-aluminates. In line with the same, evidence of magnesium bearing phases was confirmed with their significant atomic concentration upon global random point analysis.

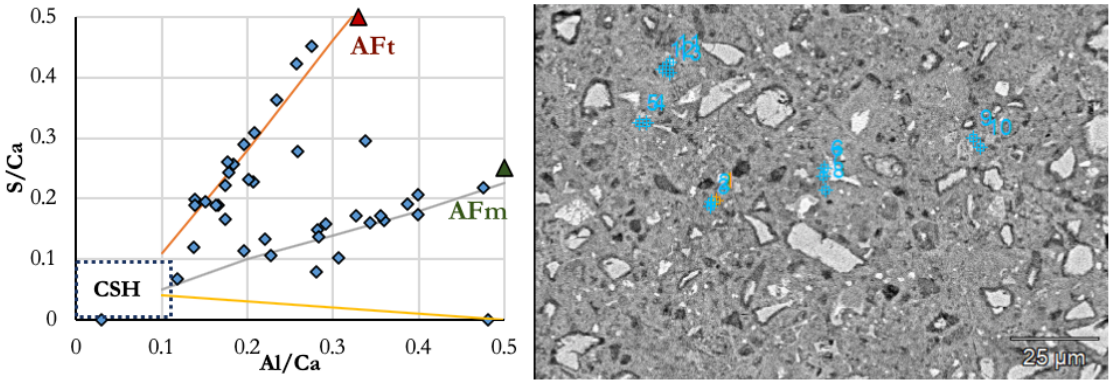

Figure 5.45: After Exposure Micro-Analysis CEM III/A .

Point analysis of CEM III-A revealed a significant scatter of the atomic concentration ratios between the AFt stretch as well as the in and around the region of AFm stretches. A number of positions under analysis indicated the presence of ettringite with higher sulphur concentrations i.e. above 0.2. and correspondingly lower aluminate ratios. A second significant concentration region was observed with a lower atomic ratio of Sulphur to Ca, with subsequent increase in Aluminium to Calcium ratio, indicative of the strong presence of AFm and/or monocarbonates phases. Since the corresponding carbon concentration at the same points were considerably high, it is expected that they were representative of carbo-aluminate phases. This observation is consistent with XRD data, that show significant peaks for ettringite and some minor peak intensity for monocarbonates.

Despite a higher percentage of slag i.e. 50% along with high fineness of 600 m^2/kg , in CEM III/A system, there appeared a presence of AFt after exposure to the lime solution. It can be concluded that the effect of indistinguishable fineness eliminated the heterogeneous nucleation of slag particles. This would thus reflect in enhanced sulphate apprehension leading to more AFt formation due to high fineness of clinker present. Also, since the sulphite to aluminate ratio of the system is closer to the pessimum value of 0.5, the complete elimination of AFt formation is averted.

Upon random point analysis surrounding outer hydration products, significant concentrations of magnesium, as well as aluminium, were identified. Thereby indicating the presence of magnesium bearing phases, consistent with XRD results, that show the presence of dolomite crystals.

Custom Blended Systems

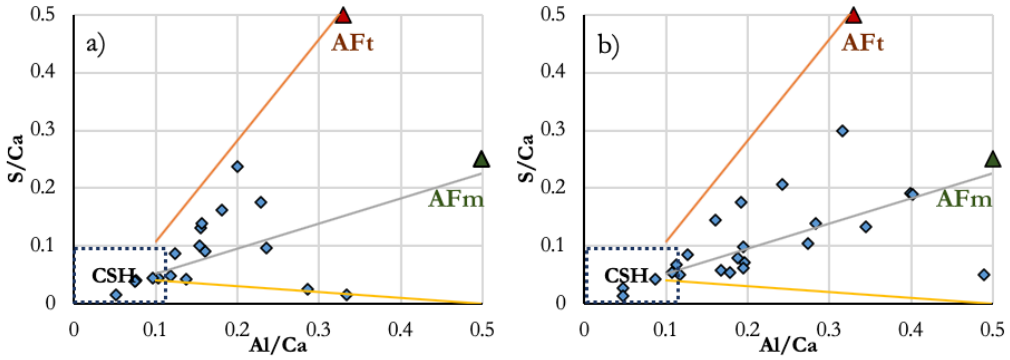

Figure 5.46: After Exposure Micro-Analysis :a)20C , b)20F .

Both lower slag systems with varying fineness showed minor traces of ettringite lying within the defined boundaries. The lower sulphate ratio even at higher aluminates is thus indicative of hydrated calcium-aluminate phases along with possible carbo-aluminate phases. For the slag systems, confirmation of monocarbonates phases was emphasized not only with lower sulphate ratios but also a subsequent clear indicative presence of carbon at the shot regions. This information is in congruence with XRD results that indicated a clear presence of carbonate phases and absence of ettringite. Although monosulphate presence was observed in chemical analysis, the possibility of minor quantities could have reflected their absence while detection using XRD technique.

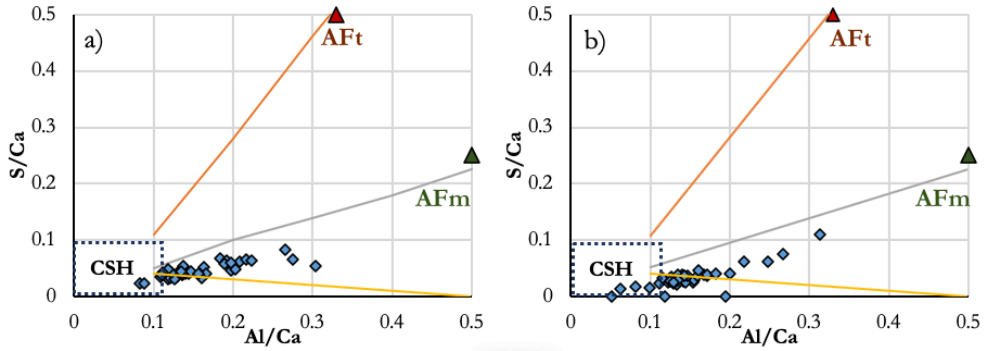

Figure 5.47: After Exposure Micro-Analysis :a)50C , b)50F .

Observing the chemical analysis for 50% slag composition systems, a distinct absence of AFt phases was confirmed. Consequently, a strong indication of carbo-aluminate phases was realised as at higher aluminate ratios, sulphate concentrations were seen at less than 0.1 ratios. The analysis also revealed the existence of carbon in the same spots as analysed for aluminate phases, thereby confirming the presence of carbo-aluminates. Traces of Mg was also revealed upon analysis, supporting the presence of hydrotalcites and other Mg bearing phases. These results were again in agreement with diffraction results that indicated the presence of carbo-aluminates and absence of AFt phase after 90 days of exposure. Here, contrary to 50% slag in Industrial blends, in the custom-blended system, the divergent fineness enables localised nucleation of the slag particles. This therein enables more competition for sulphate and aluminates in the overall binders, thereby reducing AFt formations after exposure. Also, the sulphite to aluminate ratio is much below the pessimum of 0.5, along with a strong presence of carbon surpassed the sulpho-aluminate formation to carbo-aluminate formation.

5.5. Thermodynamic Modelling Outputs

5.5.1. Hydration Phase Assemblage

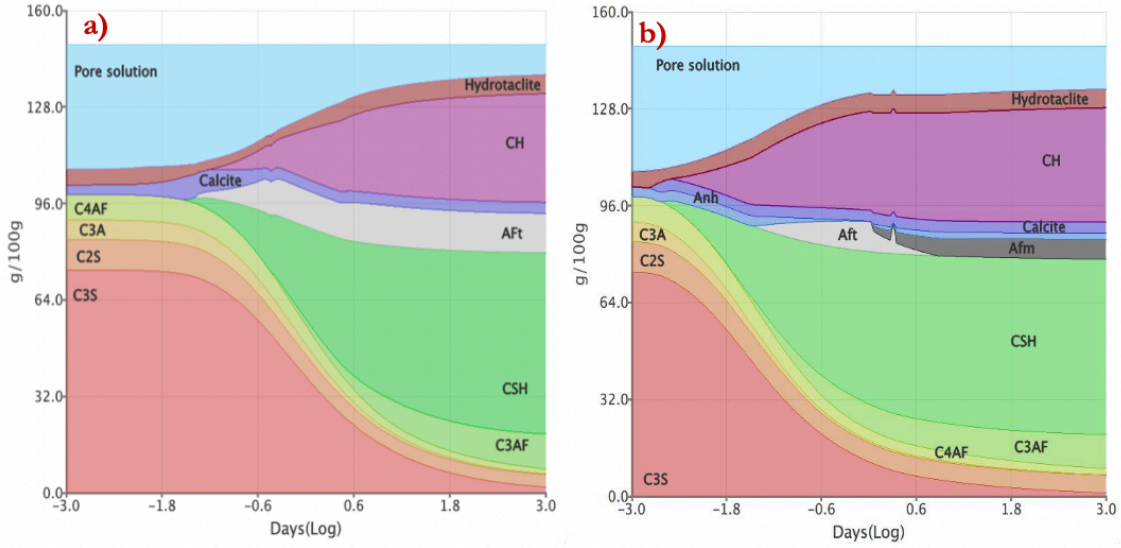

Figure 5.48: CEM I 52.5 Hydration model a)25°C and b)90°C .

In the case of CEM I system, at ambient temperature modelled the formation of only ettringite is observed. This is expected and in conjunction with the theory that ettringite persists at lower temperatures and more stable. Anhydrite minerals were not observed, re-iterating the mechanism were sulphate consumption is complete with ettringite formation during hydration.

In the case of high-temperature simulation, early hydration indicates the formation of ettringite, however, after a certain period the phase shifts to form monosulphate as a result of ettringite decomposition. Since the simulation does not account for the uptake of sulphate ions dissociated with high-temperature decomposition, the thermodynamic equilibrium is established between sulpho-aluminate phase and anhydrite phase.

A small peak due to AFt is observed in the case of high-temperature hydration, could be possibly a simulation lag when the anhydrite also persists, ettringite is formed momentarily but then later decomposed to form AFm. With respect to clinker composition, there appears the significant increase in hydration degree with high-temperature simulation, resulting in their reactivity as accounted for in the equation as discussed in section 5.2 resulting in phase changes during hydration.

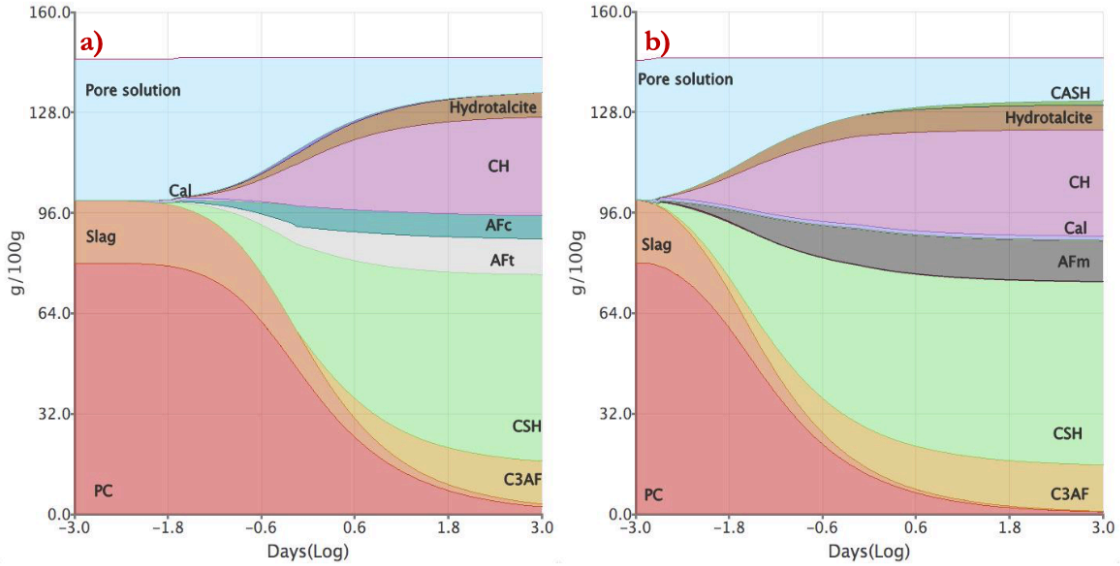

Figure 5.49: CEM II/B-S Hydration model a)25°C and b)90°C .

For CEM II/B-S system, the presence of ettringite and monocarbonate phases is observed at low-temperature hydration. Since the slag is present in the composite blends, there exists a considerable amount of carbon dioxide from the same that contributes towards the formation of monocarbonate phase. The carbo-aluminate phase replaces the ettringite phase that would have otherwise formed due to the limited amount of sulphate present initially.

In the case of high-temperature simulation, there is a clear absence of ettringite phases right from the beginning of hydration and presence of monosulphate phases only. This indicates that the decomposition ettringite is more prominent at lower sulphate ratios and enables faster persistence of monosulphate at elevated temperatures. Also, monocarbonates being thermally more stable at lower temperatures observed to have decomposed at elevated temperatures and the carbonates were present as calcite in the system. This confirms the thermodynamic balance between carbo-aluminates and calcite as a result of thermal effects.

There was no indication of anhydrite in the phase's analyses, probably due to its full consumption in the formation of monosulphate or being present in the pore solution. Formation of hydrogarnet species was observed to be more pronounced in the case of high-temperature hydration which can be understood that at normal temperature, the secondary hydration process for the reactivity of slag with portlandite is much slower. This is also confirmed by the increased formation of portlandite in the case of elevated hydration temperature. Here again, the decrease in hydration reactants is more pronounced for high-temperature hydration clearly indicating increased hydration degree.

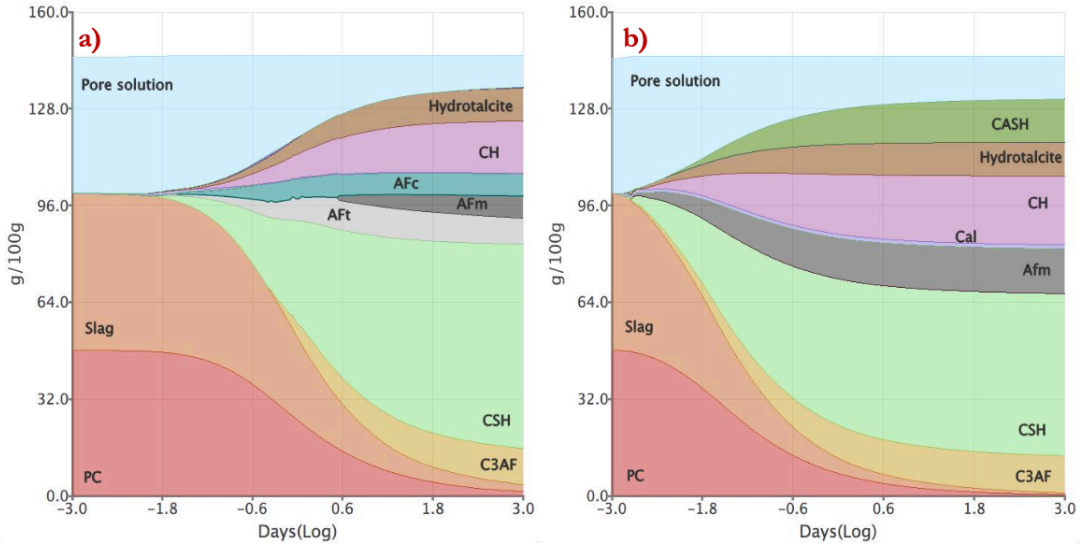

Figure 5.50: CEM III/A Hydration model a)25°C and b)90°C .

For a higher percentage of slag system, CEM III/A, the lower sulphate ratio is clearly indicative of the existence of both ettringite and monosulphate at lower temperature hydration. Also, the effect of lower sulphate ratio was also evident in the presence of carbonate species from slag composition as well as clinker was seen as the formation of monocarbonates.

At high-temperature hydration, similar to other systems absence of ettringite was seen. The presence of sulpho-aluminate phases was dominated by only AFm phase, due to the decomposition of ettringite along with monocarbonates. The released carbon was subsequently indicative of minor calcite phases being present at elevated temperatures. This once again confirms the thermodynamic balance between carbo-aluminates and calcite as a result of thermal effects.

Increased hydration degree was observed as a result of elevated temperature hydration, and subsequently higher amounts of hydrogarnet species were observed. Again, re-iterating the reaction of slag with portlandite instigated faster by elevated curing temperatures. No significant difference in portlandite amount is observed despite their consumption by slag, possibly due to accelerated formations from clinkers, overshadowing their subsequent consumption.

5.6. Pore solution Concentration

The simulations obtained for pore solution concentration changes at respective temperatures and hydration models is shown below.

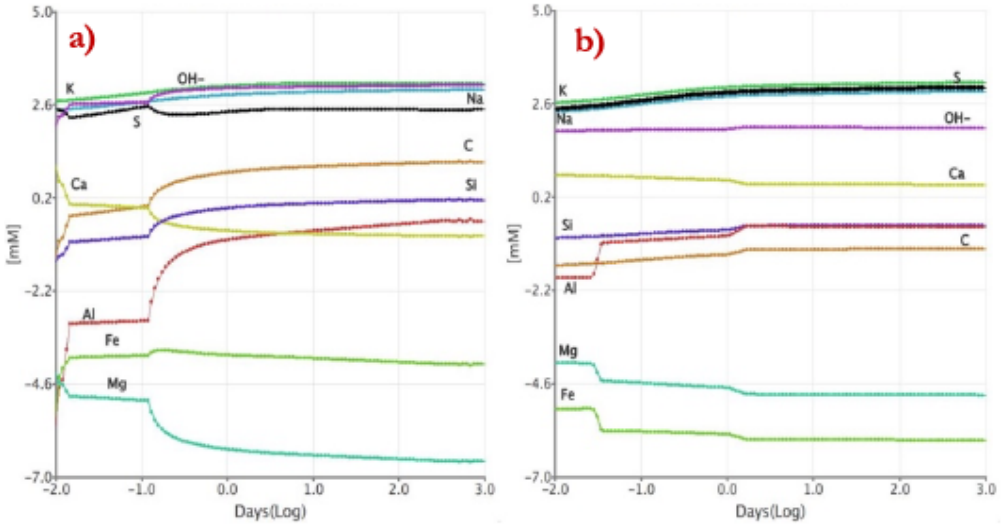

Figure 5.51: CEM I Pore solution concentration a)25°C and b)90°C .

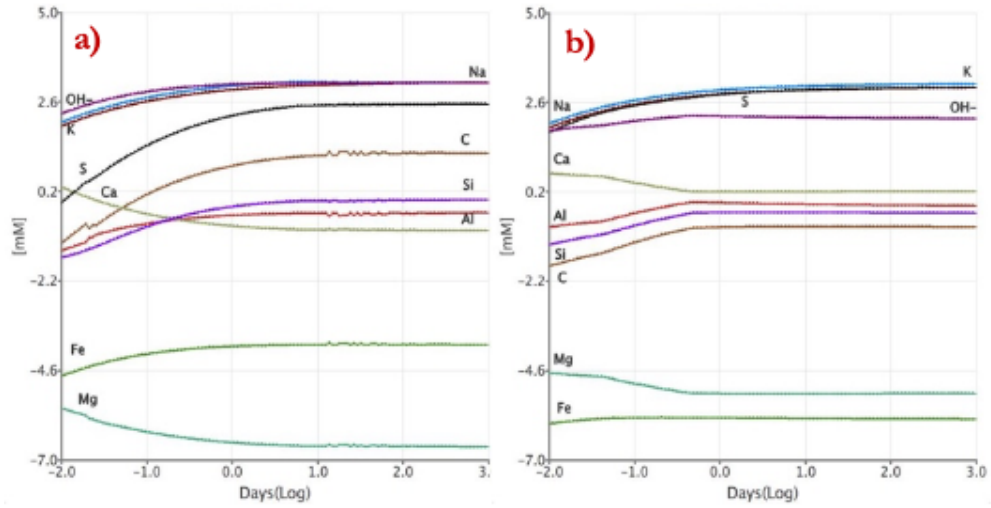

Figure 5.52: CEM II/B-S Pore solution concentration a)25°C and b)90°C .

Observing the pore solution concentration for low-temperature hydration of all the systems there exists the primary alkali ions in the pore solution throughout the low-temperature hydration such as Na, K and hydroxyl ions. There is a reduction in Ca ions which is expected due to the formation of calcium bearing phases during hydration. Also, the presence of Al, Fe and Mg ions were present in very low quantities throughout the hydration as they participate definitively in hydration phase assemblage.

With regard to slag blended systems, the amount of carbon shows a consistent increase in the

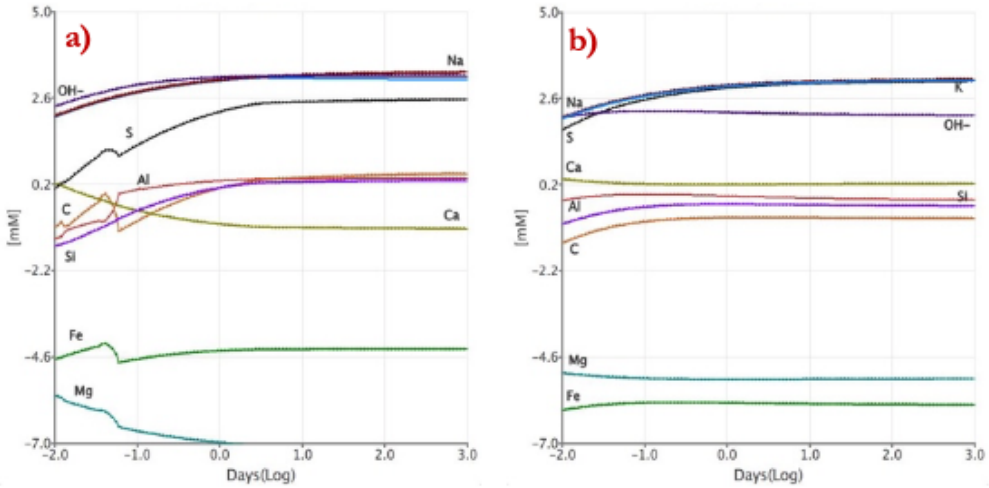

Figure 5.53: CEM III/A Pore solution concentration a)25°C and b)90°C .

case of CEM II/B-S system with higher concentration, while in for CEM III/A system, there is a small peak initially and then is followed by constant but at a lower concentration. This could be indicative of the presence of higher carbonate species present in the binder initially in the latter when compared to the former along with its competition between formation of monosulphate and monocarbonate formation being higher, with lower sulphate ratio.

In the case of high-temperature hydration similar observations were noted for all the systems. There is a minor reduction in the concentration of hydroxyl ion concentration along with calcium ions, which still persists in the solution. The presence of Ca still persistent in the pore solution indicates that it has leached as a result of ettringite decomposition due to its instability at high temperatures. This is also supported by the persistence of Sulphur ions in the pore solution during hydration. Moreover, a swap in the concentration of Fe and Mg is observed, where Mg appeared to decrease after prevalence, indicating the possibility of formation of magnesium bearing phases such as hydrotalcites.

6

Conclusion

The research's primary focus is on examination for the susceptibility of the studied binder systems for probably delayed ettringite formation, monitoring the phase changes and mechanisms involved during what is considered as induction period before the onset of physical expansion. Therefore, the subsequent study for deterioration extent is excluded from the current research. The findings of the scientific research conducted are summarized and conclusions are drawn and the research questions are answered. From the experimental program, the following conclusions are drawn.

1. **"Examination for the susceptibility of secondary ettringite formation after exposure period"**

   1.a *The presence of slag although with lower sulphite to alumina ratio revealed ettringite formations in the case of industrial blended systems and AFc in the case of custom-blended systems*.

   The pessimum value for sulphate ratio is observed to be much lower than 0.4 in combination with ferrite composition for the case of 50% slag composition. Therefore, to fully limit Aft formation, the percentage of slag is recommended to be higher than 50% along with lower pessimum ratio. This result is consistent with mineralogical change analysis and also concluded through micro-analysis study.

   1.b *The effect of binder composition appeared to have a significant role in the early hydration phase change characteristic as well as during subsequent exposure changes*.

   The effect of Al_2O_3/Fe_2O_3 ratio appears to influence the participation of available alumina considerably for sulpho-aluminate formations during both study periods. The effect of alkalis present appeared to play an important role through pH environment and competition for other hydration products, in AFt and AFc formations despite lower sulphate ratio. This translates the pH of the pore solution which affect the uptake of leached ions during the saturation period.

2. **"Observation on pore structure evolution as an effect of high-temperature curing and phase assemblage mechanism during induction period"**

   2.a *The evolution of pore structure revealed refinement during the exposure period as a result of calcium-aluminate crystal formations in combination with silicate hydrate gels.*

   The changes in pore volume variation revealed the limited crystallisation in lower pore

diameter ranges i.e. within silicate gel formations and thus the possibility of a swelling theory is suggested. The presence of cluster like AFt formations as observed in SEM image analysis also supports this theory.

2.b *The divergence of fineness along with substitution level of the slag to clinker appeared to have an influence on pore structure during the early stages of elevated temperature curing and attenuate during exposure.*

The effect of fineness of slag was more pronounced immediately after curing, however primarily for a lower percentage of replacement as a result of the possible agglomeration of particles. This effect was overshadowed by the dilution effect in the case of high replacement level of slag. However, the effect of combined high fineness of CEM III/A system also revealed agglomeration immediately after curing. This result is consistent with pore structure evolution data as well as image analysis.

3. **"Determine the effect of fineness on delayed ettringite formation and phase assemblage at a high temp."**

3.a *The impact of fineness of slag on the hydration products was confirmed during and after exposure.*

The alkalinity of pore solution appeared to have the influence of fineness of the slag system with 50% replacement levels, which showed increased activity relating to the uptake of alkali ions during elevated hydration temperature. This had a considerable impact on the availability of alumina to be present during the exposure period, leading to the formation of carbo-aluminate species. The effect of fineness in the case of 20% slag composition looked to override the effect of high Al_2O_3/Fe_2O_3 ratio for hydrogarnet formations during curing. However, in the case of 50% slag replacement, this impact was lower as a result of the dilution effect. After the exposure to the lime solution, the effect was reversed for 50% slag level, that showed a considerable increase in hydrogarnet phase in the case of finer slag. Also, the effect of fineness on portlandite consumption was limited immediately after curing was surpassed by the amount of slag replacement level. In conclusion, the fineness of slag observed to have an indirect effect on delayed ettringite formation.

Thermodynamic modelling of high temperature was conducted on the primary assumption of using empirical models for the degree of hydration for complete hydration until 1200 days. The conclusions from the simulations are summarised below:

4. **"Thermodynamic modelling investigation of cementitious systems with slag at elevated temperatures"**

4.a *Decomposition of ettringite was observed in all the industrial blended systems.*

Simulations showed clear decomposition of ettringite to monosulphate species that

were otherwise prevalent during ambient temperature hydration in the cases of all systems studied. Slag blended systems showed the presence of Monocarbonate species at 25 C hydration which also subsequently was decomposed at high temperatures. The presence of slag indicated hydrogarnet formations at high temperatures along with an increase in the degree of hydration. The results of the simulations appeared to be in correlation with the experimental study.

4.b *Changes in pore solution concentration was observed in the industrial blends at elevated temperature.*

The concentration of sulphur and calcium ions showed an increase as a result of decomposition and subsequent reduction in Mg was also recorded which reflected in the presence of hydrotalcite phase.

7

Reflection and Recommendation

Reflection

Reflecting back on conducted research, some valuable improvements are proposed:

- Repeatability of the results to obtain more statistical data for XRD, MIP,SEM and pH measurements.
- Full scan for chemical analysis on SEM specimens in order to see phase changes in other primary hydration products such as Ca/Si ratio in CSH gel.
- Quantitative measurements on mineralogical changes would enable optimisation of composition eliminating DEF mechanisms.

As part of the experimental research carried out, it primarily involved results and conclusions that aimed at understanding the mechanisms and assessing the probability for delayed ettringite formation. The work conducted was a reflection on prior works done and conducted on the basis of conceptual knowledge considering multi factorial effects.The further steps along this research propaganda would be thus to understand the extent of deteriorating nature,if any. Therefore, the following recommendations are suggested.

1. **Extend the current research work to Expansion studies in concrete specimens**

   As understood from the conclusions derived,the availability of capillary pore volume along with AFc formations,The impact of re-crystallisation need not be always deteriorating for the structure.Therefore, length change measurements are recommended.

2. **Extension for Studying the effect of internal crystallisation on transport properties**.

   Since the effect of mobility of available sulphate and alumina ions play an important role in crystal formations, the pore structure connectivity can be explored to understand its subsequent effect in relation to fineness effect.

3. **Combined effect of carbonation on delayed ettringite formation can be explored.**

Since the presence of carbonates in the raw material appear to have considerable impact on the sulpho-aluminate formations, the effect of atmospheric carbonation can be studied as they both occur under similar environmental conditions.

It was learned that thermodynamic modelling is an excellent tool to predict hydration phase assemblage for case specific environmental conditions. The current work focuses on the initial hydration mechanisms and thus further scope for research is suggested below:

1. **Translation of real-time hydration degree is recommended**

   Calorimetric study is proposed to obtain experimental data on hydration degree calculations to obtain realistic predictions reflecting on specific applications.

2. **Extending the hydration model to durability study for internal sulphate attack**

   Thermodynamic modelling accommodates computation of chemical parameters through specific codes in order to simulate exposure environment and thus its possibility to model the delayed ettringite formation is suggested.

Bibliography

[1] K. Tosun, "Effect of SO3 content and fineness on the rate of delayed ettringite formation in heat cured Portland cement mortars," *Cement and Concrete Composites*, vol. 28, no. 9, pp. 761–772, 2006.

[2] K. Van Tittelboom and N. De Belie, *Self-healing in cementitious materials-a review*, vol. 6. 2013.

[3]

[4] H. F. Taylor, C. Famy, and K. L. Scrivener, "Delayed ettringite formation," *Cement and Concrete Research*, vol. 31, no. 5, pp. 683–693, 2001.

[5] N. Leklou, V. H. Nguyen, and P. Mounanga, "The effect of the partial cement substitution with fly ash on Delayed Ettringite Formation in heat-cured mortars," *KSCE Journal of Civil Engineering*, vol. 21, no. 4, pp. 1359–1366, 2017.

[6] E. S. N. H. Xu Ma, Oguzhan Copuroglu and F. Xing, "Expansion and degradation of cement paste in sodium sulfate solutions," vol. 158, pp. 410–422, 2018.

[7] R. Barbarulo, H. Peycelon, S. Prené, and J. Marchand, "Delayed ettringite formation symptoms on mortars induced by high temperature due to cement heat of hydration or late thermal cycle," *Cement and Concrete Research*, vol. 35, no. 1, pp. 125–131, 2005.

[8] S. O. Ekolu, "Heat curing practice in concrete precasting technology–problems and future directions," *Concrete Society of Southern Africa*, vol. 114, pp. 5–10, 2006.

[9]

[10] Y. Fu and J. J. Beaudoin, "Mechanisms of delayed ettringite formation in portland cement systems," *ACI Materials Journal*, vol. 93, no. 4, pp. 327–333, 1996.

[11] R. Barbarulo, H. Peycelon, and S. Leclercq, "Chemical equilibria between C-S-H and ettringite, at 20 and 85 °C," *Cement and Concrete Research*, vol. 37, no. 8, pp. 1176–1181, 2007.

[12] J. Skalny and F. W. Locher, "Curing practices and internal sulfate attack - The European experience," *Cement, Concrete and Aggregates*, vol. 21, no. 1, pp. 59–63, 1999.

[13] Y. Fu, P. Gu, P. Xie, and J. J. Beaudoin, "A kinetic study of delayed ettringite formation in hydrated portland cement paste," *Cement and Concrete Research*, vol. 25, no. 1, pp. 63–70, 1995.

[14] H. Y. Ghorab, "On the chemistry of delayed ettringite formation," no. September, pp. 65–81, 2006.

[15] C. Famy, K. L. Scrivener, A. Atkinson, and A. R. Brough, "Influence of the storage conditions on the dimensional changes of heat-cured mortars," *Cement and Concrete Research*, vol. 31, no. 5, pp. 795–803, 2001.

[16] I. Odler and Y. Chen, "Effect of cement composition on the expansion of heat-cured cement pastes," *Cement and Concrete Research*, vol. 25, no. 4, pp. 853–862, 1995.

[17] P. L. Mulongo and S. O. Ekolu, "Kinetic model to predict cement susceptibility to delayed ettringite formation. Part 2: Model validation and application," *Magazine of Concrete Research*, vol. 65, no. 10, pp. 640–646, 2013.

[18] A. Yammine, "Micromechanical modelling of damage induced by delayed ettringite formation," 2019.

[19] L. G. Baquerizo, T. Matschei, and K. L. Scrivener, "Impact of water activity on the stability of ettringite," *Cement and Concrete Research*, vol. 79, pp. 31–44, 2016.

[20] A. Pavoine, L. Divet, and S. Fenouillet, "A concrete performance test for delayed ettringite formation: Part II validation," *Cement and Concrete Research*, vol. 36, no. 12, pp. 2144–2151, 2006.

[21] S. Kelham, "The effect of cement composition and fineness on expansion associated with delayed ettringite formation," *Cement and Concrete Composites*, vol. 18, no. 3, pp. 171–179, 1996.

[22] T. Ramlochan, M. D. Thomas, and R. D. Hooton, "The effect of pozzolans and slag on the expansion of mortars cured at elevated temperature: Part II: Microstructural and microchemical investigations," *Cement and Concrete Research*, vol. 34, no. 8, pp. 1341–1356, 2004.

[23] J. France-Mensah, "Development of Leachate Test for Delayed Ettringite Formation Potential in Cementitious Materials," no. 1, p. 87, 1989.

[24] I. Cigrovski, "Some Aspects of the Delayed Ettringite Formation in Concrete-a Review," no. 1, pp. 1–9, 2014.

[25] T. Ramlochan, M. D. Thomas, and R. D. Hooton, "The effect of pozzolans and slag on the expansion of mortars cured at elevated temperature: Part II: Microstructural and microchemical investigations," *Cement and Concrete Research*, vol. 34, no. 8, pp. 1341–1356, 2004.

[26] W. Kunther, B. Lothenbach, and J. Skibsted, "Influence of the Ca/Si ratio of the C-S-H phase on the interaction with sulfate ions and its impact on the ettringite crystallization pressure," *Cement and Concrete Research*, vol. 69, pp. 37–49, 2015.

[27] Y. Amine, N. Leklou, and O. Amiri, "Effect of supplementary cementitious materials (scm) on delayed ettringite formation in heat-cured concretes," *Energy Procedia*, vol. 139, pp. 565–570, 2017.

[28] T. Ramlochan, P. Zacarias, M. D. Thomas, and R. D. Hooton, "The effect of pozzolans and slag on the expansion of mortars cured at elevated temperature: Part I: Expansive behaviour," *Cement and Concrete Research*, vol. 33, no. 6, pp. 807–814, 2003.

[29] S. O. Ekolu, M. D. Thomas, and R. D. Hooton, "Implications of pre-formed microcracking in relation to the theories of DEF mechanism," *Cement and Concrete Research*, vol. 37, no. 2, pp. 161–165, 2007.

[30] H. F. Taylor, C. Famy, and K. L. Scrivener, "Delayed ettringite formation," *Cement and Concrete Research*, vol. 31, no. 5, pp. 683–693, 2001.

[31] W. G. Hime, S. L. Marusin, Z. T. Jugovic, R. A. Martinek, R. A. Cechner, and L. A. Backus, "Chemical and petrographic analyses and ASTM test procedures for the study of delayed ettringite formation," *Cement, Concrete and Aggregates*, vol. 22, no. 2, pp. 160–168, 2000.

[32] G. S. Barger, J. Bayles, B. Blair, D. Brown, H. Chen, T. Conway, and P. Hawkins, "Ettringite Formation and the Performance of Concrete," *Portland Cement Association*, no. 2166, pp. 1–16, 2001.

[33] W. Deboucha, N. Leklou, and A. Khelidj, "Blast Furnace Slag Addition Effects on Delayed Ettringite Formation in Heat-cured Mortars," *KSCE Journal of Civil Engineering*, vol. 22, no. 9, pp. 3484–3490, 2018.

[34] V. H. Nguyen, N. Leklou, J. E. Aubert, and P. Mounanga, "The effect of natural pozzolan on delayed ettringite formation of the heat-cured mortars," *Construction and Building Materials*, vol. 48, pp. 479–484, 2013.

[35] B. Lothenbach, "Thermodynamic equilibrium calculations in cementitious systems," *Materials and Structures/Materiaux et Constructions*, vol. 43, no. 10, pp. 1413–1433, 2010.

[36] B. Lothenbach and M. Zajac, "Application of thermodynamic modelling to hydrated cements," *Cement and Concrete Research*, vol. 123, no. January, 2019.

[37] B. Lothenbach, G. Le Saout, E. Gallucci, and K. Scrivener, "Influence of limestone on the hydration of Portland cements," *Cement and Concrete Research*, vol. 38, no. 6, pp. 848–860, 2008.

[38] B. Lothenbach and A. Nonat, "Calcium silicate hydrates: Solid and liquid phase composition," *Cement and Concrete Research*, vol. 78, pp. 57–70, 2015.

[39] B. Kolani, L. Buffo-Lacarrière, A. Sellier, G. Escadeillas, L. Boutillon, and L. Linger, "Hydration of slag-blended cements," *Cement and Concrete Composites*, vol. 34, no. 9, pp. 1009–1018, 2012.

[40] R. J. Myers, B. Lothenbach, S. A. Bernal, and J. L. Provis, "Thermodynamic modelling of alkali-activated slag cements," *Applied Geochemistry*, vol. 61, pp. 233–247, 2015.

[41] Y. Elakneswaran, E. Owaki, S. Miyahara, M. Ogino, T. Maruya, and T. Nawa, "Hydration study of slag-blended cement based on thermodynamic considerations," *Construction and Building Materials*, vol. 124, pp. 615–625, 2016.

[42] D. P. Prentice, B. Walkley, S. A. Bernal, M. Bankhead, M. Hayes, and J. L. Provis, "Thermodynamic modelling of BFS-PC cements under temperature conditions relevant to the geological disposal of nuclear wastes," *Cement and Concrete Research*, vol. 119, no. January, pp. 21–35, 2019.

[43] K. Sato, T. Saito, M. Kikuchi, and T. Saeki, "Relationship between expansion characteristics of heat-cured mortars during water curing and origins of ettringite formation," *Journal of Advanced Concrete Technology*, vol. 17, no. 5, pp. 260–268, 2019.

[44] P. Gao, G. Ye, J. Wei, and Q. Yu, "Multi-scale simulation of capillary pores and gel pores in Portland cement paste," *14th International Congress on the Chemistry of Cement*, vol. 31, no. 0, 2015.

[45] B. Lothenbach, T. Matschei, G. Möschner, and F. P. Glasser, "Thermodynamic modelling of the effect of temperature on the hydration and porosity of Portland cement," *Cement and Concrete Research*, vol. 38, no. 1, pp. 1–18, 2008.

[46] D. Damidot, B. Lothenbach, D. Herfort, and F. P. Glasser, "Thermodynamics and cement science," *Cement and Concrete Research*, vol. 41, no. 7, pp. 679–695, 2011.

[47] B. Lothenbach, "Thermodynamic equilibrium calculations in cementitious systems," *Materials and Structures/Materiaux et Constructions*, vol. 43, no. 10, pp. 1413–1433, 2010.

[48] H. J. Kuzel, "Initial hydration reactions and mechanisms of delayed ettringite formation in Portland cements," *Cement and Concrete Composites*, vol. 18, no. 3, pp. 195–203, 1996.

[49] T. Matschei, "Thermodynamics of Cement Hydration," *phd at the University of Aberdeen*, no. December, p. 222, 2007.

[50] S. Bauer, B. Cornell, D. Figurski, T. Ley, J. Miralles, and K. Folliard, "Alkali-Silica Reaction and Delayed Ettringite Formation in Concrete: A Literature Review," *Federal Highway Administration Publications FHWA-HRT-04-113 (2004) and Techbrief FHWA-HRT-06-071*, vol. 7, no. 22, p. 74, 2006.

[51] N. C. Collier, "Transition and decomposition temperatures of cement phases - a collection of thermal analysis data," *Ceramics - Silikaty*, vol. 60, no. 4, pp. 338–343, 2016.

[52] J. Dai, Q. Wang, C. Xie, Y. Xue, Y. Duan, and X. Cui, "The effect of fineness on the hydration activity index of ground granulated blast furnace slag," *Materials*, vol. 12, no. 18, pp. 1–15, 2019.

[53] Y. Gu, R. P. Martin, O. Omikrine Metalssi, T. Fen-Chong, and P. Dangla, "Pore size analyses of cement paste exposed to external sulfate attack and delayed ettringite formation," *Cement and Concrete Research*, vol. 123, no. May, p. 105766, 2019.

[54] M. Öner, K. Erdogdu, and A. Günlü, "Effect of components fineness on strength of blast furnace slag cement," *Cement and Concrete Research*, vol. 33, no. 4, pp. 463–469, 2003.

[55] A. Hadj-Sadok, S. Kenai, L. Courard, and A. Darimont, "Microstructure and durability of mortars modified with medium active blast furnace slag," *Construction and Building Materials*, vol. 25, no. 2, pp. 1018–1025, 2011.

[56] Y. Gu, R. P. Martin, O. Omikrine Metalssi, T. Fen-Chong, and P. Dangla, "Pore size analyses of cement paste exposed to external sulfate attack and delayed ettringite formation," *Cement and Concrete Research*, vol. 123, no. May, p. 105766, 2019.

[57] M. Whittaker, M. Zajac, M. Ben Haha, and L. Black, "The impact of alumina availability on sulfate resistance of slag composite cements," *Construction and Building Materials*, vol. 119, pp. 356–369, 2016.

A

Experimental Case Study

A. Experimental Case Study

S.No.	Title	Year	Specimen	Type	Dimensions (cm	Curing Temp	Exposure temp	Exposure Condition	Duration/Criteria	Description
1	Pore size analyses	2019	Paste	CEM 1 52.5	2 x 2 x 12 11 x 11 x 22			Tap water (no cycles)	Continuous (0.03% @ 200 days was observed in prism samples)	w/c = 0.55 ;Testing period :28 days ; Expansion : 0.03 % , >1%.; Vw/Vs = 26
2	Effect of SCM'S	2017	Concrete	CEM 1 52.5	11 dia x 22 L		20	Water exposure	Refreshing water at intervals	Vw/Vs = 1.5
3	Effect of Fly as for DEF Mitigation	2016	Mortar	CEM 1 52.5	4 x 4 x 16		20	De-ionized water @ 20 deg	Refreshing water every week till 24 weeks and every 4 weeks	total 650 days test; 10 % replacement showed early
4	Development of leachate test for DEF	2014	Mortar	Commercial	2.5 dia x 0.625 L			De-ionized water	90 days with testing at regular intervals	Ionic investiagtion from leached solutions
	Effect of wetting-drying cycles on mortar samples affected by DEF	2012	Mortar	CEM 1 52.5	4 x 4 x 16	80	20	Water @20 deg	5 days wetting @ 20 deg, 5 days dry @ 50 deg	Storage water NOT renewed
5	Effect of Natural Pozzolan	2013	Mortar	CEM 1 52.5 + Volcanic ash	4 x 4 x 16			De-ionized water (Continuous)	Non Renewed & Renewed water	0.1% expansion at 50 days , overall 490+ days
6	Reproduction of DEF in concrete and relationship between DEF and alkali silica reaction	2010	Mortar	HPC, OPC , White PC	4 x 4 x 16			Water @40 deg		
7	A concrete performance test for delayed ettringite formation: Part I optimisation	2006	Concrete	CEM 1 52.5	11 dia x 22 L				W/D & Permanent Immersion	Wet & Dry cylce showed accelerated results
8	effect of pozzolans and slag on the expansion of mortars cured at elevated temperature: Part I	2003	Mortar	Portland cement + Slag	2.5 x 2.5 x 28	60,70, 80,95		Lime saturated water	Complete Immersion	highest expansion at 95 deg
DEF Test Procedure (Slag Studies)										
1	Blast Furnace Slag effect	2018	Mortar	CEM 1 52.5 N + BFS	4 x 4 x 16			De-ionized water	Bath Renewal	750+ days, 10,20,40 % BFS ; 400,500 Finess
2	Relationship between expansion characteristc	2019	Mortar & Pastes		2 x 2 x 13			De-ionized water		Vw/Vs = 3:1 ; 40 ,70% BFS
3	Influence of Mineral Admixture	2010	Concrete	CEM 1 52.5 N + BFS	11 dia x 22 L			2 - Wet-Dry cycle , Tap water	7 wet, 7 dry ; Continous immersion	Water & Humidity condition ;10,15,20, 40% slag ; 450 -
4	The effect of pozzolans and slag on the expansion of mortars cured at elevated	2003	Mortar	CEM I + Slag	2.5 x 2.5 x 28	95		Lime saturated water	Complete Immersion	35 % slag showed 0.01 % expansion in 1200 days
5	Swellings due to alkali-silica reaction and delayed ettringite formation: Characterisation of expansion isotropy and effect of moisture conditions	2012	Mortar	Portland cement	4 x 4 x 16			Vw/Vs = 5 & 2 ,w/o renewal ;		

B

Material Information

Portland Cement

CEM I 52,5 R

CEM I

February 2018

MAASTRICHT

1. Standards and certificates

Cement type	Certificate	Standard	Certificate N°
CEM I 52,5 R	CE	EN 197-1	0956-CPR-1101.1032
CEM I 52,5 R	KOMO	BRL 2601	1101-16-1032
CEM I 52,5 R HES	Benor	NBN B12	18/10/108

2. Declared composition

	Units	Average Values	Requirements	
			Min	Max
	Constituents in % of the sum of the principal and secondary constituents			
Clinker (K)	%	100	95	100
Filler	%		-	5
	Additions in % of the cement			
Setting regulator	%	5,3	–	–
Grinding agent	%	0,019	–	–
Reducing agent*	%	0,28	–	–

3. Chemical properties

The chemical characteristics are determined in accordance with EN 196-2

	Units	Average Values	Requirements	
			Min.	Max.
CaO	%	64	-	-
SiO_2	%	20	-	-
Al_2O_3	%	5,06	-	-
Fe_2O_3	%	3	-	-
Sulfate SO_3	%	3,24	-	4,0
Insoluble residue	%	0,62	-	5,0
Loss on ignition	%	1	-	5,0
Chlorides	%	0,05	-	0,10
Chromium (VI)*	%	< 0,0002	-	0,0002
Na_2O equivalent	%	0,57		

* In accordance with the Regulation EC 1907/2006 (Reach), the soluble chromium (VI) content is limited to a maximum of 0.0002%. The chromium (VI) content is determined in accordance with EN 196-10.

ENCI

Technical Advise

Postbus 3233

5203 DE 's-Hertogenbosch

Tel: +31(0)73 640 12 20

tv@enci.nl

www.enci.nl

CBR Cementbedrijven

Technical Advise

Parc de l'Alliance

Boulevard de France 3-5

1420 BRAINE-L'ALLEUD

Tel: +32(0)2 678 35 10

Fax: +32(0)2 675 23 91

communications@cbr.be

www.cbr.be

Portlandslakcement CEM II/B-S

CEM II/B-S

CEM II/B-S 42,5 N

CEM II/B-S 52,5 N

ENCI
Technische Voorlichting
Postbus 3233
5203 DE 's-Hertogenbosch
Tel: 073 640 12 20
Fax: 073 640 12 18
tv@enci.nl
www.enci.nl

CBR Cementbedrijven
Afdeling Technische Voorlichting
Terhulpsesteenweg 185
1170 Brussel
Tel: 02 678 35 10
Fax: 02 675 23 91
communication@cbr.be
www.cbr.be

Productomschrijving

Portlandslakcement is een grijs cement dat verkregen wordt door het gezamenlijk malen van de hoofdcomponent portlandcementklinker met gegranuleerde hoogovenslak. Door de juiste verhouding portlandcement-klinker en hoogovenslak wordt, in combinatie met een bepaalde maalfijnheid een cement vervaardigd in de klasse 42,5 of 52,5. Afhankelijk van de sterkteklasse wordt dit cement gekenmerkt als een cement met een normale of hoge beginsterkte. Portlandslakcement CEM II/B-S voldoet aan de eisen zoals gesteld in de Europese cement-norm EN 197-1. Deze norm geeft eisen ten aanzien van de samenstel-ling op bestanddelen, chemische eisen, mechanische en fysische eisen.

Samenstelling

De eisen aan de samenstelling zijn uitgedrukt in procenten ten opzichte van de som van alle hoofd- en nevenbestanddelen. Dit totaal wordt nog vermeerderd met het nodige calciumsulfaat om het bindingsgedrag te regelen.

Cementsoort	Hoofdbestanddelen (in massa %)		Nevenbestanddelen (in massa %)
	Portlandcementklinker (K)	Hoogovenslak (S)	
CEM II/B-S	65-79	21-35	0 - 5

Mechanische en fysische eisen

De sterkteklasse van een cement bepaalt de minimale druksterkte gemeten na 28 dagen op normprisma`s. Binnen zijn normsterkteklasse heeft dit cement een normale beginsterkte, aangeduid met N. Het begin van de binding is een maat voor het opstijfgedrag van een cementpasta. Aan de eis van vormhoudendheid moet worden voldaan om te tonen dat een cementpasta niet gevoelig is voor expansie.

Sterkteklasse	Druksterkte in MPa				Begin van de binding (min.)	Vorm-houdend-heid (mm)
	Beginsterkte		Normsterkte			
	2 dagen	7 dagen	28 dagen			
42,5 N	≥ 10,0	-	≥ 42,5	≥ 62,5	≥ 60	≥ 10,0
52,5 N	≥ 20,0	-	≥ 52,5		≥ 45	≥ 10,0

Speciale eigenschappen

Cement dat voldoet aan de in EN 197-1 gestelde eisen is voorzien van een CE-markering.

ENCI HEIDELBERGCEMENT Group

CBR HEIDELBERGCEMENT Group

Hoogovencement

CEM III/A

CEM III/A 32,5 N

CEM III/A 32,5 N *LA*

CEM III/A 42,5 N *LA*

CEM III/A 42,5 N

CEM III/A 52,5 N

ENCI
Technische Voorlichting
Postbus 3233
5203 DE 's-Hertogenbosch
Tel: 073 640 12 20
Fax: 073 640 12 18
tv@enci.nl
www.enci.nl

CBR Cementbedrijven
Afdeling Technische Voorlichting
Terhulpsesteenweg 185
1170 Brussel
Tel: 02 678 35 10
Fax: 02 675 23 91
communication@cbr.be
www.cbr.be

Productomschrijving

Hoogovencement CEM III/A is een lichtgrijs cement dat verkregen wordt door het gezamenlijk malen van de hoofdcomponenten portlandcementklinker en gegranuleerde hoogovenslak. Door de juiste verhouding tussen de samenstellende bestanddelen wordt, in combinatie met een bepaalde maalfijnheid, een cement vervaardigd in de sterkteklasse 32,5, 42,5 of 52,5. Alle cementen worden binnen hun sterkteklasse gekenmerkt als een cement met een normale beginsterkte. Hoogovencement CEM III/A voldoet aan de eisen zoals gesteld in de Europese cementnorm EN 197-1, inclusief wijzigingsblad A1. Deze norm geeft eisen ten aanzien van de samenstelling op bestanddelen, chemische eisen, mechanische en fysische eisen.

Samenstelling

De eisen aan de samenstelling zijn uitgedrukt in procenten ten opzichte van de som van alle hoofd- en nevenbestanddelen. Dit totaal wordt nog vermeerderd met het nodige calciumsulfaat om het bindingsgedrag te regelen.

Cementsoort	Hoofdbestanddelen (in massa %)		Nevenbestanddelen (in massa %)
	Portlandcementklinker (K)	Hoogovenslak (S)	
CEM III/A	35 - 64	36 - 65	0 - 5

Mechanische en fysische eisen

De sterkteklasse van een cement bepaalt de minimale druksterkte gemeten na 28 dagen op normprisma's. Binnen zijn normsterkteklasse heeft dit cement een normale beginsterkte, aangeduid met N.
Het begin van de binding is een maat voor het opstijfgedrag van een cementpasta. Aan de eis van vormhoudendheid moet worden voldaan om aan te tonen dat een cementpasta niet gevoelig is voor expansie.

Sterkteklasse	Druksterkte in MPa				Begin van de binding (min.)	Vorm-houdend-heid (mm)
	Beginsterkte		Normsterkte			
	2 dagen	7 dagen	28 dagen			
32,5 N	–	≥ 16,0	≥ 32,5	≤ 52,5	≥ 75	≤ 10
42,5 N	≥ 10,0	–	≥ 42,5	≤ 62,5	≥ 60	
52,5 N	≥ 20,0	–	≥ 42,5	–	≥ 45	

Speciale eigenschappen

Cement dat voldoet aan de in EN 197-1 gestelde eisen is voorzien van een CE-markering. Daarnaast kan cement gecertificeerd worden op een aantal andere specifieke eigenschappen. Deze eigenschappen komen tot uiting in de naamgeving van het cement. De naamgeving is

ENCI HEIDELBERGCEMENT Group
CBR HEIDELBERGCEMENT Group

C

XRD results

Before Exposure

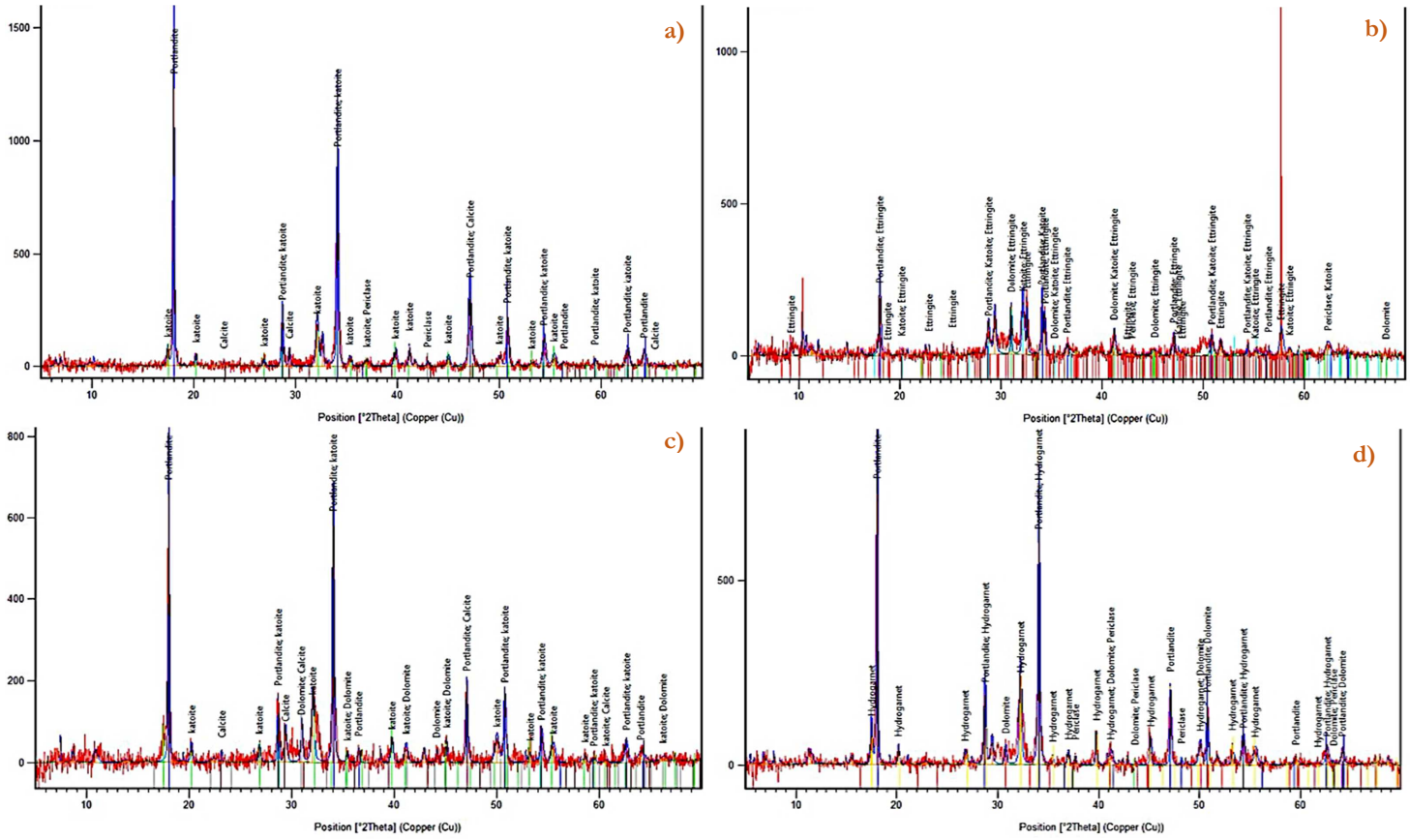

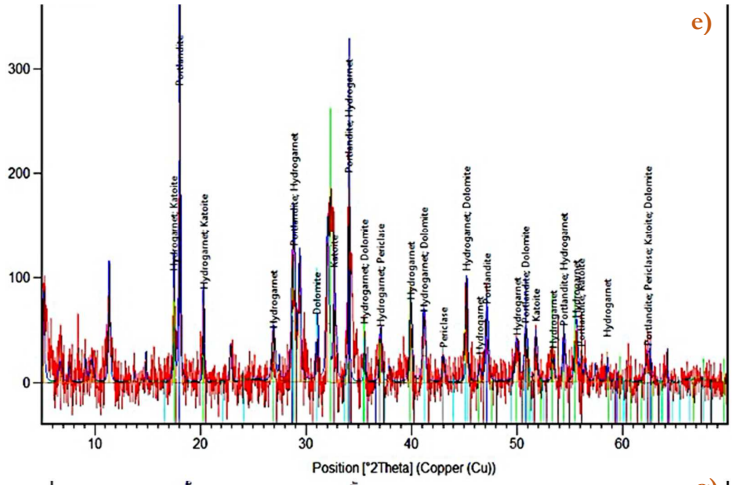

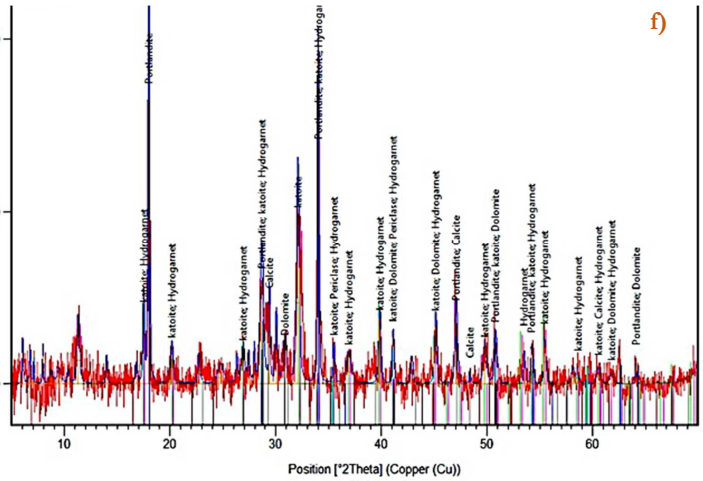

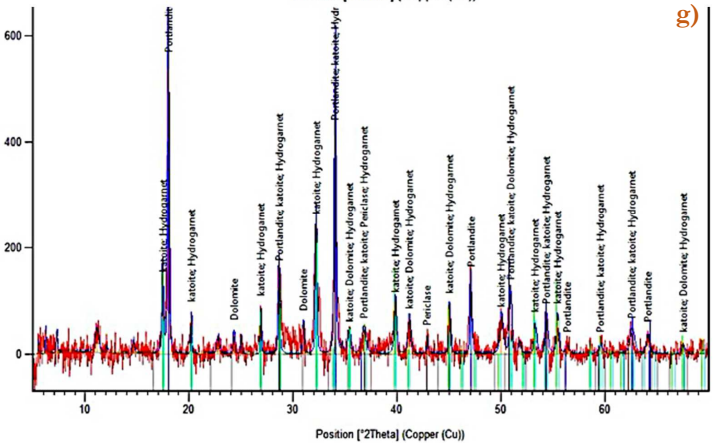

Diffraction Analysis for Before Exposure to lime solution

a) CEM I, b) CEM II/B-S, c) CEM III/A

d)20C , e)20F , f)50C , g)50F

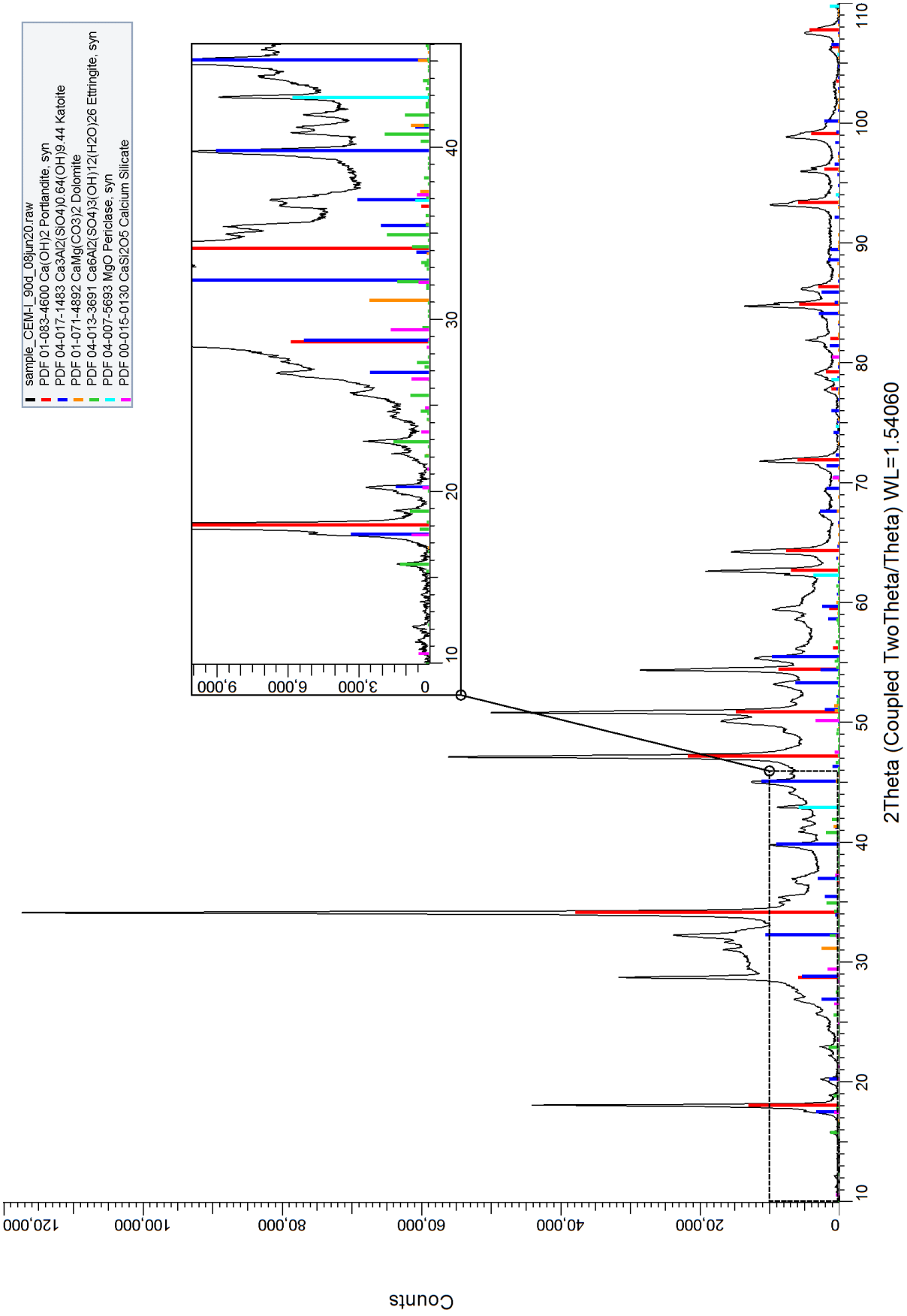

Figure 1 XRD pattern sample "CEM-I 90d"

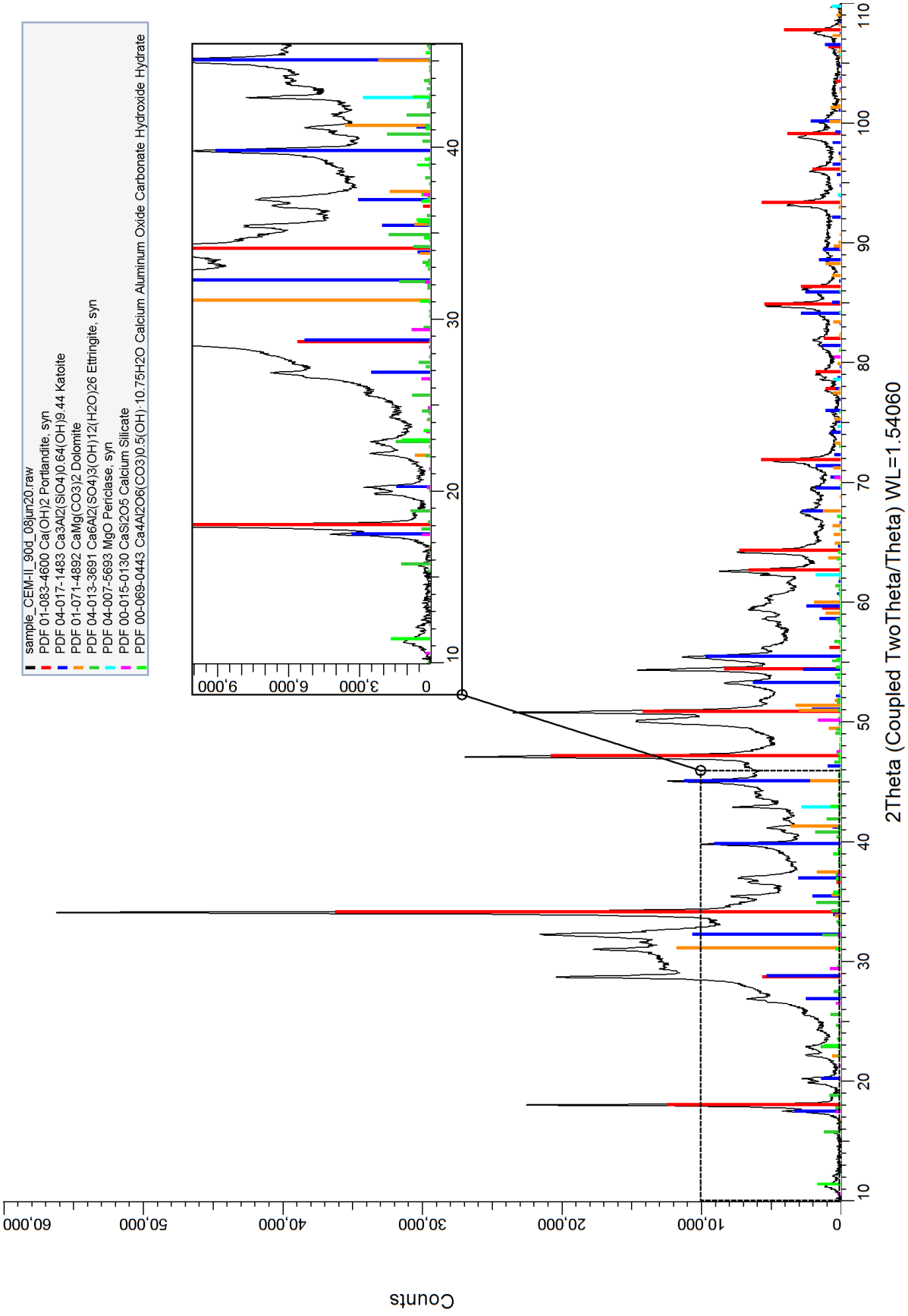

Figure 2 XRD pattern sample "CEM-II 90d "

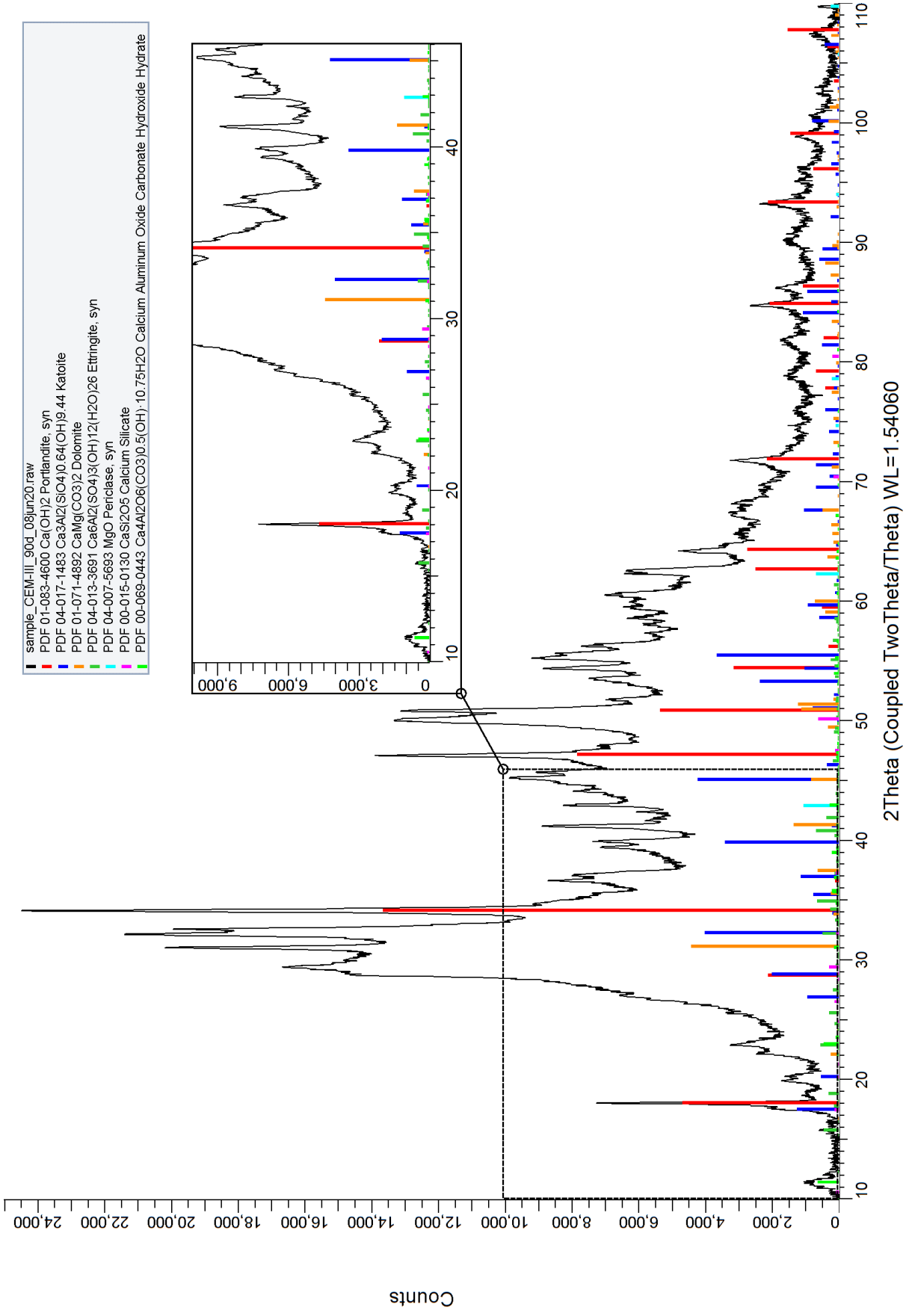

Figure 3 XRD pattern sample "CEM-III 90d"

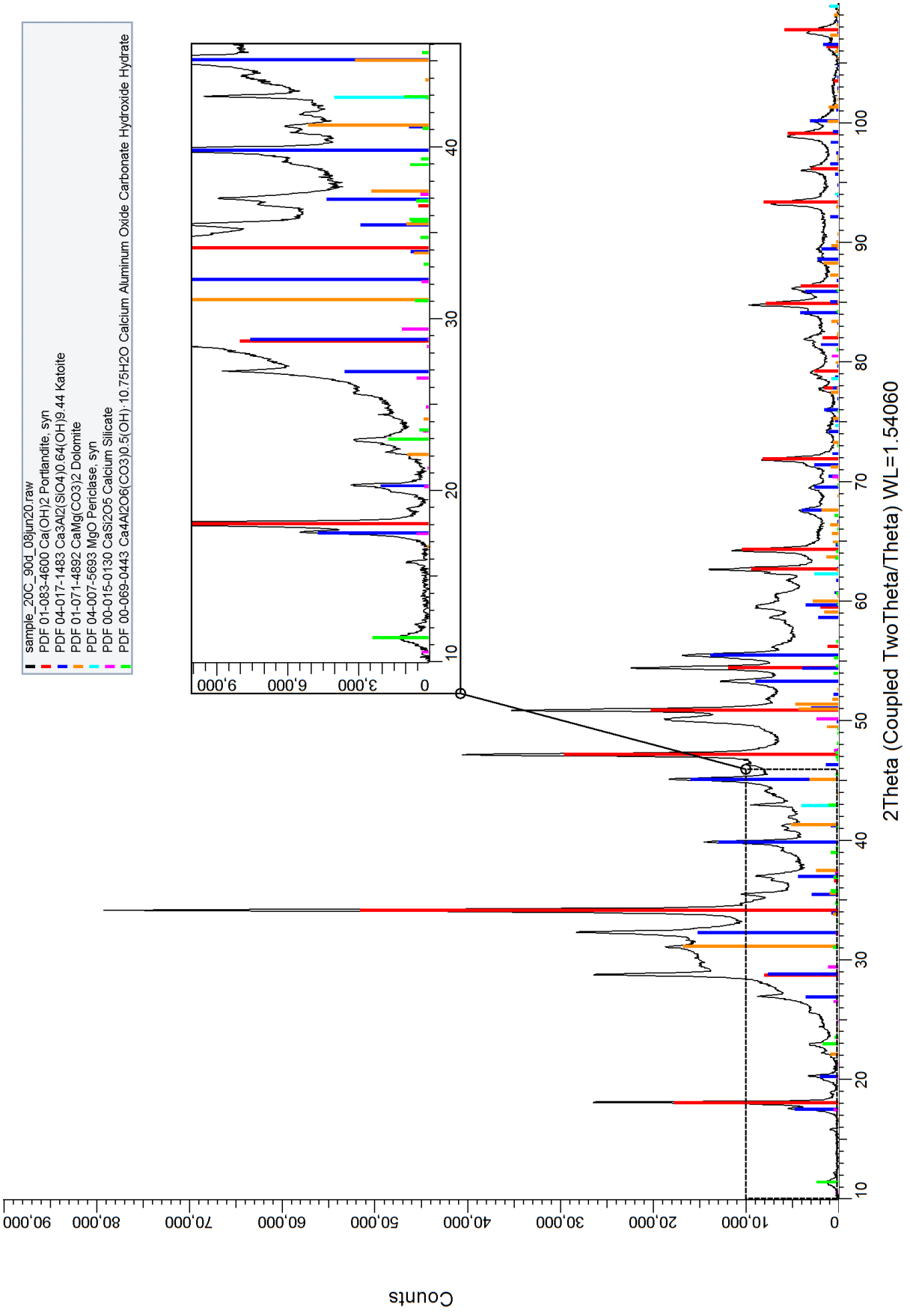

Figure 4 XRD pattern sample " 20C 90d"

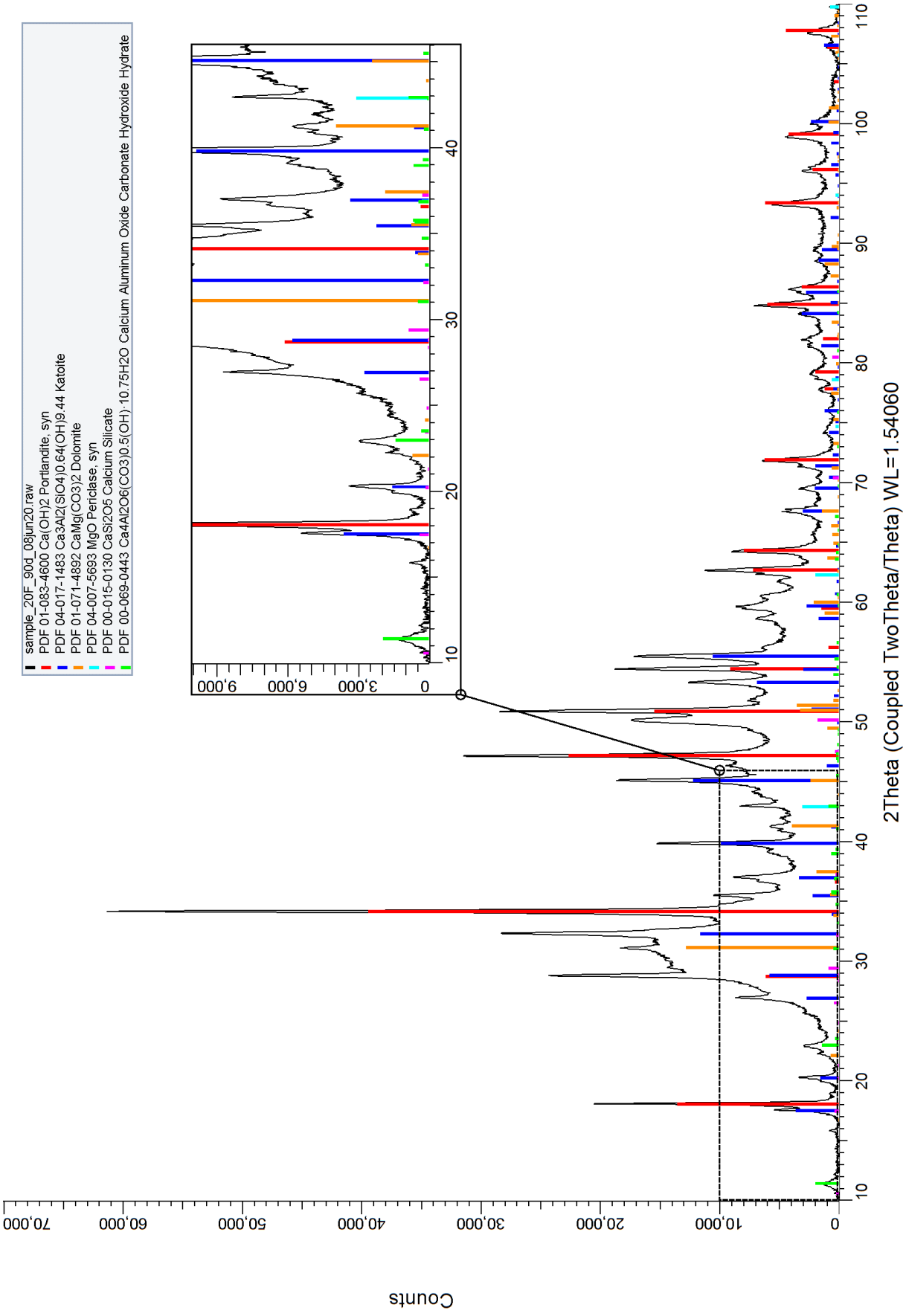

Figure 5 XRD pattern sample "20F 90d "

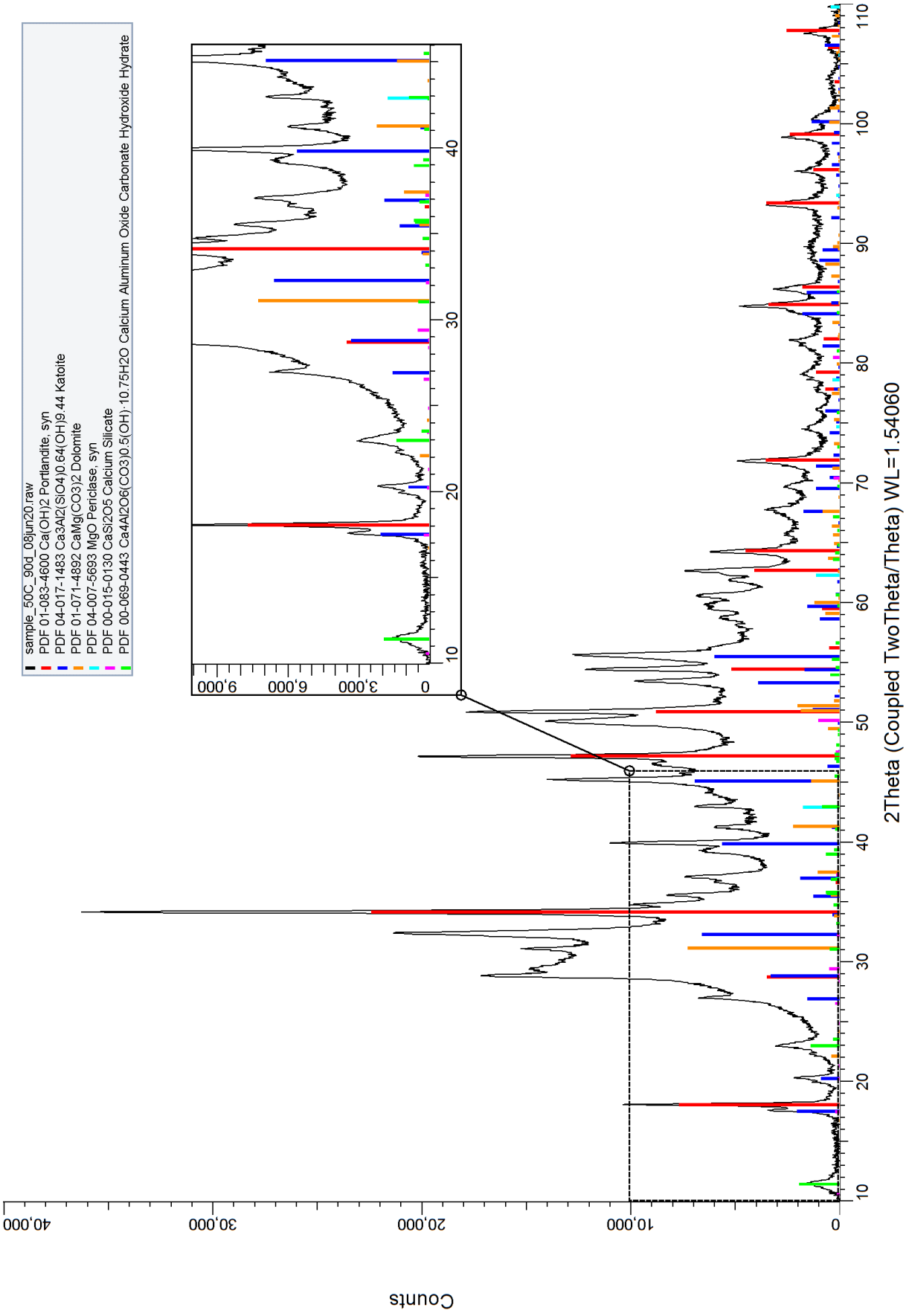

Figure 6 XRD pattern sample " 50C 90d"

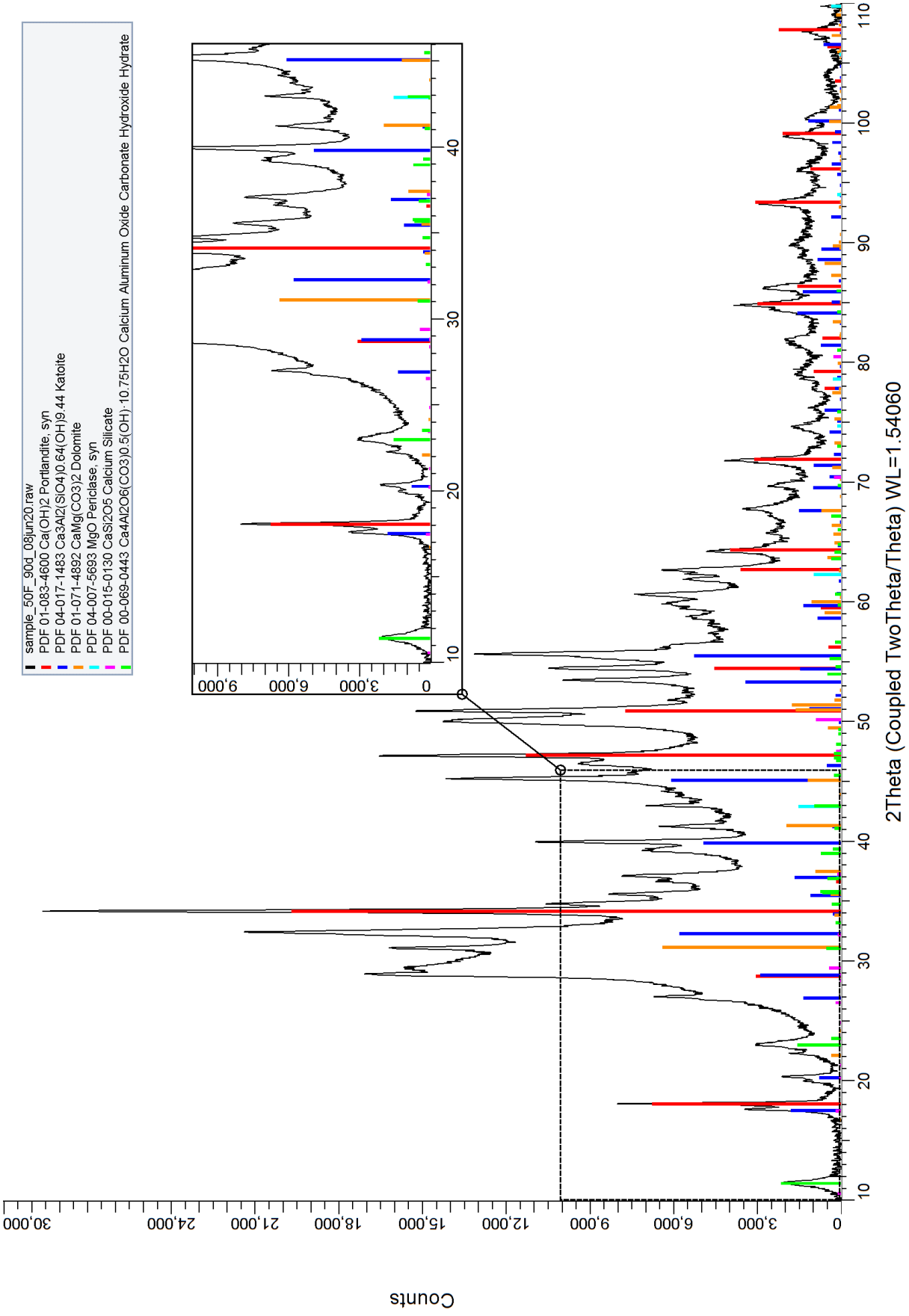

Figure 7 XRD pattern sample " 50F 90d"

D

SEM results

SEM Results

Before Exposure Micrographs

CEMI-D0

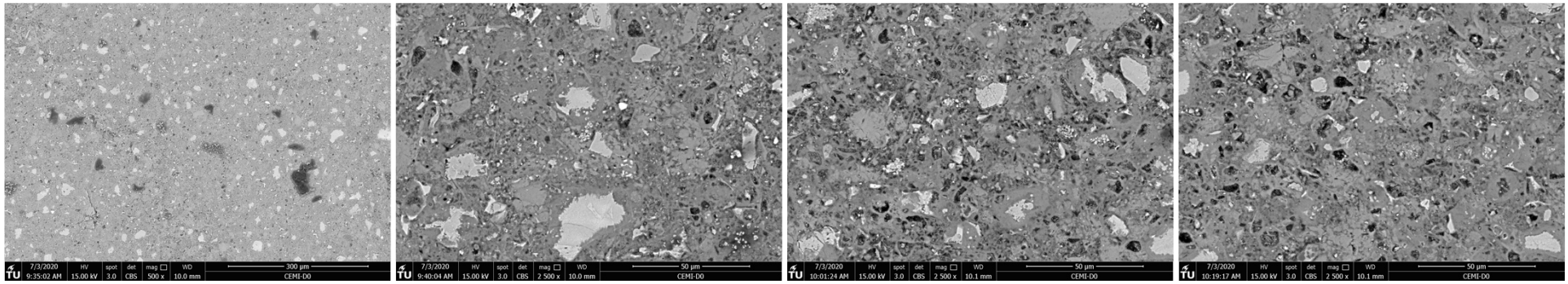

CEM II/B-S -D0

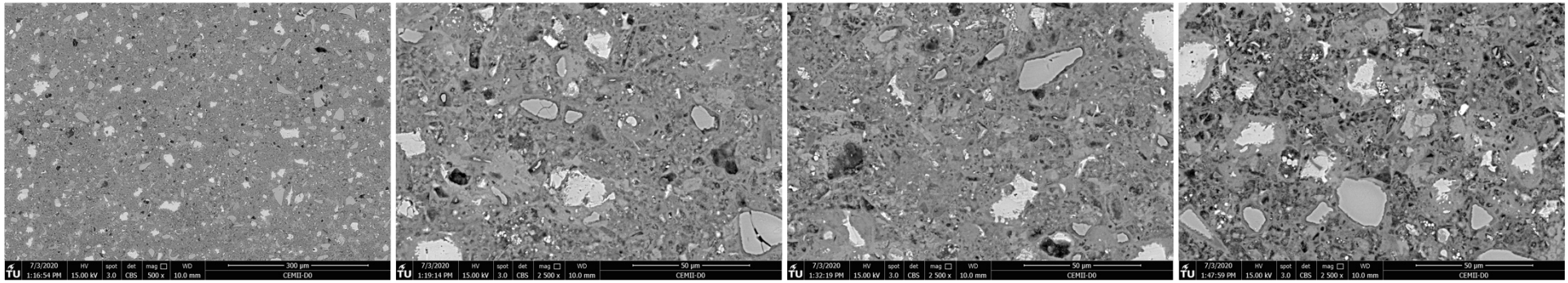

CEM III/A-D0

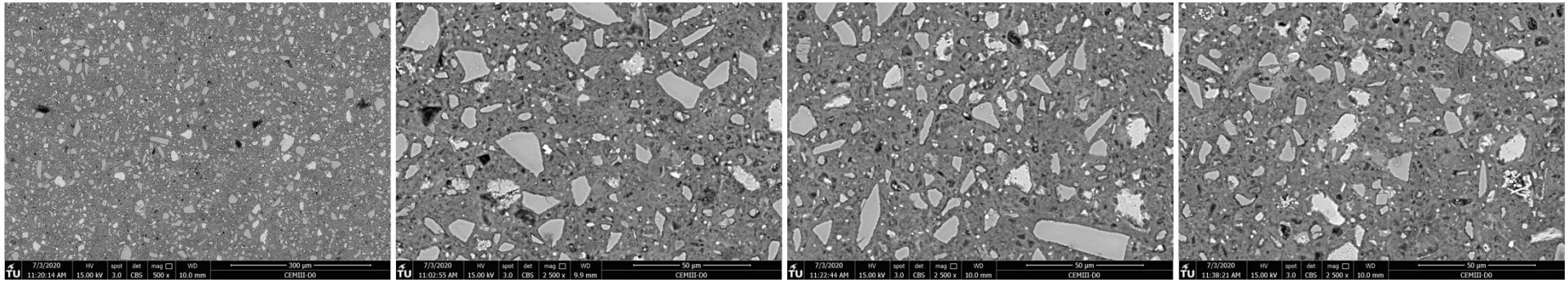

20C-D0

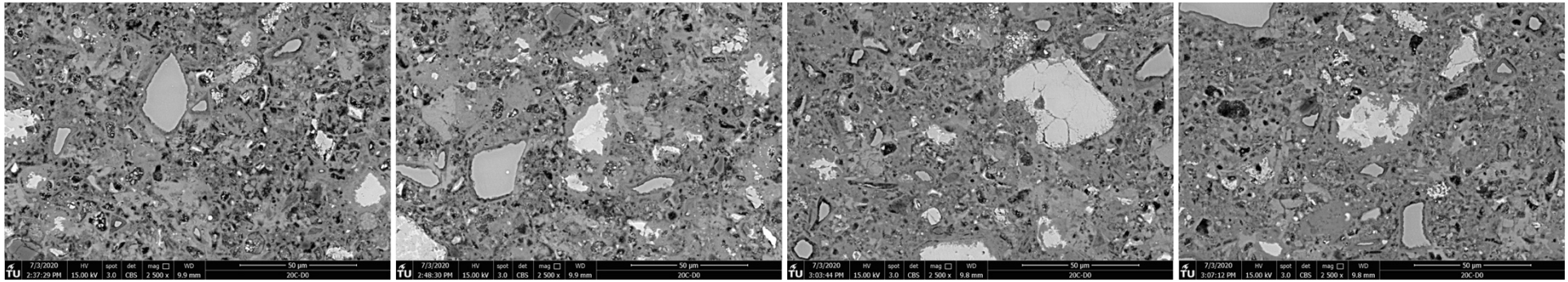

20F-D0

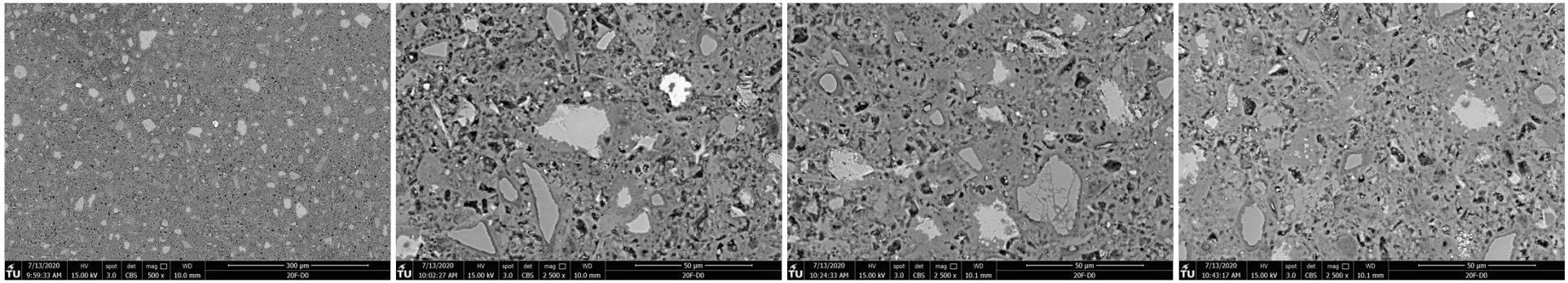

50C-D0

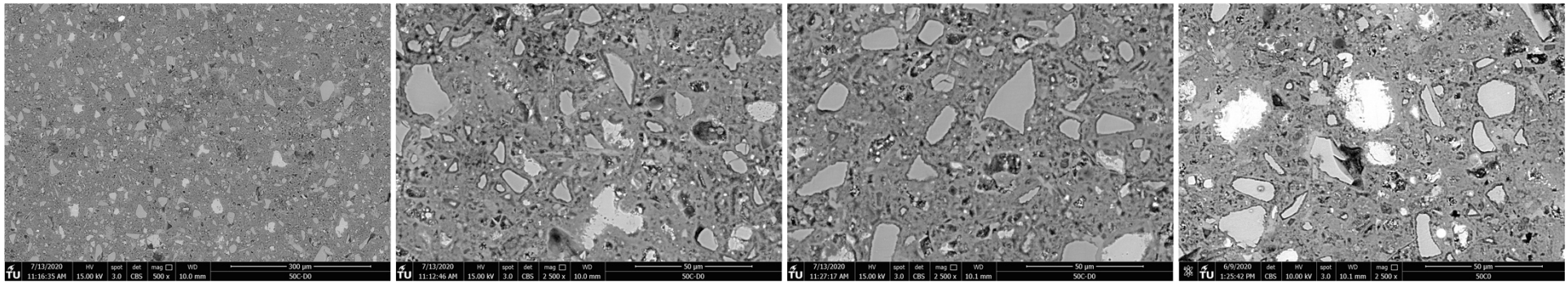

50F-D0

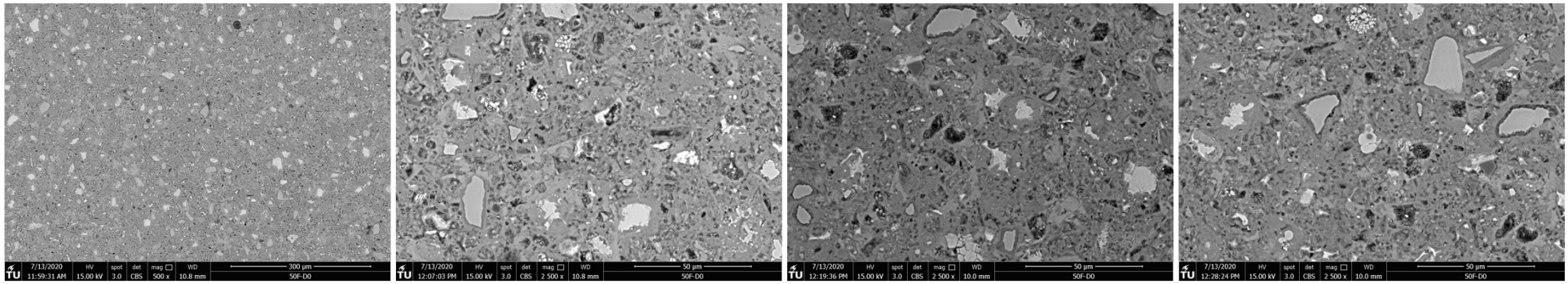

After Exposure Micrographs

CEM I-D90

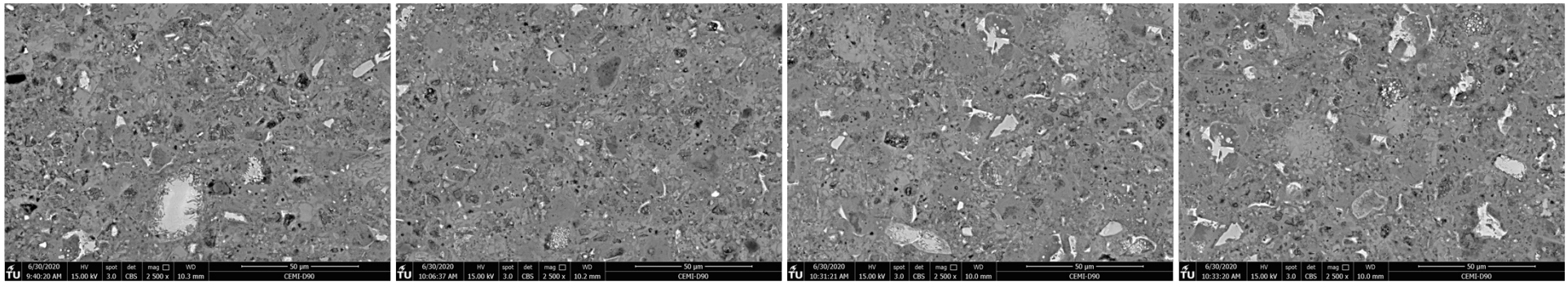

CEM II/B-S -D90

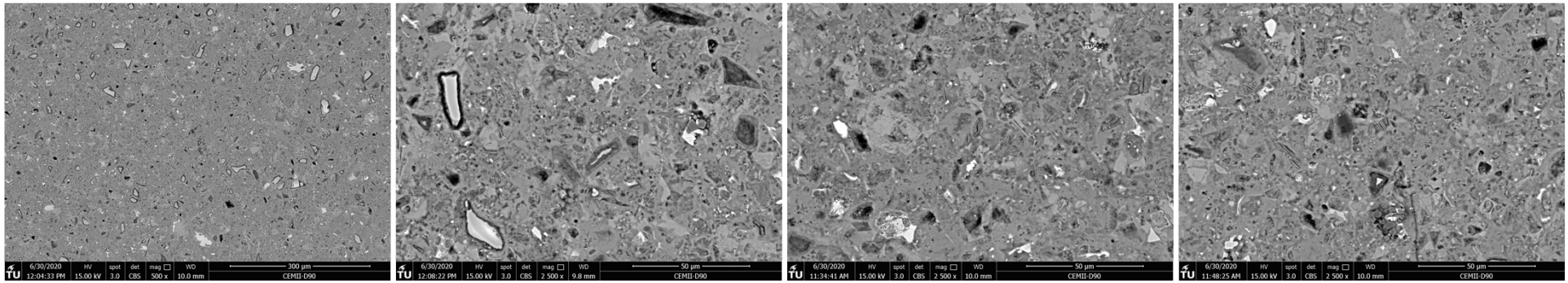

CEM III/A-D90

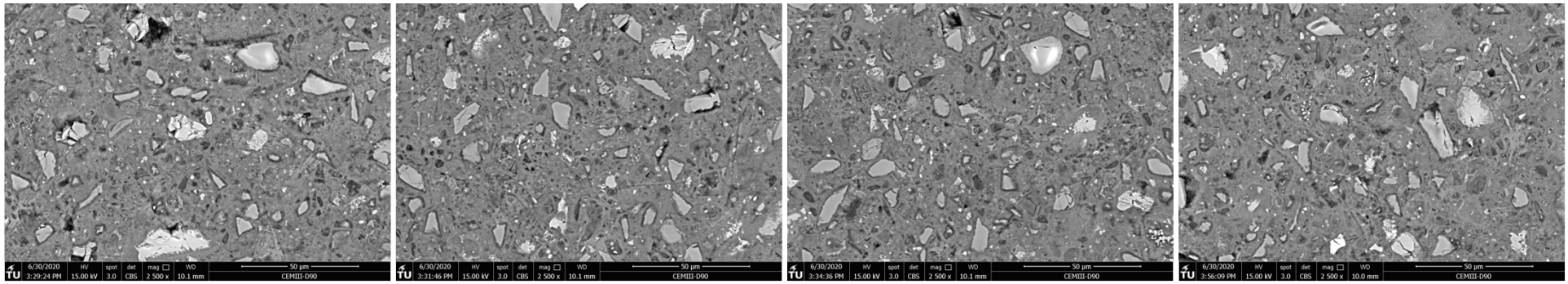

20C-D90

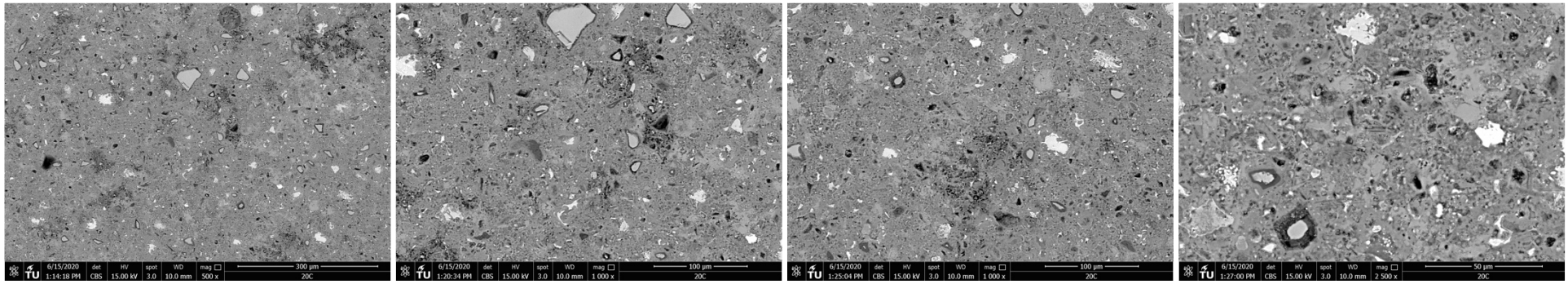

20F-D90

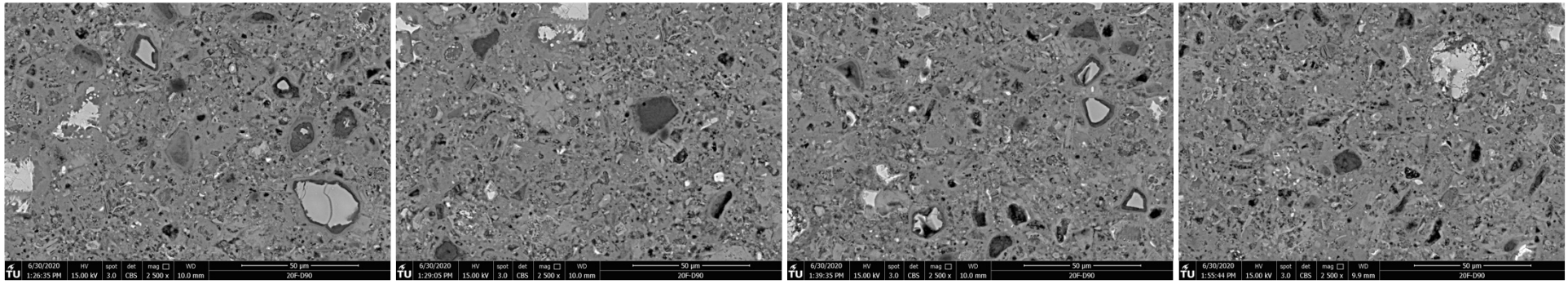

50C-D90

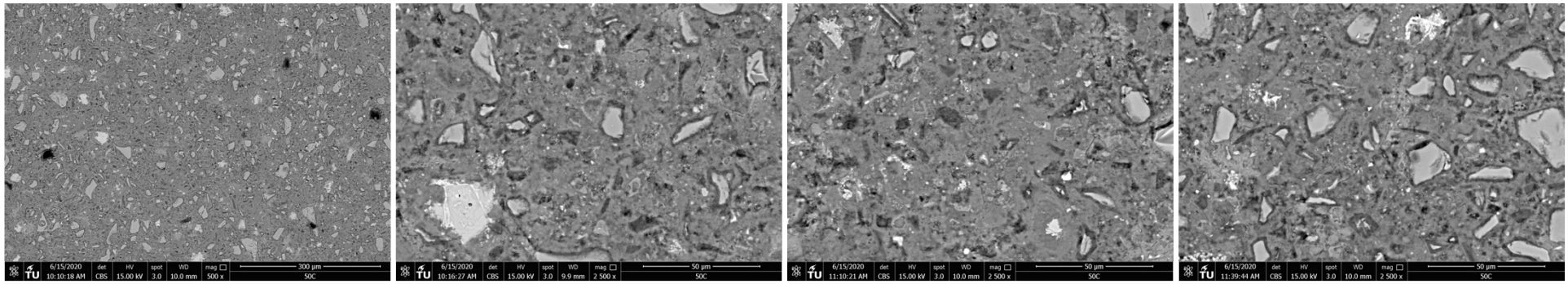

50F-D90

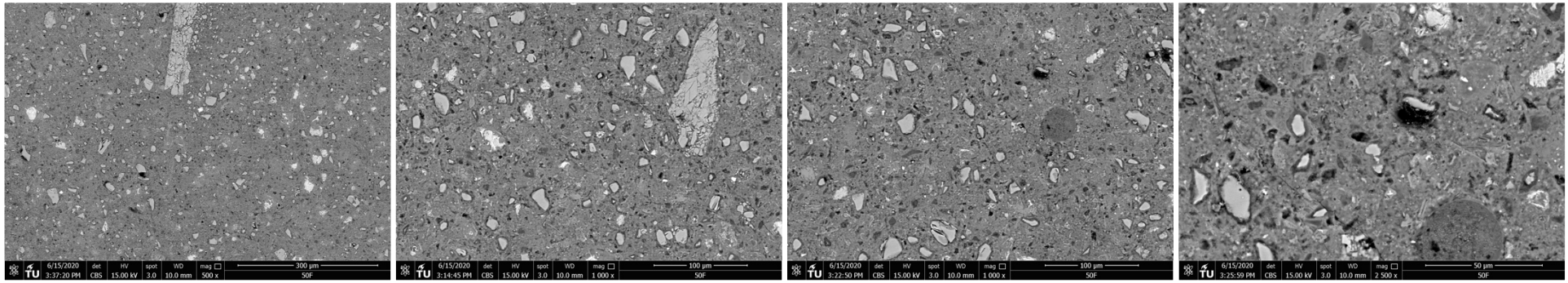

After Exposure Micro Analysis

CEM I -D90

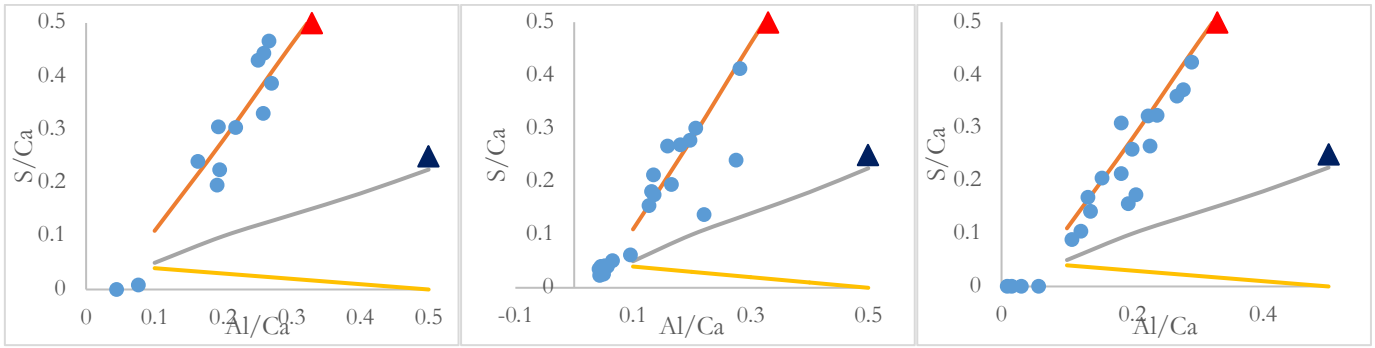

CEM II/B-S -D90

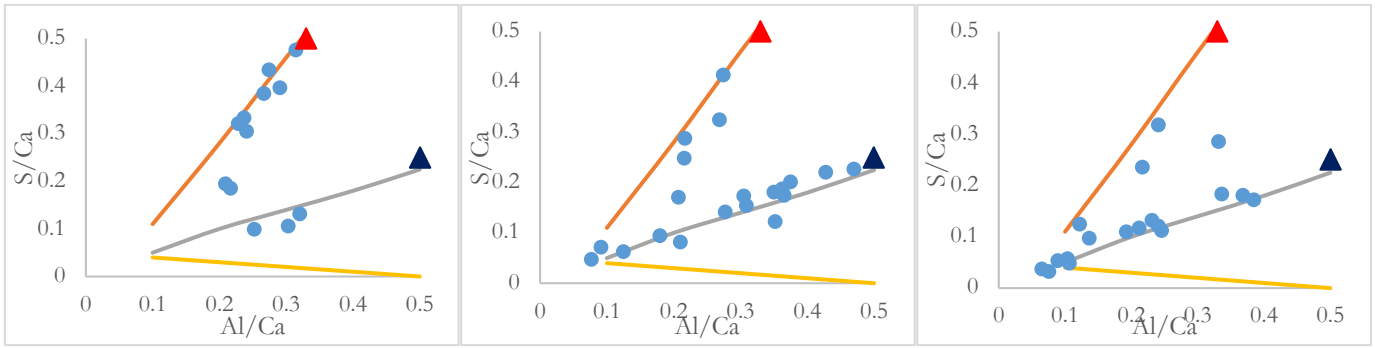

CEM III/A -D90

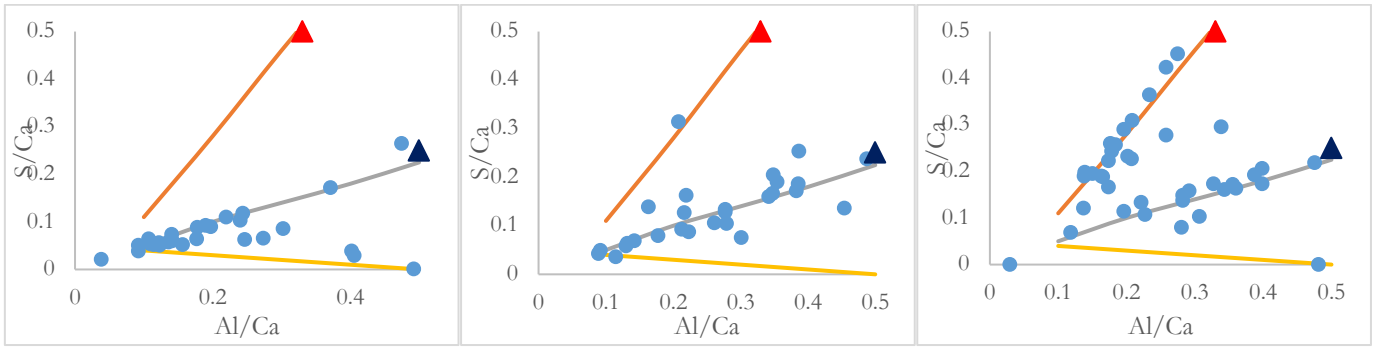

20C-D90

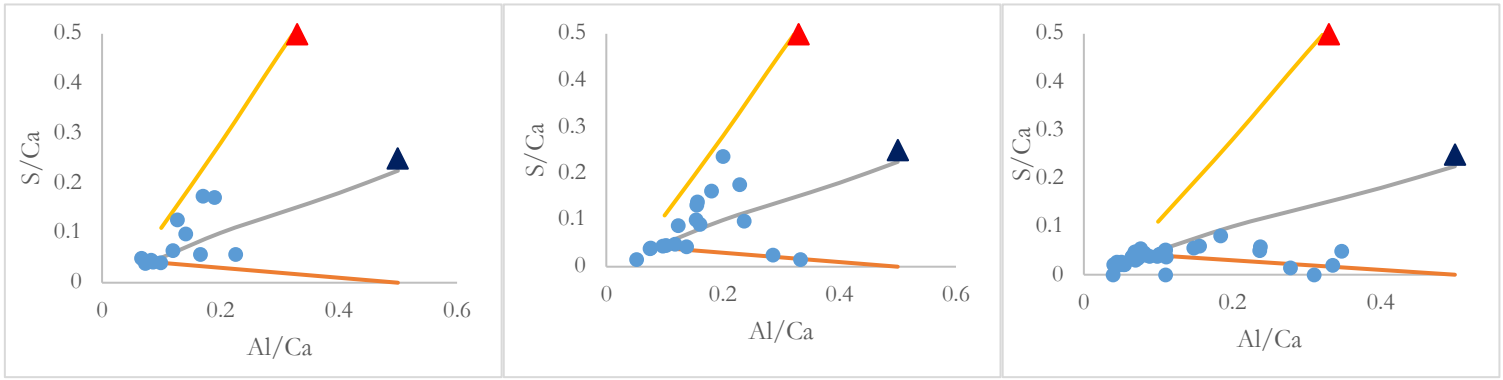

20F-D90